

Search for dijet resonances in events with an isolated charged lepton using $\sqrt{s} = 13$ TeV proton-proton collision data collected by the ATLAS detector



The ATLAS collaboration

E-mail: atlas.publications@cern.ch

ABSTRACT: A search for dijet resonances in events with at least one isolated charged lepton is performed using 139 fb^{-1} of $\sqrt{s} = 13$ TeV proton-proton collision data recorded by the ATLAS detector at the LHC. The dijet invariant-mass (m_{jj}) distribution constructed from events with at least one isolated electron or muon is searched in the region $0.22 < m_{jj} < 6.3$ TeV for excesses above a smoothly falling background from Standard Model processes. Triggering based on the presence of a lepton in the event reduces limitations imposed by minimum transverse momentum thresholds for triggering on jets. This approach allows smaller dijet invariant masses to be probed than in inclusive dijet searches, targeting a variety of new-physics models, for example ones in which a new state is produced in association with a leptonically decaying W or Z boson. No statistically significant deviation from the Standard Model background hypothesis is found. Limits on contributions from generic Gaussian signals with widths ranging from that determined by the detector resolution up to 15% of the resonance mass are obtained for dijet invariant masses ranging from 0.25 TeV to 6 TeV. Limits are set also in the context of several scenarios beyond the Standard Model, such as the Sequential Standard Model, a technicolor model, a charged Higgs boson model and a simplified Dark Matter model.

KEYWORDS: Exotics, Hadron-Hadron scattering (experiments)

ARXIV EPRINT: [2002.11325](https://arxiv.org/abs/2002.11325)

Contents

1	Introduction	1
2	ATLAS detector	2
3	Object definitions and event selection	4
4	Monte Carlo simulations	6
5	Analysis procedure	7
6	Systematic uncertainties	10
7	Results	12
7.1	Limits on BSM models	15
8	Conclusion	17
A	Dijet invariant mass in the LE-CR region	19
B	Expected limits for broad signals	19
	The ATLAS collaboration	25

1 Introduction

In the Standard Model (SM), events with two or more jets are usually produced by strong interactions described by quantum chromodynamics (QCD). Searches for resonances in dijet invariant-mass distributions provide a means to investigate a wide range of theories beyond the Standard Model (BSM). Such searches are sensitive to heavy particles that decay into two partons which, following fragmentation, form two jets. Studies of this kind were among the first published using early data from the ATLAS [1–4] and CMS [5–7] experiments at the Large Hadron Collider (LHC) at CERN, when operations at high energy first began. Later results used new datasets as the LHC increased the collision energy, from 7 TeV to 8 TeV during Run 1 [8–10], and then to 13 TeV for Run 2 [11–18]. Typically, these searches initially focused on resonances with high dijet invariant masses, m_{jj} , e.g. on enhanced event yields in the new kinematic regime opened up by the increase in energy. However, as the integrated luminosity collected at the highest available energy increased, without signs of new physics at high masses, there has been renewed interest in exploiting these large datasets to also look for signals in the region $m_{jj} < 1$ TeV. These low-mass regions are difficult to access in inclusive dijet searches due to limitations imposed by

the high transverse-momentum thresholds applied to jet triggers to keep trigger rates at manageable levels. Such studies have been performed with inclusive samples using analyses done at so-called ‘trigger level’ [10, 13]. Other strategies involve requiring the presence of an associated object that can be used for triggering, such as a photon [19, 20] or a jet [21–24] from initial-state radiation. The results presented here complement these techniques by searching for dijet resonances in events containing an isolated electron (e) or muon (μ). Besides providing access to lower dijet invariant masses, the requirement of a final-state lepton in addition to jets provides sensitivity to a set of new-physics models that cannot be studied using jet triggers.

Many BSM models predict new heavy resonances in production modes, yielding a final state consisting of jets, produced in the resonance decay, accompanied by at least one lepton. At hadron colliders, possible processes are $q\bar{q}' \rightarrow WX \rightarrow \ell\nu q\bar{q}$ and $q\bar{q}' \rightarrow X' \rightarrow WX \rightarrow \ell\nu q\bar{q}$, as well as production induced by gluon-gluon fusion, where the X and X' can be either scalar or vector particles. Examples include technicolor models, $q\bar{q} \rightarrow \rho_T \rightarrow W\pi_T \rightarrow \ell\nu q\bar{q}$ [25] (in which a technirho ρ_T decays into a W boson and a technipion π_T , see figure 1(a-b)), the Sequential Standard Model [26], $W' \rightarrow WZ' \rightarrow \ell\nu q\bar{q}$ (where W' and Z' are new heavy gauge bosons, see figure 1(c)), and charged Higgs models [27] (figure 1(d)). A number of dark-matter (DM) models also predict new resonances that can be produced in association with vector bosons [28] (figure 1(e)).

Searches for the signatures of specific models may benefit by requiring the presence of other leptons (as in the case of associated Z boson production), b -tagged jets, missing transverse momentum (in the case of W boson or top decays) or other model-specific kinematic quantities. However, the study presented in this article focuses on a generic search for BSM resonances in the dijet invariant-mass distribution constructed from events with at least one isolated electron or muon, in order to explore the potential of searches without signal-specific selections. Model-dependent limits are set by taking into account the signal shapes expected in the models described above. This search uses an integrated luminosity of 139 fb^{-1} of $\sqrt{s} = 13 \text{ TeV}$ proton-proton (pp) collision data recorded by the ATLAS detector over the full period of Run 2 of the LHC.

2 ATLAS detector

The ATLAS detector [29–31] consists of an inner tracking detector (ID), surrounded by a superconducting solenoid that provides a 2 T magnetic field, electromagnetic and hadronic calorimeters, and a muon spectrometer (MS). The ID provides tracking in the pseudorapidity¹ region $|\eta| \leq 2.5$ and consists of silicon pixel and microstrip detectors surrounded by

¹ATLAS uses a right-handed coordinate system with its origin at the nominal interaction point (IP) in the centre of the detector and the z -axis along the beam line. The x -axis points from the IP to the centre of the LHC ring, and the y -axis points upwards. Cylindrical coordinates (r, ϕ) are used in the transverse plane, ϕ being the azimuthal angle around the beam line. Transverse momentum and energy are defined as $p_T = p \sin \theta$ and $E_T = E \sin \theta$, respectively. The pseudorapidity is defined in terms of the polar angle θ as $\eta = -\ln \tan(\theta/2)$. The angular separation between two objects in η - ϕ space is defined as $\Delta R = \sqrt{(\Delta\eta)^2 + (\Delta\phi)^2}$.

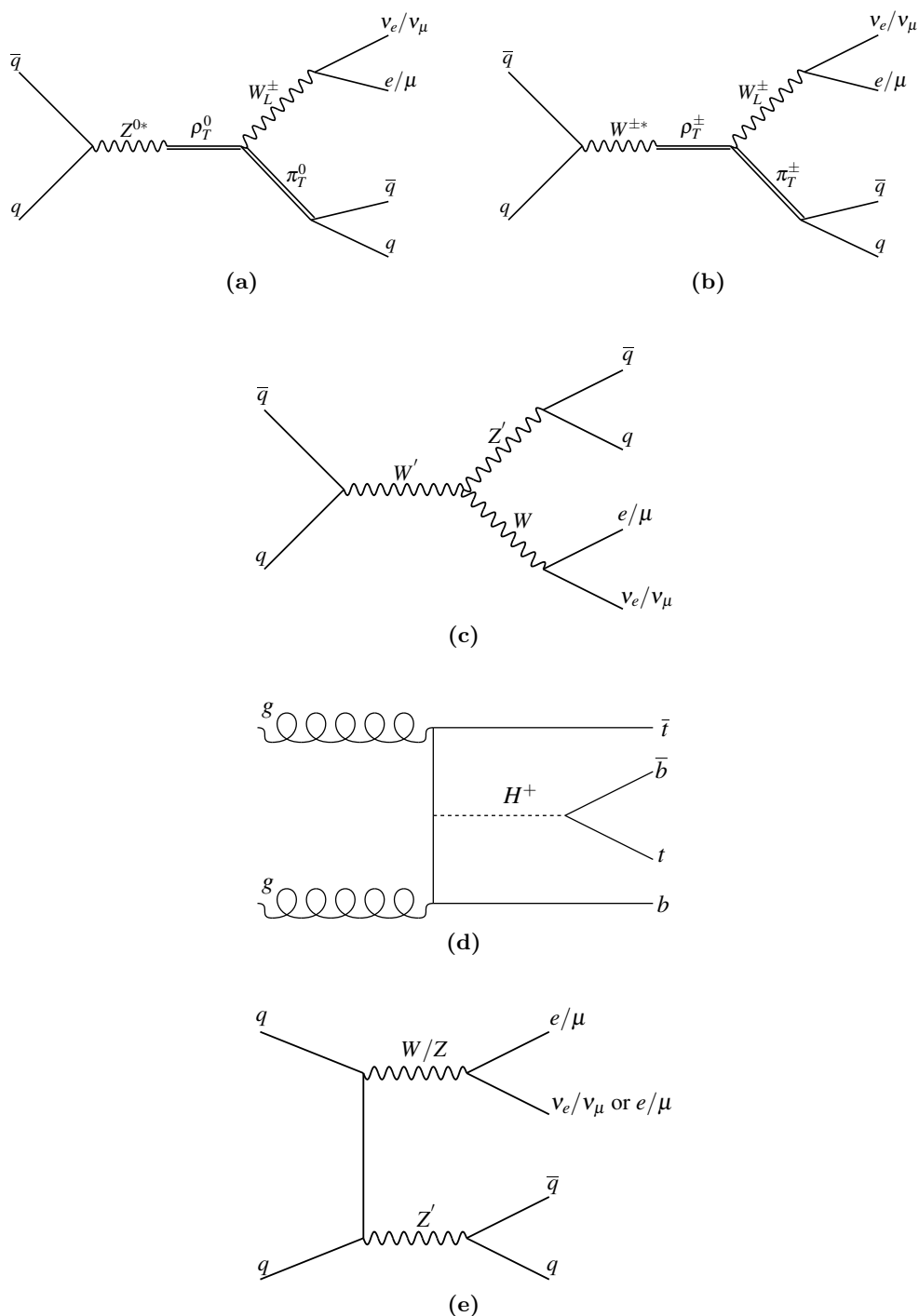


Figure 1. Representative Feynman diagrams for the processes considered in this analysis: (a)-(b) the technicolor model with production of ρ_T decaying into $\pi_T W^\pm$, (c) $W' \rightarrow Z' W^\pm$ production in the Sequential Standard Model, (d) the charged Higgs boson production in association with a top quark, $t\bar{t}H^\pm$, (e) the simplified dark-matter model.

a transition radiation tracker, which also provides information for electron identification. Each tracking detector consists of a central barrel and two endcap sections.

The electromagnetic calorimeter is a sampling device made of lead absorbers with liquid argon (LAr) as active medium. It comprises a barrel ($|\eta| \leq 1.475$) and two endcaps ($1.375 \leq |\eta| \leq 3.2$). To facilitate corrections for energy losses upstream of the calorimeter, the cryostat is equipped with a presampler layer in the region $|\eta| \leq 1.8$. Hadronic sampling calorimetry is provided by a steel and scintillator-tile calorimeter in the region $|\eta| \leq 1.7$, complemented by a copper/LAr system in the region $1.5 \leq |\eta| \leq 3.2$. The forward region ($3.1 \leq |\eta| \leq 4.9$) is equipped with both electromagnetic and hadronic calorimeters composed of copper/LAr and tungsten/LAr, respectively.

The muon spectrometer is the outermost ATLAS subsystem. It detects muons in the pseudorapidity region up to $|\eta| = 2.7$, with triggering capability up to $|\eta| = 2.4$. The MS consists of a barrel ($|\eta| \leq 1.05$) and two endcap sections ($1.05 \leq |\eta| \leq 2.7$). A system of three large superconducting air-core toroid magnets, each with eight coils, provides a magnetic field with a bending integral of about 2.5 Tm in the barrel and up to 6 Tm in the endcaps.

The trigger system [32] consists of a first-level trigger implemented in hardware using a subset of the detector information to accept events from the 40 MHz bunch crossings at a rate of 100 kHz, followed by a software-based trigger implemented in a large computer farm, which reduces the acceptance rate so that events are recorded at about 1 kHz.

3 Object definitions and event selection

The analysis presented in this paper is based on data collected with the ATLAS detector during the 2015–2018 data-taking period, referred to as Run 2. The data were recorded under stable beam conditions while all relevant subdetectors were fully operational, and were subject to detailed quality checks. The data sample corresponds to an integrated luminosity of 139 fb^{-1} with an uncertainty of 1.7%. This uncertainty was derived from calibration of the luminosity scale using x - y beam-separation scans, following a methodology similar to that detailed in ref. [33] using data from the LUCID-2 detector [34] for the baseline measurement.

Candidate events were accepted by either single-muon or single-electron triggers [32] with various transverse momentum p_T (muons) or transverse energy E_T (electrons) thresholds, as well as data quality and lepton isolation requirements. The lowest p_T (E_T) threshold without trigger prescaling is 24 (26) GeV and includes a lepton isolation requirement that is not applied for triggers with higher thresholds. A trigger matching requirement [32] is applied where the reconstructed lepton must lie within the vicinity of the corresponding trigger-level object. This requirement reduces the fake rate and allows a consistent definition of efficiencies between Monte Carlo simulations and data.

Muons are reconstructed by using a combined fit to hits in the ID and MS, and are required to have $p_T \geq 7 \text{ GeV}$ and $|\eta| \leq 2.5$ and to satisfy ‘medium’ quality criteria, in order to select particles from the primary interaction [35]. Identification requirements based on the number of hits in the ID and MS subsystems, as well as the significance of the difference

$|q/p_{\text{MS}} - q/p_{\text{ID}}|$, where q is the charge and p_{MS} (p_{ID}) is the momentum as measured in the MS (ID), are applied to the combined tracks. Muon tracks are required to satisfy $|d_0/\sigma(d_0)| \leq 3$ and $|z_0 \times \sin \theta| \leq 0.5$ mm, where d_0 is the transverse impact parameter relative to the beam line, $\sigma(d_0)$ is its uncertainty, z_0 is the distance along the beam line to the primary vertex from the point where d_0 is measured, and θ is the polar angle. The primary vertex is chosen as the vertex with the highest $\sum p_{\text{T}}^2$, where the sum is over tracks associated with that vertex and having $p_{\text{T}} > 500$ MeV; at least two such tracks are required.

Electrons are identified as energy clusters formed in the electromagnetic calorimeter [36] matched to tracks in the ID, with requirements of $E_{\text{T}} > 7$ GeV and $|\eta| \leq 2.47$. Candidate electrons must have tracks satisfying $|d_0/\sigma(d_0)| \leq 5$ and $|z_0 \times \sin \theta| \leq 0.5$ mm and meet ‘tight’ quality criteria [36]. Electrons within the barrel-endcap transition region of the electromagnetic calorimeter, $1.37 \leq |\eta| \leq 1.52$, or which share a track with an identified muon, are discarded.

Leptons are further required to be isolated from other objects in the event using p_{T} -dependent criteria based on calorimeter and tracking information. The isolation parameters were tuned to provide a constant efficiency as a function of transverse momentum, and the highest background rejection below 60 GeV (‘FCTight’). The lepton isolation and p_{T} requirements allow a consistent definition of lepton candidates when considering data-taking periods in which different trigger configurations were used. Lepton misidentification rates for the chosen isolation requirements are discussed in refs. [35, 36]. The combined trigger efficiency is about 88%, averaged over the two lepton flavours.

Jets are reconstructed using the anti- k_t algorithm [37] with a radius parameter of $R = 0.4$, as implemented in the FastJet package [38], using topological clusters of energy deposits in the calorimeters [39] as inputs. These jets are corrected for contributions arising from additional collisions in the same and nearby bunch crossings (pile-up) [40], and calibrated to the particle energy scale (i.e. before interaction with the detector) [41]. Jet candidates are required to have $p_{\text{T}} \geq 20$ GeV and to be within $|\eta| \leq 2.4$. To suppress jets arising from pile-up, a jet-vertex-tagging technique [42] is applied to jets with $p_{\text{T}} \leq 60$ GeV, requiring that at least 60% of the total p_{T} of tracks in the jet be associated with the primary vertex in each event. Candidate jets with fewer than three associated tracks are discarded if they lie within a cone of $\Delta R = 0.2$ around a muon candidate, and disregarded irrespective of the track requirement for the electron candidates. The track-multiplicity requirement is effective in rejection of misreconstructed jets originating from muons. Electron and muon candidates are discarded if they are within a cone of $\Delta R = 0.4$ around a remaining jet’s axis.

Following this object selection, a signal region is defined by requiring at least one isolated lepton (e or μ) with $p_{\text{T}}^{\ell} \geq 60$ GeV and at least two jets. Dijet invariant masses are constructed by combining the two jets having the highest p_{T} . Only events with $m_{\text{jj}} \geq 0.22$ TeV are considered; this minimum value is chosen in order to avoid the low- m_{jj} region where the event rate does not monotonically decrease due to a kinematic bias in jet p_{T} from the minimum p_{T}^{ℓ} of leptons. The m_{jj} mass distribution that includes a region below 0.22 TeV is difficult to describe with a function that falls smoothly over the entire range of m_{jj} .

4 Monte Carlo simulations

Monte Carlo (MC) simulations are used to investigate contributions to the m_{jj} distribution from various SM processes, as well as to estimate the background from data. The sources of background modelled using MC simulation are the QCD multijet, $t\bar{t}$ and W +jets processes. The multijet event sample was simulated with the PYTHIA 8.186 [43] generator with the NNPDF2.3 [44] set of parton distribution functions (PDF) and a set of tuned parameters called the A14 tune [45]. The $t\bar{t}$ and W +jet events were produced using the POWHEGBOX [46–49] v2 generator interfaced with PYTHIA 8. This simulation used the CT10 NLO PDF set [50] and the AZNLO tune [51].

For the model-dependent searches, MC simulations are also used to predict the expected signal shapes for the BSM models discussed earlier: (1) $W' \rightarrow WZ' \rightarrow \ell\nu q\bar{q}$; (2) $\rho_T \rightarrow W^\pm\pi_T \rightarrow \ell\nu q\bar{q}$; (3) charged Higgs boson production in association with a top quark, tbH^+ ; and (4) a simplified DM model with an axial-vector mediator, Z' .

The $W' \rightarrow WZ' \rightarrow \ell\nu q\bar{q}$ and $\rho_T \rightarrow W^\pm\pi_T \rightarrow \ell\nu q\bar{q}$ simulations are performed at leading-order QCD using PYTHIA 8 and PYTHIA 6 [52], respectively, with the CT10 NLO PDF set. The parton showering and hadronisation of the latter simulation are performed using the A14 tune of PYTHIA 8. The first model assumes a Z' dijet resonance produced in association with a leptonically decaying W from the $q\bar{q} \rightarrow W'$ process. The relative width of the Z' is set to 3.2%, which is the default value in PYTHIA. The W' to WZ' branching fraction is chosen to be 0.5 and the mass difference between the W' and Z' was set to 250 GeV. This latter requirement yields the largest predicted cross-section for the desired final state. This model is also used to estimate systematic uncertainties in generic signals approximated by Gaussian functions with widths varying between 5% and 15% of the dijet invariant mass.

The second model considered is a generic technicolor model [53] that assumes the production of a technirho, ρ_T , that decays into a leptonically decaying W boson and a technipion π_T , decaying into two jets. The mass of the ρ_T is chosen to be a factor of two larger than the mass of the π_T , which maximises the cross-section for the $\ell\nu q\bar{q}$ final state. The signal width for this model is approximately 15% of the predicted technipion mass.

The tbH^+ process is modelled with MADGRAPH5_aMC@NLO [54] at next-to-leading order (NLO) in QCD [55], based on a two-Higgs-doublet model (2HDM) in the $m_h^{\text{mod-}}$ scenario [56] and a four-flavour scheme implementation with the NNPDF2.3 PDF set. The H^+ decay into $t\bar{b}$ is assumed. Parton showering and hadronisation are modelled using PYTHIA 8 with the A14 tune. This simulation uses the narrow-width approximation [57], and effects related to W boson polarisation and the interference between tbH^+ and the SM $t\bar{t} + b\bar{b}$ background are not included. The narrow-width approximation has a negligible impact on the limit presented in this paper since the peak in the m_{jj} distribution has a relative half width at half maximum (HWHM) of about 30% of the m_{jj} peak position. This width is much larger than the H^+ natural width of about 4% of the H^+ mass for $\tan\beta = 1$, where $\tan\beta$ is the ratio of the vacuum expectation values of the two scalar doublets in the 2HDM. While the $t\bar{b}$ final state includes more than two jets, simulation studies indicate that, for events arising from the tbH^+ process, m_{jj} distributions obtained from the two

highest- p_T jets have well-defined peaks for m_{H^+} values above 600 GeV. The reconstructed m_{jj} peak position is shifted from the m_{H^+} value by about 30% to lower masses since the two leading jets used for m_{jj} do not contain the complete information about the H^+ decays.

This analysis also studies a benchmark simplified DM model with an axial-vector mediator Z' , in which the lepton originates from the decay of a W boson, e.g. $q\bar{q} \rightarrow Z'W$ where the Z' decays into jets and the W via $W \rightarrow \ell\nu$. This model assumes the leptophobic couplings $g_q = 0.25$, $g_\ell = 0$, and $g_{DM} = 1$, following the recommendations of the LHC-DMWG [28]. Here g_q , g_ℓ and g_{DM} are the couplings of the mediator to quarks, leptons and the DM particle, respectively. Signal MC events were generated with MADGRAPH5_aMC@NLO at leading order in QCD. Possible interference between SM and DM processes was studied at parton level and shown not to affect the shape or normalisation of the resonance mass peaks, so is not included in the simulation sample.

All MC samples, with the exception of the tbH^+ and DM models, were passed through the full ATLAS detector simulation [58] based on GEANT4 [59]; the tbH^+ and DM processes were simulated using the ATLAS fast simulation framework, ATLFast-II [60], which uses parameterisations of electromagnetic and hadronic showers in the calorimeters. All simulated events are corrected so that the object identification, reconstruction and trigger efficiencies, energy scales and energy resolutions match those determined from data control samples. After this correction, additional systematic uncertainties were applied to cover for the difference between the data and MC simulations as described in section 6. Additional simulated pp collisions generated using PYTHIA 8, with the A3 set of tuned parameters [61] and the NNPDF2.3 PDF set, were overlaid to simulate the effects of pile-up in a manner that matches the multiplicity distribution of additional collisions in the data. Simulated events were reconstructed and analysed with the same algorithms as used for data.

5 Analysis procedure

The existence of a new resonant state of mass m_X decaying into partons that hadronise to two jets could lead to an observable excess of events at $m_{jj} \approx m_X$ on an otherwise smooth and monotonically decreasing dijet invariant-mass distribution. This analysis presents a search for such an excess in the range $0.22 < m_{jj} < 6.3$ TeV.

The bin widths of the m_{jj} distribution are chosen to be approximately equal to the dijet mass resolution at a given mass and therefore widen from 13 GeV to 120 GeV, over the specified range in m_{jj} . The following fit function [8, 13, 19] is used to model the shape of the estimated background,

$$f(x) = p_1(1-x)^{p_2} x^{p_3+p_4 \ln x + p_5 \ln^2 x}, \tag{5.1}$$

where $x \equiv m_{jj}/\sqrt{s}$ and the p_i are free parameters.

To investigate the ability of eq. (5.1) to accurately describe the background in the signal region, a likelihood fit is performed to the background estimate obtained from MC simulations of QCD multijet, W +jets and $t\bar{t}$ samples. The combined contribution from W and top-quark processes in the MC simulations varies from 1% to 10% as a function of m_{jj} . The five-parameter fit function provides a good description of the signal region in this

MC sample. However, eq. (5.1) with $p_5 = 0$ also provides an adequate description of this distribution, which has far fewer events than are available in data. Additional studies were therefore undertaken, as described below. One is based on a control region (CR) defined for MC simulation, and the other on a CR defined for data; both provide far more events than are available in the MC distribution discussed above. These studies are also used to investigate possible effects related to jet reconstruction, or to leptons misidentified as jets, which may lead to structures in the m_{jj} distribution that can be difficult to describe with a smoothly falling distribution and could be misinterpreted as a potential signal. In the first of these, a three-jet control region, referred to as the ‘2+1 jets’ CR is constructed using MC events. This is identical to the signal region with the exception that a third jet with $p_T > 60$ GeV is required instead of the charged lepton. Removing the requirement of a final-state lepton increases the number of events in the dominant multijet background sample by more than an order of magnitude. No significant deviations of the MC distribution from the fit hypothesis of eq. (5.1) are observed in the 2+1 jets CR. The composition of this CR illustrates the decreased relative contributions from W and top-quark processes when requiring a third jet instead of a final-state lepton. Here, in the 2+1 jets CR, W and top processes contribute to the overall background at a level of less than 0.1% relative to QCD multijets.

The fit hypothesis of eq. (5.1) models the 2+1 jets CR well, giving $\chi^2/\text{ndf} \simeq 1.2$ (where $\chi^2 = 130$ and $\text{ndf} = 109$) and a ratio of the MC distribution to the fit that is within 5% of unity over the full range of m_{jj} . The distribution of the fit residuals is consistent with a normal distribution with a mean of zero. It is observed that all five fit parameters are strongly constrained by the low-mass region, $m_{jj} < 1$ TeV, which has the most events. Functions of the form of eq. (5.1) with fewer than five parameters fail to adequately describe the dijet mass distribution in this CR.

To complement the 2+1 jets CR used in MC studies, a ‘loose electron’ control region (LE-CR) is defined for the data. It is populated by selecting dijet events with at least one electron that satisfies a set of loose identification criteria but not the more stringent tight identification criteria, ensuring orthogonality with the signal region. The LE-CR is expected to have an increased multijet contribution due to the contamination from misidentified electrons. The main goal of this region is to verify that the data do not show structures that can be interpreted as signals when using the analytic fits. The number of events in the LE-CR is a factor of ten larger than in the 2+1 jets CR used in MC studies. Studies of this control region demonstrate that jet reconstruction does not lead to structures that can be interpreted as signals. The fit hypothesis of eq. (5.1) models the LE-CR with $\chi^2/\text{ndf} \simeq 1.6$, where $\chi^2 = 172$ and $\text{ndf} = 109$ (see the appendix A). The residuals are distributed according to a normal distribution with a mean consistent with zero. The fit with eq. (5.1) performs poorly when the minimum value of m_{jj} is below 200 GeV. The minimum value of m_{jj} value is therefore set to 216 GeV, which is defined by the lower bin edge of the chosen binning. Fit functions with $p_5 = 0$ fail to describe the LE-CR.

Several alternative five-parameter functions for the description of the LE-CR region have been investigated. It was found that the only five-parameter function that adequately describes the LE-CR as a whole, and shows some systematic difference with respect to

eq. (5.1) in the tail of the m_{jj} distribution, is a function obtained after replacing $p_5 \ln^2 x$ to p_5/\sqrt{x} . The application of this alternative function to the LE-CR region leads to residuals distributed according to a normal distribution with a mean consistent with zero. Functions with more than five parameters have also been investigated. A test based on the Wilks' theorem [62] shows that no additional parameters are needed.

To investigate potential biases in the description of the LE-CR by eq. (5.1), ‘signal-injection’ and ‘closure’ tests are performed. For the signal-injection test, signal events modelled according to Gaussian distributions are added to the expected background distribution to assess whether or not the correct numbers of events can be extracted using signal-plus-background fits, assuming the known Gaussian signal shape. For the closure test, signal-plus-background fits are run on the background-only spectra of the LE-CR for different signal masses and the extracted signal yield is taken as an estimate of a false signal. In the first case, the extracted signal yield is consistent with the injected number of events within the statistical uncertainty. The number of extracted events in the closure tests was significantly smaller than the statistical uncertainty of the data points. This event rate for the signal region is considered as a source of systematic uncertainty in the limit values (discussed in section 6).

Based on the studies of the control regions, the background-only hypothesis for the signal region is constructed using eq. (5.1), over the m_{jj} range from 216 GeV to 6.3 TeV.

To determine if the data deviate significantly from the background-only hypothesis prediction, the BumpHunter [63] test is used. This test calculates the significance of any excess found in mass intervals in all possible locations of the binned m_{jj} . The width of the search window varies from a minimum of two m_{jj} bins up to half the extent of the full m_{jj} mass distribution. For each of the chosen intervals in m_{jj} , a local p -value is calculated from a unique hypothesis test statistic. The method takes into account the look-elsewhere effect [64] by combining each of the hypothesis tests to form a new hypothesis test, and calculating the minimum p -value amongst all tests. A global p -value is then calculated and transformed to a significance assuming that bin-by-bin fluctuations of the data follow a Poisson distribution. Pseudo-experiments are then used to determine the most significant local excess and, finally, a global significance is calculated. A null result from the BumpHunter test can only be used as an indication for non-observation of the searched-for processes but not as the necessary condition. Signal-injection tests using the BumpHunter background-only fit show a lower signal extraction efficiency for wide signals than for the signal-plus-background fit.

The Bayesian Analysis Toolkit [65] is used to set 95% credibility level (CL) upper limits on the cross-section for new processes that have a signature of a new particle decaying into partons which fragment to two jets in events with at least one isolated lepton of $p_T^\ell > 60$ GeV. In the case where no statistically significant deviations are observed according to the BumpHunter test, the exclusion limits are set at the 95% CL on the production cross-section times branching ratio for generic resonances, as well as for a range of theories beyond the Standard Model. For each test contribution from a signal model, a simultaneous likelihood fit of data using the signal contribution plus the background function is performed, with an additional parameter describing the normalisation of the

signal template. The free parameters of the fit function are considered as nuisance parameters. Systematic uncertainties are also included as nuisance parameters. To make sure the convergence of the likelihood fits, the initial parameters of the background function are set to the values determined during the search phase, but the parameters were not fixed or constrained during the fits. For a given mass, a number of such fits are performed for a range of possible signal yields. The resulting likelihood function is multiplied by a flat prior to give a posterior probability density. The 95% quantile in the signal contribution is calculated for each pseudo-experiment determined by integration of the posterior probability distribution; this is taken as the upper limit on the number of possible signal events in the data, for each resonance mass and width hypothesis. This value, divided by the integrated luminosity, provides a measure of the upper limit on the cross-section times acceptance times efficiency times branching ratio for a resonance with that mass and width. This method was also used to determine the expected limits, along with the corresponding 1 and 2 standard deviation (σ) uncertainty bands. The expected limits are evaluated by replacing actual data by pseudo-data generated using the background function determined in the search phase. This limit-setting technique is described in [1] and was used in the previous ATLAS papers [2–4, 8, 11–13, 13, 16, 19].

Detector-level limits for the BSM models are corrected by the acceptance and efficiency as a function of the mass. The acceptance is defined by the p_T and η requirements on the leptons and jets, and the requirement on the minimum dijet invariant mass used in this analysis. The acceptance is typically 40% for the lowest mass point, and increases to 60–90% for the highest mass, depending on the model. The efficiency correction includes various instrumental effects, such as the efficiencies for the trigger, lepton identification and lepton reconstruction efficiencies. A typical efficiency, averaged over the two lepton flavours, is 65–75%, depending on the particle mass and the type of BSM model. The efficiency is somewhat lower (about 50%) for the tbH^+ channel than for the other models due to a more complex final state leading to fewer isolated leptons.

6 Systematic uncertainties

The systematic uncertainties considered include those associated with the background description, the jet energy scale, jet energy resolution, lepton reconstruction, and luminosity.

The effects of jet energy scale (JES) and jet energy resolution (JER) uncertainties [41] are estimated using signal model MC events. These uncertainties cause shifts in the dijet masses by as much as $\pm 1.4\%$. The combined effect from all systematic uncertainties leads to a 6% increase in the limits relative to the limits without uncertainties. This increase is typically within the 1σ band around the expected limits shown later. The uncertainty associated with the JES and JER dominates the total systematic uncertainty for $m_{jj} \lesssim 2$ TeV. At $m_{jj} > 2$ TeV the uncertainties associated with the background description become comparable. The effect of lepton energy scale uncertainties is found to be negligible. Systematic effects from the lepton trigger, and from lepton identification and reconstruction are taken into account by assigning a constant systematic uncertainty of 1%. This group of uncertainties accounts for differences between data and MC modelling. The effect of the trigger

on the shape of the m_{jj} distribution is found to be negligible. An additional uncertainty in the limits is associated with variations of the shapes of the m_{jj} signal distributions due to the PDF choice [12]. This arises from the fact that PDF uncertainty affects the angular distributions between the two jets, thus affecting simulated signal shapes used to derive the limits. Such shape-related systematic effects on the m_{jj} distribution are accounted for by assigning a 1% PDF uncertainty to the calculated limits [12]. The PDF uncertainty is found to have a negligible effect on the acceptance corrections, which are dominated by the selection cut on the leptons. The uncertainty of 1.7% in the integrated luminosity is also accounted for.

For the generic Gaussian signals, JES and JER systematic uncertainties from the $W' \rightarrow WZ' \rightarrow \ell\nu q\bar{q}$ MC events are used, parameterised as a function of mass to generate uncertainties for masses that are not covered by the $W' \rightarrow WZ' \rightarrow \ell\nu q\bar{q}$ samples. As a cross-check, other models predicting different signal widths are also used, but no significant differences are observed.

The uncertainties arising from imperfect knowledge of the background shapes are estimated by using an alternative fit function, given by eq. (5.1), with the replacement $p_5 \ln^2 x \rightarrow p_5/\sqrt{x}$. In the region $m_{jj} < 2\text{ TeV}$, the uncertainty related to this alternative function is negligible compared to the statistical variation of the nominal fit. The background shape uncertainty becomes comparable to the size of the statistical variations of the fit function at higher values of m_{jj} . To account for the effects of the fit function choice on the extracted limits, the largest difference in the event yields between the nominal and the alternative background hypothesis is taken as a systematic uncertainty. The possibility of statistical biases related to the choice of functional form used to estimate the background is investigated using a closure test. To do this, pseudo-random distributions were created according to eq. (5.1) with the parameters obtained from the data and allowing bin-by-bin fluctuations. These were fitted using eq. (5.1) plus a Gaussian (signal) component with various fixed mean and width values, similar to what is done in the limit calculations. The distributions of the amplitude of the Gaussian components in these fits have mean values close to zero for all masses and widths, with RMS values indicating a negligible effect on the limits. This was also verified using more complex signal shapes predicted by the H^+ model.

Several theoretical uncertainties associated with the H^+ model are considered. The uncertainty due to the choice of PDF is found to have a negligible effect on the m_{jj} distribution for H^+ masses below 2 TeV used for the calculation of limits in this analysis. The narrow-width approximation used by MADGRAPH5_aMC@NLO for $\tan\beta = 0.5$ also has a negligible impact on the limit presented in this paper. This is checked by applying a smearing of the m_{jj} distribution using the Breit-Wigner distribution with a width of 18% as predicted in the 2HDM model. The polarisation effect for top-quark production was studied using leading-order QCD simulations since no spin dependence is implemented in MADGRAPH5_aMC@NLO at NLO. No statistically observable effect on the m_{jj} distribution is found.

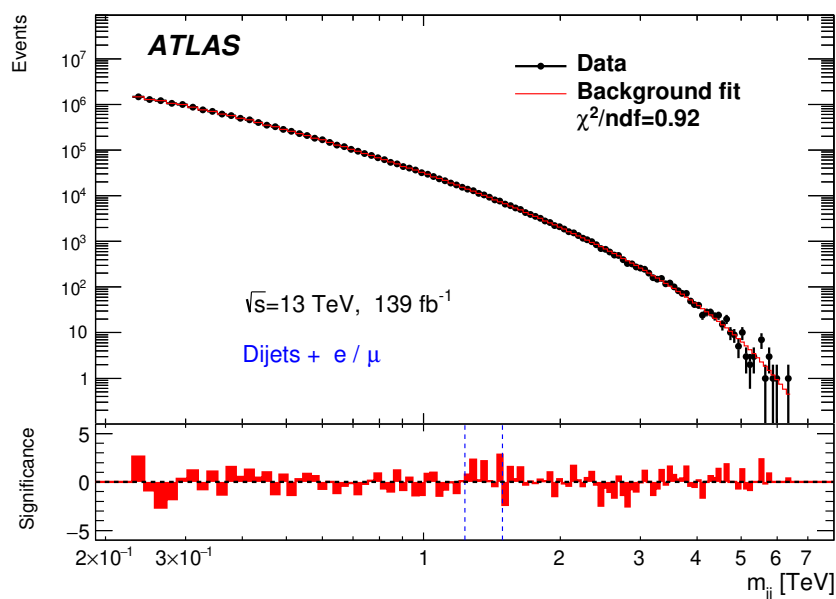
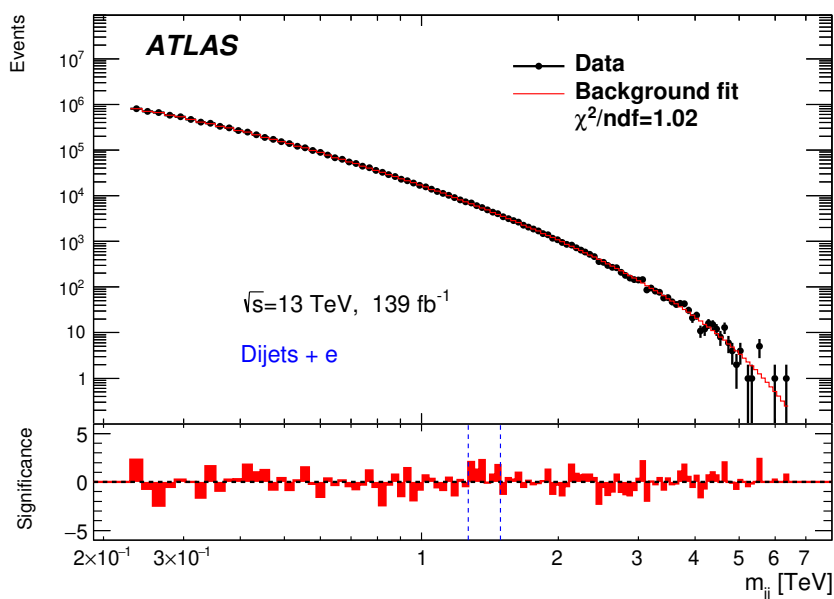


Figure 2. Dijet invariant-mass distribution from the 2015–2018 data, from events with a high- p_T lepton ($e+\mu$ combined). The distribution is calculated from the two leading jets selected from events with at least one isolated lepton with $p_T^\ell > 60$ GeV. Also shown is the result of the fit with the five-parameter background function. The lower panel shows the bin-by-bin significances of deviations from the background hypothesis. The largest deviation reported by BumpHunter is indicated by the vertical dashed lines. The global p -value of this deviation is 0.31.

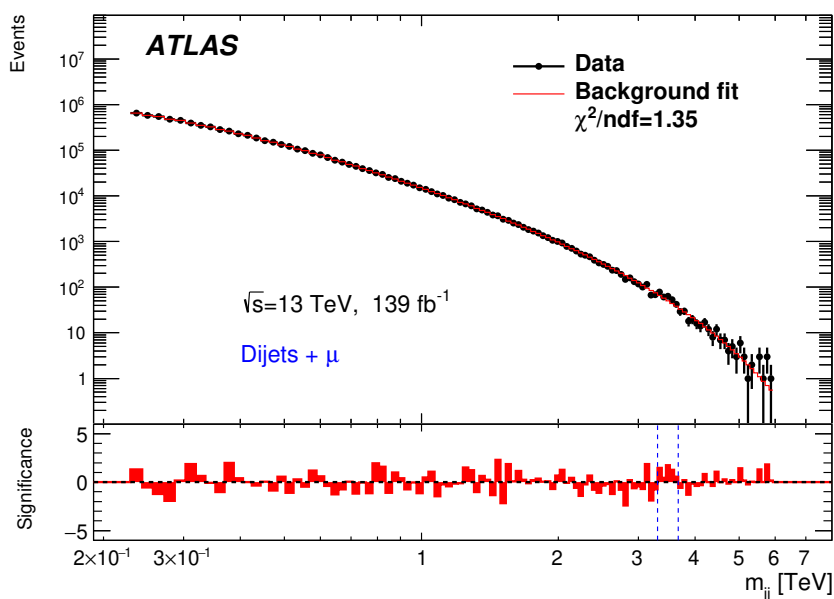
7 Results

Figure 2 shows the m_{jj} distribution obtained from the selected events in the combined electron-plus-muon channel. The result of applying the BumpHunter procedure is also shown, using a background fit with the five-parameter function from eq. (5.1). The data are well described by the fit function, with $\chi^2 = 99.8$ and the number of degrees of freedom (ndf) of 109 leading to $\chi^2/\text{ndf} = 0.92$. The lower panel shows the significances [66] of deviations from the background hypothesis, which can be approximated by $(d_i - f_i)/\delta$, where d_i is the value of the data points, f_i is the fit value, and δ is an uncertainty. This uncertainty includes statistical and systematic uncertainties of the data points and the value of the fit in the i th bin. These significances are consistent with a normal distribution with a mean of zero and unit width (not shown). Figure 3 shows the results of the analysis applied separately to events containing a high- p_T (a) electron or (b) muon, including the results from BumpHunter. The χ^2/ndf values are indicated on each figure.

The largest deviation of the data from the background-only hypothesis reported by BumpHunter in the combined channel is near 1.3 TeV, with a local p -value of 10^{-3} , corresponding to a significance of 2.8 standard deviations. The second largest deviation near 400 GeV has a local significance of 1.3σ . Accounting for the look-elsewhere effect, the global p -value for the largest deviation for the electron-plus-muon channel is 0.3, leading to a significance of 0.5σ . This deviation from the background hypothesis is consistent with a



(a)



(b)

Figure 3. Dijet invariant-mass distributions for events with a high- p_T (a) electron or (b) muon. The distributions are calculated from the two leading jets selected from events with at least one isolated lepton with $p_T^\ell > 60$ GeV. In each case, the result of the fit to the five-parameter background function is also shown. The lower panels show the bin-by-bin significances of deviations from the background hypothesis. The largest deviations reported by BumpHunter are indicated by the vertical dashed lines. The global p -values of the deviations are 0.12 (for electrons) and 0.63 (for muons).

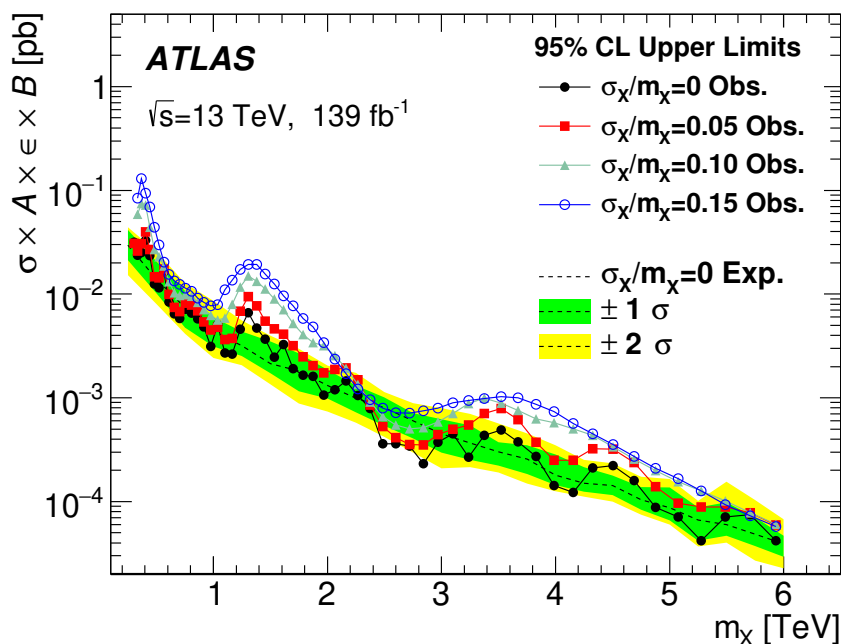


Figure 4. The 95% CL observed limits for a hypothetical particle X resulting in a contribution to the observed m_{jj} distribution with a Gaussian shape and various widths σ_X . The m_{jj} distribution is obtained from the two leading jets in events with at least one isolated lepton with $p_T^\ell > 60$ GeV. The limits, presented for the fine steps in masses that correspond to the bin sizes times two, are calculated assuming widths of the Gaussian signal corresponding to 0%, 5%, 10% and 15% of the signal mass. For the latter two cases, the points below $m_{jj} = 0.3$ TeV are excluded since the signal would, in part, be at masses below the minimum value considered here. The limits are set on the cross-section times the acceptance A , the efficiency ϵ and branching ratio B . The expected limit and the corresponding $\pm 1\sigma$ and $\pm 2\sigma$ bands are shown for the $\sigma_X/m_X=0$ signals.

statistical fluctuation, and results mainly from the electron channel. The largest deviation from the background hypothesis for the muon channel shown in figure 3(b) is near 3.5 TeV, with the global p -value of 0.6.

In the absence of any significant signals indicating the presence of new phenomena beyond the SM, limits are set in the manner described in section 5. The limits include the systematic uncertainties described in section 6.

Figure 4 shows the 95% CL observed limits for a hypothetical particle X resulting in a contribution to the observed m_{jj} distribution with a Gaussian shape and various widths σ_X . The limits are presented as a function of the mass m_X in steps that correspond to the bin sizes times two. The background hypothesis is defined as the five-parameter fit described earlier. The expected limit and the corresponding $\pm 1\sigma$ and $\pm 2\sigma$ bands are shown for $\sigma_X/m_X=0$ signals. Appendix B shows the expected limit and the corresponding $\pm 1\sigma$ and $\pm 2\sigma$ bands for the $\sigma_X/m_X=0.15$ signals. Contributions from a Gaussian-shaped signal with minimum effective cross-sections ranging from approximately 100 fb to 0.1 fb are excluded in the mass range of 0.25–6 TeV.

The oscillations in the observed limits shown in figure 4 for wide Gaussian signals are due to correlations between the points in the limit calculation, which uses the background function with unconstrained parameters. The correlation length between neighbouring mass points is proportional to the width of the resonances used for the limits. The correlation lengths increase with the width of the assumed Gaussian signal.

As a check, the statistical significance of the largest excess is studied under the signal-plus-background hypothesis. The function used to describe the data is constructed by adding a Gaussian distribution to the background shape described by eq. (5.1). All the parameters but the Gaussian width are allowed to vary during the minimisation procedure. The local significance of the largest excess, calculated from the Gaussian normalisation factor and its uncertainty, does not exceed 2.6σ , i.e. it is smaller than the local significance reported by the BumpHunter. The same conclusion is obtained by using the test based on the likelihood ratio $-2 \ln L(0)/L(1)$, with $L(0)$ and $L(1)$ being the likelihoods of the null hypothesis and the signal-plus-background hypothesis from the global likelihood fits of the data, assuming the asymptotic approximation [67]. Systematic uncertainties are not included in this check.

7.1 Limits on BSM models

Exclusion limits are also set for the four BSM models discussed earlier. As discussed before, the analysis requires well-reconstructed jets and leptons, without additional selections tuned to the specific model under study. For the limit calculations, the shape of the m_{jj} distribution for each model considered is taken from MC simulation, after detector simulation and reconstruction. The m_{jj} distributions for the π_T and Z' decays have Gaussian-like shapes around the nominal generated masses, with a HWHM ranging from 10% to 20% in their Gaussian cores. The H^+ model has an m_{jj} shape with a HWHM of about 30%, with the peak position shifted to a lower mass compared to m_{H^+} as discussed in section 4.

The Bayesian limits are calculated using the m_{jj} distribution with the background description discussed earlier, and then are corrected by the acceptance and efficiency corrections. The values of the calculated limits depend on the shape of the signal m_{jj} distributions, e.g. broader distributions typically lead to higher values of the limits. All calculated limits account for the previously discussed systematic uncertainties. In each case, the minimum m_{jj} value for the limits is selected to ensure that the signal acceptance is at least 30% for the mass points considered.

The limits on the $\rho_T \rightarrow \pi_T W^\pm$ and $W' \rightarrow Z' W^\pm$ signal models are shown in figure 5(a) and figure 5(b), respectively. For the technicolor model, in which the mass of the ρ_T is twice that of the π_T , values of m_{π_T} below 350 GeV are excluded for the range of technipion masses considered. A small deviation of the observed limits from the expected limits near 400 GeV is consistent with a statistical fluctuation, as follows from the BumpHunter background-only hypothesis (see section 7). It is not observed for the Gaussian limits due to the minimum m_{jj} requirement for the Gaussian signals with widths above 10%. The $W' \rightarrow Z' W^\pm$ model is excluded for Z' masses up to 2 TeV, assuming the maximal cross-section, which occurs when the mass difference between the W' and Z' is 250 GeV (see section 4).

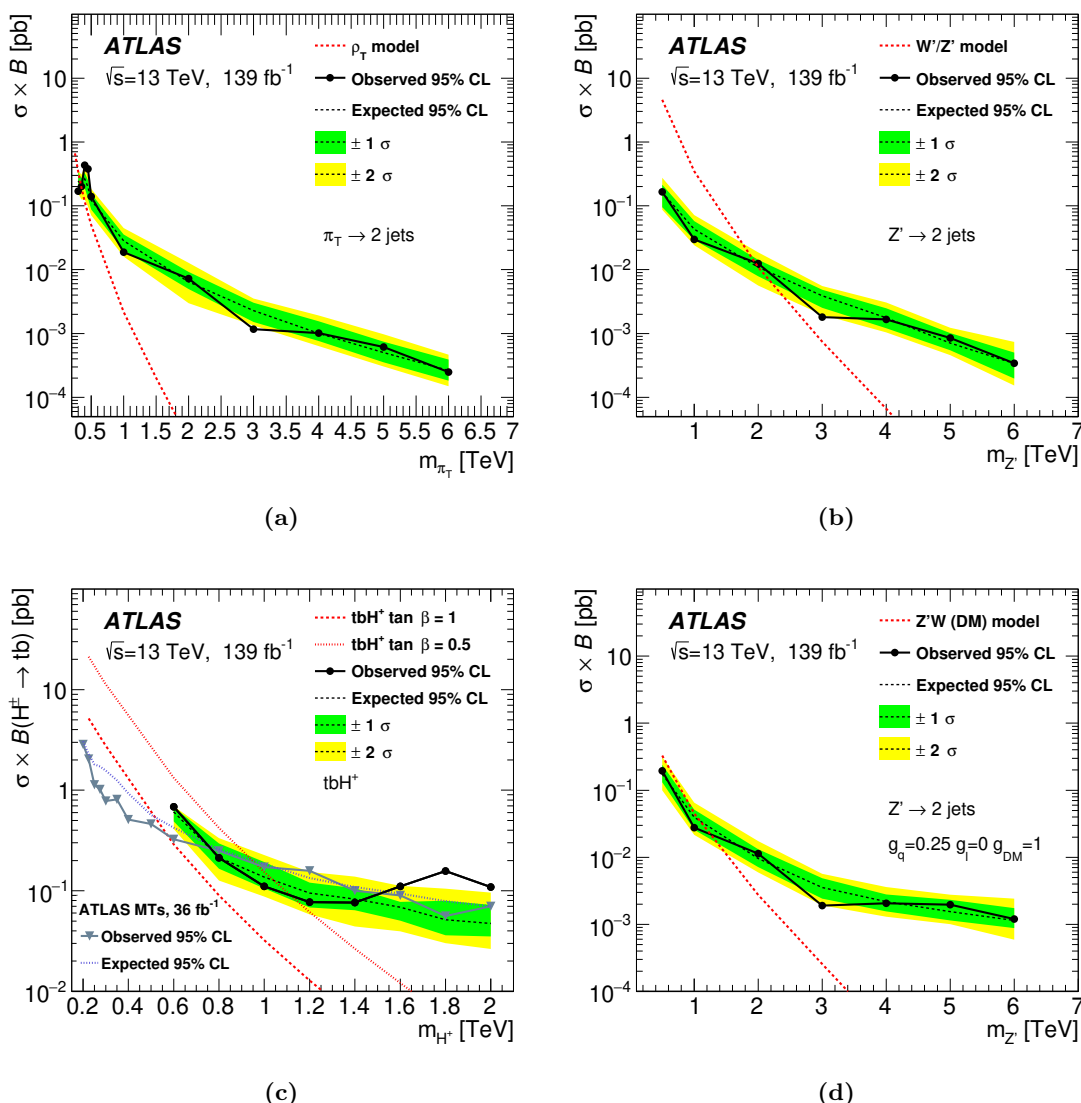


Figure 5. Observed (filled circles) and expected (dotted line with uncertainty bands) 95% credibility-level upper limits on the cross-section (σ) times branching ratio (B) for (a) the technicolor model with production of ρ_T decaying into $\pi_T W^\pm$, (b) $W' \rightarrow Z' W^\pm$ production in the Sequential Standard Model, (c) the tbH^+ model for $\tan\beta = 1$ (thick red dashed line) and $\tan\beta = 0.5$ (thin red dashed line), (d) the simplified dark-matter model. Figure (c) also shows the expected and observed limits (without indicating the 1 and 2 σ bands) from the early Run 2 paper [68] based on the multivariate techniques (MTs) in the signal regions to enhance the separation of signal from background. The presented limits are obtained using two leading jets in events with at least one isolated lepton with $p_T^\ell > 60$ GeV.

The m_{jj} distributions obtained using model-independent selection criteria can also be used to set limits on complex decay topologies. This is illustrated in the context of the H^+ signal model discussed in section 4. The limits obtained without a channel-specific selection of this process are shown in figure 5(c). The data exclude a charged Higgs particle

with a mass below 1.2 TeV, assuming $\tan\beta = 0.5$, the 2HDM type-2 model with the four-flavour scheme and the narrow-width approximation. The H^+ limits are compared with the result [68] based on multivariate techniques and an early subset of the Run 2 data corresponding to 36.1 fb^{-1} of integrated luminosity. On average, the observed and expected limits in the mass range 0.8 TeV–1.4 TeV are about a factor of two better, and the highest excluded H^+ mass is 200 GeV higher for $\tan\beta = 0.5$, than for the earlier Run 2 analysis. The observed differences in the limits between the previous analysis and the current analysis are due to differences in experimental methods adopted in these two studies, as well as due to differences in the integrated luminosities. The excess above the expected limit near an H^+ mass of 1.8 TeV corresponds to the excess near 1.3 TeV for the background-only hypothesis, which is also observed in the Gaussian limits as discussed in section 7. The limits shown in figure 5(c) are correlated since the reconstructed width of the signal is larger than the mass difference between the limit points. To verify the local statistical significance for the H^+ signal model under the signal-plus-background hypothesis, the likelihood fit of the data with the test statistic is performed using the asymptotic approximation [67]. Alternatively, the significance is calculated from the amplitude of the signal component of the signal-plus-background fit, after modelling the shape of the m_{jj} distribution analytically. No systematic uncertainties are included. In all cases the local significance does not exceed 2.4σ , i.e. it is smaller than the significance reported by the background-only hypothesis discussed earlier.

The limits on the simplified dark-matter model, for the leptophobic couplings $g_q = 0.25$, $g_\ell = 0$ and $g_{DM} = 1$, are shown in figure 5(d). These exclude Z' masses for this model below 1.2 TeV, complementing exclusions set previously by the ATLAS inclusive dijet search [16] for $m_{Z'} < 1.5$ TeV. It was checked that changing $g_\ell = 0$ to a small value ($g_\ell = 0.01$) leads to a negligible effect on the presented limits.

8 Conclusion

A search for resonances in dijet invariant-mass distributions is presented, based on the analysis of events in which the jets are accompanied by at least one isolated high- p_T lepton (e or μ). Events are selected from a data sample corresponding to an integrated luminosity of 139 fb^{-1} of proton-proton collisions at $\sqrt{s} = 13$ TeV, recorded by the ATLAS detector during Run 2 of the LHC.

In the dijet invariant-mass range considered, 0.22–6.3 TeV, the most significant deviation from data-derived estimate of the Standard Model background in the combined electron and muon channel is observed around $m_{jj} = 1.3$ TeV. Taking into account both the systematic uncertainties and the look-elsewhere effect, this excess has a p -value of 0.3. The data are thus consistent with the background-only hypothesis.

This analysis has set 95% credibility-level upper limits on the signal cross-section times acceptance times efficiency times branching ratio for new processes that can produce a Gaussian contribution to the dijet invariant-mass distribution in events having at least one isolated lepton with $p_T^\ell > 60$ GeV. Limits are calculated in different scenarios for the width of these Gaussian signals, ranging from that determined by the detector resolution up to

15% of the resonance mass. The limits obtained range from 100 fb to 0.1 fb for resonance masses between 0.25 and 6 TeV.

Model-dependent limits are also set on a variety of BSM models, without the use of additional selection criteria tailored to the specific final states investigated. These results exclude contributions from the $W' \rightarrow WZ'$ process in the Sequential Standard Model for masses of the Z' (decaying into jet pairs) below 2 TeV, assuming the mass difference between the W' and Z' is 250 GeV to maximise the cross-section for this process. For a technicolor model in which the relationship between the ρ_T and π_T masses maximises the cross-section for the final state of interest, technipion masses below 350 GeV are excluded for the range of technipion masses considered.

The model-dependent limits obtained without optimisation for the specific signal models are shown to have the potential to exclude heavy states with complex decays, such as in charged Higgs boson production in association with a top quark, tbH^+ . For this model, the data exclude H^+ masses below 1.2 TeV assuming $\tan\beta = 0.5$. These results complement those from the dedicated H^+ studies [68] that employ a selection optimised for the charged Higgs event topology.

The data also exclude Z' mediator with masses below 1.2 TeV in a simplified Dark Matter model with leptophobic couplings ($g_q = 0.25$, $g_\ell = 0$ and $g_{DM} = 1$), in which the lepton originates from the decay of an associated W boson.

Acknowledgments

We thank CERN for the very successful operation of the LHC, as well as the support staff from our institutions without whom ATLAS could not be operated efficiently.

We acknowledge the support of ANPCyT, Argentina; YerPhI, Armenia; ARC, Australia; BMWFW and FWF, Austria; ANAS, Azerbaijan; SSTC, Belarus; CNPq and FAPESP, Brazil; NSERC, NRC and CFI, Canada; CERN; CONICYT, Chile; CAS, MOST and NSFC, China; COLCIENCIAS, Colombia; MSMT CR, MPO CR and VSC CR, Czech Republic; DNRF and DNSRC, Denmark; IN2P3-CNRS and CEA-DRF/IRFU, France; SRNSFG, Georgia; BMBF, HGF and MPG, Germany; GSRT, Greece; RGC and Hong Kong SAR, China; ISF and Benoziyo Center, Israel; INFN, Italy; MEXT and JSPS, Japan; CNRST, Morocco; NWO, Netherlands; RCN, Norway; MNiSW and NCN, Poland; FCT, Portugal; MNE/IFA, Romania; MES of Russia and NRC KI, Russia Federation; JINR; MESTD, Serbia; MSSR, Slovakia; ARRS and MIZŠ, Slovenia; DST/NRF, South Africa; MINECO, Spain; SRC and Wallenberg Foundation, Sweden; SERI, SNSF and Cantons of Bern and Geneva, Switzerland; MOST, Taiwan; TAEK, Turkey; STFC, U.K.; DOE and NSF, United States of America. In addition, individual groups and members have received support from BCKDF, CANARIE, Compute Canada and CRC, Canada; ERC, ERDF, Horizon 2020, Marie Skłodowska-Curie Actions and COST, European Union; Investissements d'Avenir Labex, Investissements d'Avenir Idex and ANR, France; DFG and AvH Foundation, Germany; Herakleitos, Thales and Aristeia programmes co-financed by EU-ESF and the Greek NSRF, Greece; BSF-NSF and GIF, Israel; CERCA Programme

Generalitat de Catalunya and PROMETEO Programme Generalitat Valenciana, Spain; Göran Gustafssons Stiftelse, Sweden; The Royal Society and Leverhulme Trust, U.K.

The crucial computing support from all WLCG partners is acknowledged gratefully, in particular from CERN, the ATLAS Tier-1 facilities at TRIUMF (Canada), NDGF (Denmark, Norway, Sweden), CC-IN2P3 (France), KIT/GridKA (Germany), INFN-CNAF (Italy), NL-T1 (Netherlands), PIC (Spain), ASGC (Taiwan), RAL (UK) and BNL (USA), the Tier-2 facilities worldwide and large non-WLCG resource providers. Major contributors of computing resources are listed in ref. [69].

We thank Dr. G. Bodwin for the studies of the analytic properties of eq. (5.1).

A Dijet invariant mass in the LE-CR region

Figure 6 illustrates the distribution of events in the LE-CR defined for the data. Also shown is the five-parameter fit function used to describe this region.

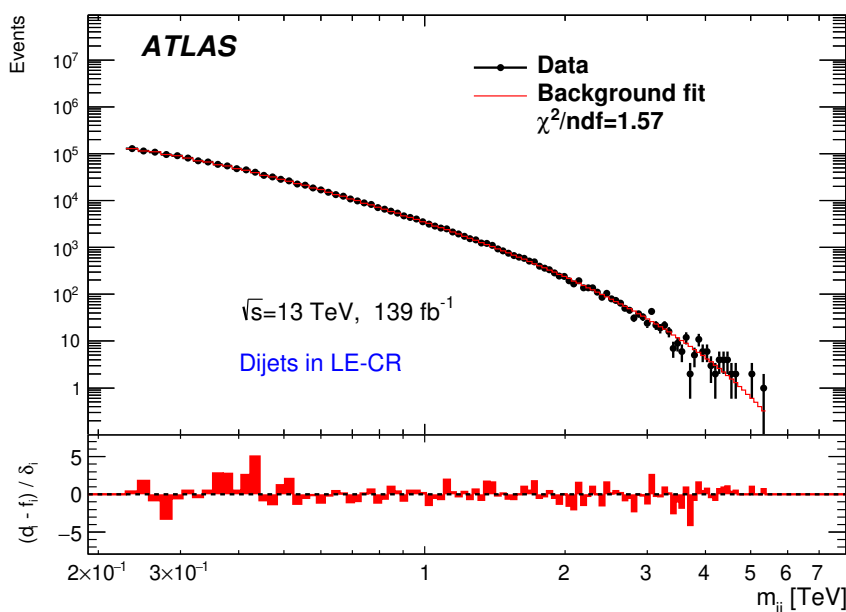


Figure 6. Dijet invariant-mass distribution for the LE-CR region for the 2015–2018 data. Also shown is the result of the fit with the five-parameter background function. The lower panel shows the fit residuals divided by the uncertainty on data points. No systematic uncertainties are included.

B Expected limits for broad signals

Figure 7 shows the comparison of the observed limits with the expected limit, including the corresponding $\pm 1\sigma$ and $\pm 2\sigma$ bands, for the $\sigma_X/m_X = 0.15$ signals. The observed limits are the same as for figure 4.

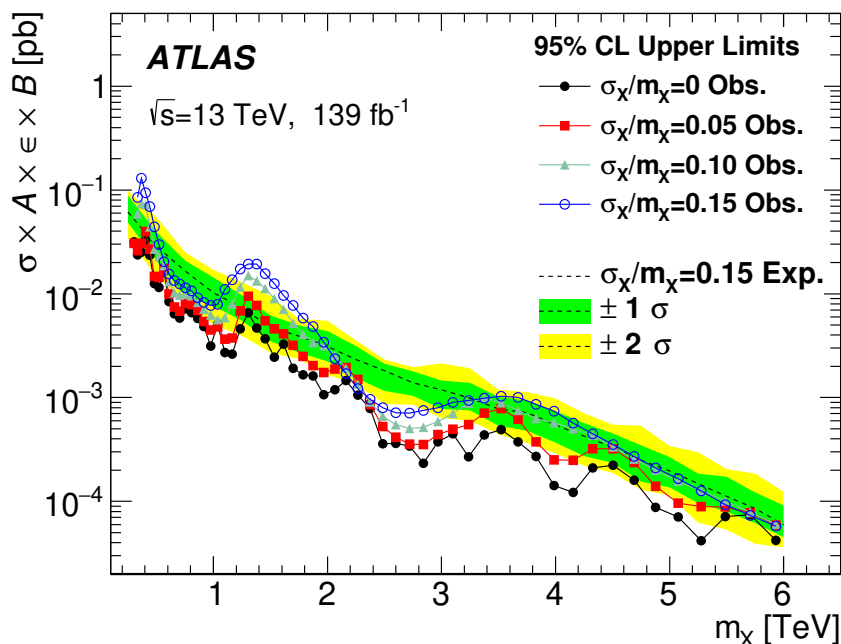


Figure 7. The 95% CL observed limits for a hypothetical particle X resulting in a contribution to the observed m_{jj} distribution with a Gaussian shape and various widths σ_X . The m_{jj} distribution is obtained from the two leading jets in events with at least one isolated lepton with $p_T^\ell > 60$ GeV. The limits, presented for the fine steps in masses that correspond to the bin sizes times two, are calculated assuming widths of the Gaussian signal corresponding to 0%, 5%, 10% and 15% of the signal mass. The limits are set on the cross-section times the acceptance A , the efficiency ϵ and branching ratio B . The expected limit and the corresponding $\pm 1\sigma$ and $\pm 2\sigma$ bands are shown for the $\sigma_X/m_X=0.15$ signals.

Open Access. This article is distributed under the terms of the Creative Commons Attribution License ([CC-BY 4.0](https://creativecommons.org/licenses/by/4.0/)), which permits any use, distribution and reproduction in any medium, provided the original author(s) and source are credited.

References

- [1] ATLAS collaboration, *Search for New Particles in Two-Jet Final States in 7 TeV Proton-Proton Collisions with the ATLAS Detector at the LHC*, *Phys. Rev. Lett.* **105** (2010) 161801 [[arXiv:1008.2461](https://arxiv.org/abs/1008.2461)] [[INSPIRE](https://inspirehep.net/literature/900000)].
- [2] ATLAS collaboration, *Search for New Physics in the Dijet Mass Distribution using 1 fb⁻¹ of pp Collision Data at $\sqrt{s} = 7$ TeV collected by the ATLAS Detector*, *Phys. Lett. B* **708** (2012) 37 [[arXiv:1108.6311](https://arxiv.org/abs/1108.6311)] [[INSPIRE](https://inspirehep.net/literature/1000000)].
- [3] ATLAS collaboration, *Search for New Physics in Dijet Mass and Angular Distributions in pp Collisions at $\sqrt{s} = 7$ TeV Measured with the ATLAS Detector*, *New J. Phys.* **13** (2011) 053044 [[arXiv:1103.3864](https://arxiv.org/abs/1103.3864)] [[INSPIRE](https://inspirehep.net/literature/900000)].

- [4] ATLAS collaboration, *ATLAS search for new phenomena in dijet mass and angular distributions using pp collisions at $\sqrt{s} = 7$ TeV*, *JHEP* **01** (2013) 029 [[arXiv:1210.1718](#)] [[INSPIRE](#)].
- [5] CMS collaboration, *Search for Dijet Resonances in 7 TeV pp Collisions at CMS*, *Phys. Rev. Lett.* **105** (2010) 211801 [[arXiv:1010.0203](#)] [[INSPIRE](#)].
- [6] CMS collaboration, *Search for Resonances in the Dijet Mass Spectrum from 7 TeV pp Collisions at CMS*, *Phys. Lett. B* **704** (2011) 123 [[arXiv:1107.4771](#)] [[INSPIRE](#)].
- [7] CMS collaboration, *Search for Narrow Resonances and Quantum Black Holes in Inclusive and b-Tagged Dijet Mass Spectra from pp Collisions at $\sqrt{s} = 7$ TeV*, *JHEP* **01** (2013) 013 [[arXiv:1210.2387](#)] [[INSPIRE](#)].
- [8] ATLAS collaboration, *Search for new phenomena in the dijet mass distribution using p – p collision data at $\sqrt{s} = 8$ TeV with the ATLAS detector*, *Phys. Rev. D* **91** (2015) 052007 [[arXiv:1407.1376](#)] [[INSPIRE](#)].
- [9] CMS collaboration, *Search for narrow resonances in the b-tagged dijet mass spectrum in proton-proton collisions at $\sqrt{s} = 8$ TeV*, *Phys. Rev. Lett.* **120** (2018) 201801 [[arXiv:1802.06149](#)] [[INSPIRE](#)].
- [10] CMS collaboration, *Search for narrow resonances in dijet final states at $\sqrt{s} = 8$ TeV with the novel CMS technique of data scouting*, *Phys. Rev. Lett.* **117** (2016) 031802 [[arXiv:1604.08907](#)] [[INSPIRE](#)].
- [11] ATLAS collaboration, *Search for new phenomena in dijet mass and angular distributions from pp collisions at $\sqrt{s} = 13$ TeV with the ATLAS detector*, *Phys. Lett. B* **754** (2016) 302 [[arXiv:1512.01530](#)] [[INSPIRE](#)].
- [12] ATLAS collaboration, *Search for new phenomena in dijet events using 37fb^{-1} of pp collision data collected at $\sqrt{s} = 13$ TeV with the ATLAS detector*, *Phys. Rev. D* **96** (2017) 052004 [[arXiv:1703.09127](#)] [[INSPIRE](#)].
- [13] ATLAS collaboration, *Search for low-mass dijet resonances using trigger-level jets with the ATLAS detector in pp collisions at $\sqrt{s} = 13$ TeV*, *Phys. Rev. Lett.* **121** (2018) 081801 [[arXiv:1804.03496](#)] [[INSPIRE](#)].
- [14] CMS collaboration, *Search for dijet resonances in proton–proton collisions at $\sqrt{s} = 13$ TeV and constraints on dark matter and other models*, *Phys. Lett. B* **769** (2017) 520 [Erratum *ibid.* **772** (2017) 882] [[arXiv:1611.03568](#)] [[INSPIRE](#)].
- [15] CMS collaboration, *Search for narrow and broad dijet resonances in proton-proton collisions at $\sqrt{s} = 13$ TeV and constraints on dark matter mediators and other new particles*, *JHEP* **08** (2018) 130 [[arXiv:1806.00843](#)] [[INSPIRE](#)].
- [16] ATLAS collaboration, *Search for new resonances in mass distributions of jet pairs using 139fb^{-1} of pp collisions at $\sqrt{s} = 13$ TeV with the ATLAS detector*, *JHEP* **03** (2020) 145 [[arXiv:1910.08447](#)] [[INSPIRE](#)].
- [17] CMS collaboration, *Search for high mass dijet resonances with a new background prediction method in proton-proton collisions at $\sqrt{s} = 13$ TeV*, *JHEP* **05** (2020) 033 [[arXiv:1911.03947](#)] [[INSPIRE](#)].
- [18] CMS collaboration, *Search for dijet resonances using events with three jets in proton-proton collisions at $\sqrt{s} = 13$ TeV*, *Phys. Lett. B* **805** (2020) 135448 [[arXiv:1911.03761](#)] [[INSPIRE](#)].

- [19] ATLAS collaboration, *Search for low-mass resonances decaying into two jets and produced in association with a photon using pp collisions at $\sqrt{s} = 13$ TeV with the ATLAS detector*, *Phys. Lett. B* **795** (2019) 56 [[arXiv:1901.10917](#)] [[INSPIRE](#)].
- [20] CMS collaboration, *Search for Low-Mass Quark-Antiquark Resonances Produced in Association with a Photon at $\sqrt{s} = 13$ TeV*, *Phys. Rev. Lett.* **123** (2019) 231803 [[arXiv:1905.10331](#)] [[INSPIRE](#)].
- [21] CMS collaboration, *Search for Low Mass Vector Resonances Decaying to Quark-Antiquark Pairs in Proton-Proton Collisions at $\sqrt{s} = 13$ TeV*, *Phys. Rev. Lett.* **119** (2017) 111802 [[arXiv:1705.10532](#)] [[INSPIRE](#)].
- [22] CMS collaboration, *Search for low mass vector resonances decaying into quark-antiquark pairs in proton-proton collisions at $\sqrt{s} = 13$ TeV*, *JHEP* **01** (2018) 097 [[arXiv:1710.00159](#)] [[INSPIRE](#)].
- [23] CMS collaboration, *Search for low-mass resonances decaying into bottom quark-antiquark pairs in proton-proton collisions at $\sqrt{s} = 13$ TeV*, *Phys. Rev. D* **99** (2019) 012005 [[arXiv:1810.11822](#)] [[INSPIRE](#)].
- [24] CMS collaboration, *Search for low mass vector resonances decaying into quark-antiquark pairs in proton-proton collisions at $\sqrt{s} = 13$ TeV*, *Phys. Rev. D* **100** (2019) 112007 [[arXiv:1909.04114](#)] [[INSPIRE](#)].
- [25] E. Eichten, K.D. Lane and J. Womersley, *Finding low scale technicolor at hadron colliders*, *Phys. Lett. B* **405** (1997) 305 [[hep-ph/9704455](#)] [[INSPIRE](#)].
- [26] G. Altarelli, B. Mele and M. Ruiz-Altaba, *Searching for New Heavy Vector Bosons in $p\bar{p}$ Colliders*, *Z. Phys. C* **45** (1989) 109 [Erratum *ibid.* **C 47** (1990) 676] [[INSPIRE](#)].
- [27] A.G. Akeroyd et al., *Prospects for charged Higgs searches at the LHC*, *Eur. Phys. J. C* **77** (2017) 276 [[arXiv:1607.01320](#)] [[INSPIRE](#)].
- [28] AUTHOR NEEDED, *Dark Matter Benchmark Models for Early LHC Run-2 Searches: Report of the ATLAS/CMS Dark Matter Forum*, [FERMILAB-PUB-15-282](#) (2015).
- [29] ATLAS collaboration, *The ATLAS Experiment at the CERN Large Hadron Collider*, **2008 JINST** **3** S08003 [[INSPIRE](#)].
- [30] ATLAS collaboration, *ATLAS Insertable B-Layer Technical Design Report*, [ATLAS-TDR-19](#) (2010).
- [31] ATLAS IBL collaboration, *Production and Integration of the ATLAS Insertable B-Layer*, **2018 JINST** **13** T05008 [[arXiv:1803.00844](#)] [[INSPIRE](#)].
- [32] ATLAS collaboration, *Performance of the ATLAS Trigger System in 2015*, *Eur. Phys. J. C* **77** (2017) 317 [[arXiv:1611.09661](#)] [[INSPIRE](#)].
- [33] ATLAS collaboration, *Luminosity determination in pp collisions at $\sqrt{s} = 8$ TeV using the ATLAS detector at the LHC*, *Eur. Phys. J. C* **76** (2016) 653 [[arXiv:1608.03953](#)] [[INSPIRE](#)].
- [34] G. Avoni et al., *The new LUCID-2 detector for luminosity measurement and monitoring in ATLAS*, **2018 JINST** **13** P07017 [[INSPIRE](#)].
- [35] ATLAS collaboration, *Muon reconstruction performance of the ATLAS detector in proton-proton collision data at $\sqrt{s} = 13$ TeV*, *Eur. Phys. J. C* **76** (2016) 292 [[arXiv:1603.05598](#)] [[INSPIRE](#)].

- [36] ATLAS collaboration, *Electron and photon performance measurements with the ATLAS detector using the 2015–2017 LHC proton-proton collision data*, *2019 JINST* **14** P12006 [[arXiv:1908.00005](#)] [[INSPIRE](#)].
- [37] M. Cacciari, G.P. Salam and G. Soyez, *The anti- k_t jet clustering algorithm*, *JHEP* **04** (2008) 063 [[arXiv:0802.1189](#)] [[INSPIRE](#)].
- [38] M. Cacciari, G.P. Salam and G. Soyez, *FastJet User Manual*, *Eur. Phys. J. C* **72** (2012) 1896 [[arXiv:1111.6097](#)] [[INSPIRE](#)].
- [39] ATLAS collaboration, *Topological cell clustering in the ATLAS calorimeters and its performance in LHC Run 1*, *Eur. Phys. J. C* **77** (2017) 490 [[arXiv:1603.02934](#)] [[INSPIRE](#)].
- [40] ATLAS collaboration, *Performance of pile-up mitigation techniques for jets in pp collisions at $\sqrt{s} = 8$ TeV using the ATLAS detector*, *Eur. Phys. J. C* **76** (2016) 581 [[arXiv:1510.03823](#)] [[INSPIRE](#)].
- [41] ATLAS collaboration, *Jet energy scale measurements and their systematic uncertainties in proton-proton collisions at $\sqrt{s} = 13$ TeV with the ATLAS detector*, *Phys. Rev. D* **96** (2017) 072002 [[arXiv:1703.09665](#)] [[INSPIRE](#)].
- [42] ATLAS collaboration, *Tagging and suppression of pileup jets with the ATLAS detector*, *ATLAS-CONF-2014-018* (2014).
- [43] T. Sjöstrand, S. Mrenna and P.Z. Skands, *A Brief Introduction to PYTHIA 8.1*, *Comput. Phys. Commun.* **178** (2008) 852 [[arXiv:0710.3820](#)] [[INSPIRE](#)].
- [44] R.D. Ball et al., *Parton distributions with LHC data*, *Nucl. Phys. B* **867** (2013) 244 [[arXiv:1207.1303](#)] [[INSPIRE](#)].
- [45] ATLAS collaboration, *ATLAS PYTHIA 8 tunes to 7 TeV datas*, *ATL-PHYS-PUB-2014-021* (2014).
- [46] P. Nason, *A New method for combining NLO QCD with shower Monte Carlo algorithms*, *JHEP* **11** (2004) 040 [[hep-ph/0409146](#)] [[INSPIRE](#)].
- [47] S. Frixione, P. Nason and C. Oleari, *Matching NLO QCD computations with Parton Shower simulations: the POWHEG method*, *JHEP* **11** (2007) 070 [[arXiv:0709.2092](#)] [[INSPIRE](#)].
- [48] S. Alioli, P. Nason, C. Oleari and E. Re, *A general framework for implementing NLO calculations in shower Monte Carlo programs: the POWHEG BOX*, *JHEP* **06** (2010) 043 [[arXiv:1002.2581](#)] [[INSPIRE](#)].
- [49] S. Frixione, P. Nason and G. Ridolfi, *A Positive-weight next-to-leading-order Monte Carlo for heavy flavour hadroproduction*, *JHEP* **09** (2007) 126 [[arXiv:0707.3088](#)] [[INSPIRE](#)].
- [50] H.-L. Lai et al., *New parton distributions for collider physics*, *Phys. Rev. D* **82** (2010) 074024 [[arXiv:1007.2241](#)] [[INSPIRE](#)].
- [51] ATLAS collaboration, *Measurement of the Z/γ^* boson transverse momentum distribution in pp collisions at $\sqrt{s} = 7$ TeV with the ATLAS detector*, *JHEP* **09** (2014) 145 [[arXiv:1406.3660](#)] [[INSPIRE](#)].
- [52] T. Sjöstrand, S. Mrenna and P.Z. Skands, *PYTHIA 6.4 Physics and Manual*, *JHEP* **05** (2006) 026 [[hep-ph/0603175](#)] [[INSPIRE](#)].
- [53] K. Lane and L. Pritchett, *The light composite Higgs boson in strong extended technicolor*, *JHEP* **06** (2017) 140 [[arXiv:1604.07085](#)] [[INSPIRE](#)].

- [54] J. Alwall et al., *The automated computation of tree-level and next-to-leading order differential cross sections and their matching to parton shower simulations*, *JHEP* **07** (2014) 079 [[arXiv:1405.0301](#)] [[INSPIRE](#)].
- [55] C. Degrande, M. Ubiali, M. Wiesemann and M. Zaro, *Heavy charged Higgs boson production at the LHC*, *JHEP* **10** (2015) 145 [[arXiv:1507.02549](#)] [[INSPIRE](#)].
- [56] M. Carena, S. Heinemeyer, O. Stål, C.E.M. Wagner and G. Weiglein, *MSSM Higgs Boson Searches at the LHC: Benchmark Scenarios after the Discovery of a Higgs-like Particle*, *Eur. Phys. J. C* **73** (2013) 2552 [[arXiv:1302.7033](#)] [[INSPIRE](#)].
- [57] C.F. Uhlemann and N. Kauer, *Narrow-width approximation accuracy*, *Nucl. Phys. B* **814** (2009) 195 [[arXiv:0807.4112](#)] [[INSPIRE](#)].
- [58] ATLAS collaboration, *The ATLAS Simulation Infrastructure*, *Eur. Phys. J. C* **70** (2010) 823 [[arXiv:1005.4568](#)] [[INSPIRE](#)].
- [59] GEANT4 collaboration, *GEANT4: A Simulation toolkit*, *Nucl. Instrum. Meth. A* **506** (2003) 250 [[INSPIRE](#)].
- [60] ATLAS collaboration, *The ATLAS Simulation Infrastructure*, *Eur. Phys. J. C* **70** (2010) 823 [[arXiv:1005.4568](#)] [[INSPIRE](#)].
- [61] ATLAS collaboration, *The PYTHIA 8 A3 tune description of ATLAS minimum bias and inelastic measurements incorporating the Donnachie-Landshoff diffractive model*, *ATL-PHYS-PUB-2016-017* (2016).
- [62] S.S. Wilks, *The Large-Sample Distribution of the Likelihood Ratio for Testing Composite Hypotheses*, *Annals Math. Statist.* **9** (1938) 60 [[INSPIRE](#)].
- [63] G. Choudalakis, *On hypothesis testing, trials factor, hypertexts and the BumpHunter*, in *Proceedings, PHYSTAT 2011 Workshop on Statistical Issues Related to Discovery Claims in Search Experiments and Unfolding*, CERN, Geneva, Switzerland 17-20 January 2011, 2011, [[arXiv:1101.0390](#)] [[INSPIRE](#)].
- [64] E. Gross and O. Vitells, *Trial factors for the look elsewhere effect in high energy physics*, *Eur. Phys. J. C* **70** (2010) 525 [[arXiv:1005.1891](#)] [[INSPIRE](#)].
- [65] A. Caldwell, D. Kollar and K. Kroninger, *BAT: The Bayesian Analysis Toolkit*, *Comput. Phys. Commun.* **180** (2009) 2197 [[arXiv:0808.2552](#)] [[INSPIRE](#)].
- [66] *Plotting the differences between data and expectation*, *Eur. Phys. J. Plus* **127** (2012) 25 [[arXiv:1111.2062](#)].
- [67] G. Cowan, K. Cranmer, E. Gross and O. Vitells, *Asymptotic formulae for likelihood-based tests of new physics*, *Eur. Phys. J. C* **71** (2011) 1554 [*Erratum ibid.* **C 73** (2013) 2501] [[arXiv:1007.1727](#)] [[INSPIRE](#)].
- [68] ATLAS collaboration, *Search for charged Higgs bosons decaying into top and bottom quarks at $\sqrt{s} = 13$ TeV with the ATLAS detector*, *JHEP* **11** (2018) 085 [[arXiv:1808.03599](#)] [[INSPIRE](#)].
- [69] ATLAS collaboration, *ATLAS Computing Acknowledgements*, *ATL-SOFT-PUB-2020-001* (2020).

The ATLAS collaboration

G. Aad¹⁰², B. Abbott¹²⁹, D.C. Abbott¹⁰³, A. Abed Abud³⁶, K. Abeling⁵³, D.K. Abhayasinghe⁹⁴, S.H. Abidi¹⁶⁷, O.S. AbouZeid⁴⁰, N.L. Abraham¹⁵⁶, H. Abramowicz¹⁶¹, H. Abreu¹⁶⁰, Y. Abulaiti⁶, B.S. Acharya^{67a,67b,n}, B. Achkar⁵³, S. Adachi¹⁶³, L. Adam¹⁰⁰, C. Adam Bourdarios⁵, L. Adamczyk^{84a}, L. Adamek¹⁶⁷, J. Adelman¹²¹, M. Adersberger¹¹⁴, A. Adiguzel^{12c}, S. Adorni⁵⁴, T. Adye¹⁴⁴, A.A. Affolder¹⁴⁶, Y. Afik¹⁶⁰, C. Agapopoulou⁶⁵, M.N. Agaras³⁸, A. Aggarwal¹¹⁹, C. Agheorghiesei^{27c}, J.A. Aguilar-Saavedra^{140f,140a,af}, F. Ahmadov⁸⁰, W.S. Ahmed¹⁰⁴, X. Ai¹⁸, G. Aielli^{74a,74b}, S. Akatsuka⁸⁶, T.P.A. Åkesson⁹⁷, E. Akilli⁵⁴, A.V. Akimov¹¹¹, K. Al Khoury⁶⁵, G.L. Alberghi^{23b,23a}, J. Albert¹⁷⁶, M.J. Alconada Verzini¹⁶¹, S. Alderweireldt³⁶, M. Aleksa³⁶, I.N. Aleksandrov⁸⁰, C. Alexa^{27b}, T. Alexopoulos¹⁰, A. Alfonsi¹²⁰, F. Alfonsi^{23b,23a}, M. Alhroob¹²⁹, B. Ali¹⁴², M. Aliev¹⁶⁶, G. Alimonti^{69a}, C. Allaire⁶⁵, B.M.M. Allbrooke¹⁵⁶, B.W. Allen¹³², P.P. Allport²¹, A. Aloisio^{70a,70b}, F. Alonso⁸⁹, C. Alpigiani¹⁴⁸, A.A. Alshehri⁵⁷, E. Alunno Camelia^{74a,74b}, M. Alvarez Estevez⁹⁹, M.G. Alviggi^{70a,70b}, Y. Amaral Coutinho^{81b}, A. Ambler¹⁰⁴, L. Ambroz¹³⁵, C. Amelung²⁶, D. Amidei¹⁰⁶, S.P. Amor Dos Santos^{140a}, S. Amoroso⁴⁶, C.S. Amrouche⁵⁴, F. An⁷⁹, C. Anastopoulos¹⁴⁹, N. Andari¹⁴⁵, T. Andeen¹¹, C.F. Anders^{61b}, J.K. Anders²⁰, A. Andreazza^{69a,69b}, V. Andrei^{61a}, C.R. Anelli¹⁷⁶, S. Angelidakis³⁸, A. Angerami³⁹, A.V. Anisenkov^{122b,122a}, A. Annovi^{72a}, C. Antel⁵⁴, M.T. Anthony¹⁴⁹, E. Antipov¹³⁰, M. Antonelli⁵¹, D.J.A. Antrim¹⁷¹, F. Anulli^{73a}, M. Aoki⁸², J.A. Aparisi Pozo¹⁷⁴, L. Aperio Bella^{15a}, J.P. Araque^{140a}, V. Araujo Ferraz^{81b}, R. Araujo Pereira^{81b}, C. Arcangeletti⁵¹, A.T.H. Arce⁴⁹, F.A. Arduh⁸⁹, J-F. Arguin¹¹⁰, S. Argyropoulos⁵², J.-H. Arling⁴⁶, A.J. Armbruster³⁶, A. Armstrong¹⁷¹, O. Arnaez¹⁶⁷, H. Arnold¹²⁰, Z.P. Arrubarrena Tame¹¹⁴, G. Artoni¹³⁵, S. Artz¹⁰⁰, S. Asai¹⁶³, T. Asawatonvanich¹⁶⁵, N. Asbah⁵⁹, E.M. Asimakopoulou¹⁷², L. Asquith¹⁵⁶, J. Assahsah^{35d}, K. Assamagan²⁹, R. Astalos^{28a}, R.J. Atkin^{33a}, M. Atkinson¹⁷³, N.B. Atlay¹⁹, H. Atmani⁶⁵, K. Augsten¹⁴², G. Avolio³⁶, M.K. Ayoub^{15a}, G. Azuelos^{110,ao}, H. Bachacou¹⁴⁵, K. Bachas^{68a,68b}, M. Backes¹³⁵, F. Backman^{45a,45b}, P. Bagnaia^{73a,73b}, M. Bahmani⁸⁵, H. Bahrasemani¹⁵², A.J. Bailey¹⁷⁴, V.R. Bailey¹⁷³, J.T. Baines¹⁴⁴, C. Bakalis¹⁰, O.K. Baker¹⁸³, P.J. Bakker¹²⁰, D. Bakshi Gupta⁸, S. Balaji¹⁵⁷, E.M. Baldin^{122b,122a}, P. Balek¹⁸⁰, F. Balli¹⁴⁵, W.K. Balunas¹³⁵, J. Balz¹⁰⁰, E. Banas⁸⁵, A. Bandyopadhyay²⁴, Sw. Banerjee^{181,i}, A.A.E. Bannoura¹⁸², L. Barak¹⁶¹, W.M. Barbe³⁸, E.L. Barberio¹⁰⁵, D. Barberis^{55b,55a}, M. Barbero¹⁰², G. Barbour⁹⁵, T. Barillari¹¹⁵, M.-S. Barisits³⁶, J. Barkeloo¹³², T. Barklow¹⁵³, R. Barnea¹⁶⁰, B.M. Barnett¹⁴⁴, R.M. Barnett¹⁸, Z. Barnovska-Blenessy^{60a}, A. Baroncelli^{60a}, G. Barone²⁹, A.J. Barr¹³⁵, L. Barranco Navarro^{45a,45b}, F. Barreiro⁹⁹, J. Barreiro Guimarães da Costa^{15a}, S. Barsov¹³⁸, R. Bartoldus¹⁵³, G. Bartolini¹⁰², A.E. Barton⁹⁰, P. Bartos^{28a}, A. Basalae⁴⁶, A. Basan¹⁰⁰, A. Bassalat^{65,ak}, M.J. Basso¹⁶⁷, R.L. Bates⁵⁷, S. Batlamous^{35e}, J.R. Batley³², B. Batool¹⁵¹, M. Battaglia¹⁴⁶, M. Bauge^{73a,73b}, F. Bauer¹⁴⁵, K.T. Bauer¹⁷¹, H.S. Bawa³¹, J.B. Beacham⁴⁹, T. Beau¹³⁶, P.H. Beauchemin¹⁷⁰, F. Becherer⁵², P. Bechtel²⁴, H.C. Beck⁵³, H.P. Beck^{20,r}, K. Becker¹⁷⁸, C. Becot⁴⁶, A. Beddall^{12d}, A.J. Beddall^{12a}, V.A. Bednyakov⁸⁰, M. Bedognetti¹²⁰, C.P. Bee¹⁵⁵, T.A. Beermann¹⁸², M. Begalli^{81b}, M. Begel²⁹, A. Behera¹⁵⁵, J.K. Behr⁴⁶, F. Beisiegel²⁴, A.S. Bell⁹⁵, G. Bella¹⁶¹, L. Bellagamba^{23b}, A. Bellerive³⁴, P. Bellos⁹, K. Beloborodov^{122b,122a}, K. Belotskiy¹¹², N.L. Belyaev¹¹², D. Benchekroun^{35a}, N. Benekos¹⁰, Y. Benhammou¹⁶¹, D.P. Benjamin⁶, M. Benoit⁵⁴, J.R. Bensinger²⁶, S. Bentvelsen¹²⁰, L. Beresford¹³⁵, M. Beretta⁵¹, D. Berge¹⁹, E. Bergeaas Kuutmann¹⁷², N. Berger⁵, B. Bergmann¹⁴², L.J. Bergsten²⁶, J. Beringer¹⁸, S. Berlendis⁷, G. Bernardi¹³⁶, C. Bernius¹⁵³, F.U. Bernlochner²⁴, T. Berry⁹⁴, P. Berta¹⁰⁰, C. Bertella^{15a}, I.A. Bertram⁹⁰, O. Bessidskaia Bylund¹⁸², N. Besson¹⁴⁵, A. Bethani¹⁰¹, S. Bethke¹¹⁵, A. Betti⁴², A.J. Bevan⁹³, J. Beyer¹¹⁵, D.S. Bhattacharya¹⁷⁷, P. Bhattarai²⁶, R. Bi¹³⁹, R.M. Bianchi¹³⁹, O. Biebel¹¹⁴,

D. Biedermann¹⁹, R. Bielski³⁶, K. Bierwagen¹⁰⁰, N.V. Biesuz^{72a,72b}, M. Biglietti^{75a},
 T.R.V. Billoud¹¹⁰, M. Bindi⁵³, A. Bingul^{12d}, C. Bini^{73a,73b}, S. Biondi^{23b,23a}, M. Birman¹⁸⁰,
 T. Bisanz⁵³, J.P. Biswal³, D. Biswas^{181,i}, A. Bitadze¹⁰¹, C. Bittrich⁴⁸, K. Bjørke¹³⁴,
 T. Blazek^{28a}, I. Bloch⁴⁶, C. Blocker²⁶, A. Blue⁵⁷, U. Blumenschein⁹³, G.J. Bobbink¹²⁰,
 V.S. Bobrovnikov^{122b,122a}, S.S. Bocchetta⁹⁷, A. Bocci⁴⁹, D. Boerner⁴⁶, D. Bogavac¹⁴,
 A.G. Bogdanchikov^{122b,122a}, C. Bohm^{45a}, V. Boisvert⁹⁴, P. Bokan^{53,172}, T. Bold^{84a},
 A.E. Bolz^{61b}, M. Bomben¹³⁶, M. Bona⁹³, J.S. Bonilla¹³², M. Boonekamp¹⁴⁵, C.D. Booth⁹⁴,
 H.M. Borecka-Bielska⁹¹, L.S. Borgna⁹⁵, A. Borisov¹²³, G. Borissov⁹⁰, J. Bortfeldt³⁶,
 D. Bortoletto¹³⁵, D. Boscherini^{23b}, M. Bosman¹⁴, J.D. Bossio Sola¹⁰⁴, K. Bouaouda^{35a},
 J. Boudreau¹³⁹, E.V. Bouhova-Thacker⁹⁰, D. Boumediene³⁸, S.K. Boutle⁵⁷, A. Boveia¹²⁷,
 J. Boyd³⁶, D. Boye^{33c,al}, I.R. Boyko⁸⁰, A.J. Bozson⁹⁴, J. Bracinik²¹, N. Brahimi¹⁰²,
 G. Brandt¹⁸², O. Brandt³², F. Braren⁴⁶, B. Brau¹⁰³, J.E. Brau¹³², W.D. Breaden Madden⁵⁷,
 K. Brendlinger⁴⁶, L. Brenner⁴⁶, R. Brenner¹⁷², S. Bressler¹⁸⁰, B. Brickwedde¹⁰⁰, D.L. Briglin²¹,
 D. Britton⁵⁷, D. Britzger¹¹⁵, I. Brock²⁴, R. Brock¹⁰⁷, G. Brooijmans³⁹, W.K. Brooks^{147d},
 E. Brost²⁹, J.H. Broughton²¹, P.A. Bruckman de Renstrom⁸⁵, D. Bruncko^{28b}, A. Bruni^{23b},
 G. Bruni^{23b}, L.S. Bruni¹²⁰, S. Bruno^{74a,74b}, M. Bruschi^{23b}, N. Brusino^{73a,73b}, P. Bryant³⁷,
 L. Bryngemark⁹⁷, T. Buanes¹⁷, Q. Buat³⁶, P. Buchholz¹⁵¹, A.G. Buckley⁵⁷, I.A. Budagov⁸⁰,
 M.K. Bugge¹³⁴, F. Bühner⁵², O. Bulekov¹¹², T.J. Burch¹²¹, S. Burdin⁹¹, C.D. Burgard¹²⁰,
 A.M. Burger¹³⁰, B. Burghgrave⁸, J.T.P. Burr⁴⁶, C.D. Burton¹¹, J.C. Burzynski¹⁰³, V. Büscher¹⁰⁰,
 E. Buschmann⁵³, P.J. Bussey⁵⁷, J.M. Butler²⁵, C.M. Buttar⁵⁷, J.M. Butterworth⁹⁵, P. Butti³⁶,
 W. Buttinger³⁶, C.J. Buxo Vazquez¹⁰⁷, A. Buzatu¹⁵⁸, A.R. Buzykaev^{122b,122a}, G. Cabras^{23b,23a},
 S. Cabrera Urbán¹⁷⁴, D. Caforio⁵⁶, H. Cai¹⁷³, V.M.M. Cairo¹⁵³, O. Cakir^{4a}, N. Calace³⁶,
 P. Calafiura¹⁸, A. Calandri¹⁰², G. Calderini¹³⁶, P. Calfayan⁶⁶, G. Callea⁵⁷, L.P. Caloba^{81b},
 A. Caltabiano^{74a,74b}, S. Calvente Lopez⁹⁹, D. Calvet³⁸, S. Calvet³⁸, T.P. Calvet¹⁵⁵,
 M. Calvetti^{72a,72b}, R. Camacho Toro¹³⁶, S. Camarda³⁶, D. Camarero Munoz⁹⁹, P. Camarri^{74a,74b},
 D. Cameron¹³⁴, C. Camincher³⁶, S. Campana³⁶, M. Campanelli⁹⁵, A. Camplani⁴⁰,
 A. Campoverde¹⁵¹, V. Canale^{70a,70b}, A. Canesse¹⁰⁴, M. Cano Bret^{60c}, J. Cantero¹³⁰, T. Cao¹⁶¹,
 Y. Cao¹⁷³, M.D.M. Capeans Garrido³⁶, M. Capua^{41b,41a}, R. Cardarelli^{74a}, F. Cardillo¹⁴⁹,
 G. Carducci^{41b,41a}, I. Carli¹⁴³, T. Carli³⁶, G. Carlino^{70a}, B.T. Carlson¹³⁹, L. Carminati^{69a,69b},
 R.M.D. Carney¹⁵³, S. Caron¹¹⁹, E. Carquin^{147d}, S. Carrá⁴⁶, J.W.S. Carter¹⁶⁷, M.P. Casado^{14,e},
 A.F. Casha¹⁶⁷, R. Castelijm¹²⁰, F.L. Castillo¹⁷⁴, L. Castillo Garcia¹⁴, V. Castillo Gimenez¹⁷⁴,
 N.F. Castro^{140a,140e}, A. Catinaccio³⁶, J.R. Catmore¹³⁴, A. Cattai³⁶, V. Cavaliere²⁹,
 E. Cavallaro¹⁴, M. Cavalli-Sforza¹⁴, V. Cavasinni^{72a,72b}, E. Celebi^{12b}, L. Cerda Alberich¹⁷⁴,
 K. Cerny¹³¹, A.S. Cerqueira^{81a}, A. Cerri¹⁵⁶, L. Cerrito^{74a,74b}, F. Cerutti¹⁸, A. Cervelli^{23b,23a},
 S.A. Cetin^{12b}, Z. Chadi^{35a}, D. Chakraborty¹²¹, J. Chan¹⁸¹, W.S. Chan¹²⁰, W.Y. Chan⁹¹,
 J.D. Chapman³², B. Chargeishvili^{159b}, D.G. Charlton²¹, T.P. Charman⁹³, C.C. Chau³⁴,
 S. Che¹²⁷, S. Chekanov⁶, S.V. Chekulaev^{168a}, G.A. Chelkov⁸⁰, B. Chen⁷⁹, C. Chen^{60a},
 C.H. Chen⁷⁹, H. Chen²⁹, J. Chen^{60a}, J. Chen³⁹, J. Chen²⁶, S. Chen¹³⁷, S.J. Chen^{15c}, X. Chen^{15b},
 Y-H. Chen⁴⁶, H.C. Cheng^{63a}, H.J. Cheng^{15a}, A. Cheplakov⁸⁰, E. Cheremushkina¹²³,
 R. Cherkaoui El Moursli^{35e}, E. Cheu⁷, K. Cheung⁶⁴, T.J.A. Chevaléras¹⁴⁵, L. Chevalier¹⁴⁵,
 V. Chiarella⁵¹, G. Chiarelli^{72a}, G. Chiodini^{68a}, A.S. Chisholm²¹, A. Chitan^{27b}, I. Chiu¹⁶³,
 Y.H. Chiu¹⁷⁶, M.V. Chizhov⁸⁰, K. Choi¹¹, A.R. Chomont^{73a,73b}, S. Chouridou¹⁶², Y.S. Chow¹²⁰,
 M.C. Chu^{63a}, X. Chu^{15a,15d}, J. Chudoba¹⁴¹, J.J. Chwastowski⁸⁵, L. Chytka¹³¹, D. Cieri¹¹⁵,
 K.M. Ciesla⁸⁵, D. Cinca⁴⁷, V. Cindro⁹², I.A. Cioară^{27b}, A. Ciocio¹⁸, F. Ciotto^{70a,70b},
 Z.H. Citron^{180j}, M. Citterio^{69a}, D.A. Ciubotaru^{27b}, B.M. Ciungu¹⁶⁷, A. Clark⁵⁴, M.R. Clark³⁹,
 P.J. Clark⁵⁰, C. Clement^{45a,45b}, Y. Coadou¹⁰², M. Cobal^{67a,67c}, A. Coccaro^{55b}, J. Cochran⁷⁹,
 R. Coelho Lopes De Sa¹⁰³, H. Cohen¹⁶¹, A.E.C. Coimbra³⁶, B. Cole³⁹, A.P. Colijn¹²⁰,
 J. Collot⁵⁸, P. Conde Muiño^{140a,140h}, S.H. Connell^{33c}, I.A. Connolly⁵⁷, S. Constantinescu^{27b},

F. Conventi^{70a,ap}, A.M. Cooper-Sarkar¹³⁵, F. Cormier¹⁷⁵, K.J.R. Cormier¹⁶⁷, L.D. Corpe⁹⁵, M. Corradi^{73a,73b}, E.E. Corrigan⁹⁷, F. Corriveau^{104,ad}, A. Cortes-Gonzalez³⁶, M.J. Costa¹⁷⁴, F. Costanza⁵, D. Costanzo¹⁴⁹, G. Cowan⁹⁴, J.W. Cowley³², J. Crane¹⁰¹, K. Cranmer¹²⁵, S.J. Crawley⁵⁷, R.A. Creager¹³⁷, S. Crépé-Renaudin⁵⁸, F. Crescioli¹³⁶, M. Cristinziani²⁴, V. Croft¹⁷⁰, G. Crosetti^{41b,41a}, A. Cueto⁵, T. Cuhadar Donszelmann¹⁴⁹, A.R. Cukierman¹⁵³, W.R. Cunningham⁵⁷, S. Czekierda⁸⁵, P. Czodrowski³⁶, M.J. Da Cunha Sargedas De Sousa^{60b}, J.V. Da Fonseca Pinto^{81b}, C. Da Via¹⁰¹, W. Dabrowski^{84a}, F. Dachs³⁶, T. Dado^{28a}, S. Dahbi^{33e}, T. Dai¹⁰⁶, C. Dallapiccola¹⁰³, M. Dam⁴⁰, G. D'amen²⁹, V. D'Amico^{75a,75b}, J. Damp¹⁰⁰, J.R. Dandoy¹³⁷, M.F. Daneri³⁰, N.S. Dann¹⁰¹, M. Danninger¹⁵², V. Dao³⁶, G. Darbo^{55b}, O. Dartsis⁵, A. Dattagupta¹³², T. Daubney⁴⁶, S. D'Auria^{69a,69b}, C. David^{168b}, T. Davidek¹⁴³, D.R. Davis⁴⁹, I. Dawson¹⁴⁹, K. De⁸, R. De Asmundis^{70a}, M. De Beurs¹²⁰, S. De Castro^{23b,23a}, S. De Cecco^{73a,73b}, N. De Groot¹¹⁹, P. de Jong¹²⁰, H. De la Torre¹⁰⁷, A. De Maria^{15c}, D. De Pedis^{73a}, A. De Salvo^{73a}, U. De Sanctis^{74a,74b}, M. De Santis^{74a,74b}, A. De Santo¹⁵⁶, K. De Vasconcelos Corga¹⁰², J.B. De Vivie De Regie⁶⁵, C. Debenedetti¹⁴⁶, D.V. Dedovich⁸⁰, A.M. Deiana⁴², J. Del Peso⁹⁹, Y. Delabat Diaz⁴⁶, D. Delgove⁶⁵, F. Deliot^{145,q}, C.M. Delitzsch⁷, M. Della Pietra^{70a,70b}, D. Della Volpe⁵⁴, A. Dell'Acqua³⁶, L. Dell'Asta^{74a,74b}, M. Delmastro⁵, C. Delporte⁶⁵, P.A. Delsart⁵⁸, D.A. DeMarco¹⁶⁷, S. Demers¹⁸³, M. Demichev⁸⁰, G. Demontigny¹¹⁰, S.P. Denisov¹²³, L. D'Eramo¹³⁶, D. Derendarz⁸⁵, J.E. Derkaoui^{35d}, F. Derue¹³⁶, P. Dervan⁹¹, K. Desch²⁴, C. Deterre⁴⁶, K. Dette¹⁶⁷, C. Deutsch²⁴, M.R. Devesa³⁰, P.O. Deviveiros³⁶, F.A. Di Bello^{73a,73b}, A. Di Ciaccio^{74a,74b}, L. Di Ciaccio⁵, W.K. Di Clemente¹³⁷, C. Di Donato^{70a,70b}, A. Di Girolamo³⁶, G. Di Gregorio^{72a,72b}, B. Di Micco^{75a,75b}, R. Di Nardo^{75a,75b}, K.F. Di Petrillo⁵⁹, R. Di Sipio¹⁶⁷, C. Diaconu¹⁰², F.A. Dias⁴⁰, T. Dias Do Vale^{140a}, M.A. Diaz^{147a}, J. Dickinson¹⁸, E.B. Diehl¹⁰⁶, J. Dietrich¹⁹, S. Díez Cornell⁴⁶, A. Dimitrievska¹⁸, W. Ding^{15b}, J. Dingfelder²⁴, F. Dittus³⁶, F. Djama¹⁰², T. Djobava^{159b}, J.I. Djuvsland¹⁷, M.A.B. Do Vale^{81c}, M. Dobre^{27b}, D. Dodsworth²⁶, C. Doglioni⁹⁷, J. Dolejsi¹⁴³, Z. Dolezal¹⁴³, M. Donadelli^{81d}, B. Dong^{60c}, J. Donini³⁸, A. D'onofrio^{15c}, M. D'Onofrio⁹¹, J. Dopke¹⁴⁴, A. Doria^{70a}, M.T. Dova⁸⁹, A.T. Doyle⁵⁷, E. Drechsler¹⁵², E. Dreyer¹⁵², T. Dreyer⁵³, A.S. Drobac¹⁷⁰, D. Du^{60b}, Y. Duan^{60b}, F. Dubinin¹¹¹, M. Dubovsky^{28a}, A. Dubreuil⁵⁴, E. Duchovni¹⁸⁰, G. Duckeck¹¹⁴, A. Ducourthial¹³⁶, O.A. Ducu¹¹⁰, D. Duda¹¹⁵, A. Dudarev³⁶, A.C. Dudder¹⁰⁰, E.M. Duffield¹⁸, L. Dufflot⁶⁵, M. Dührssen³⁶, C. Dülsen¹⁸², M. Dumancic¹⁸⁰, A.E. Dumitriu^{27b}, A.K. Duncan⁵⁷, M. Dunford^{61a}, A. Duperrin¹⁰², H. Duran Yildiz^{4a}, M. Düren⁵⁶, A. Durglishvili^{159b}, D. Duschinger⁴⁸, B. Dutta⁴⁶, D. Duvnjak¹, G.I. Dyckes¹³⁷, M. Dyndal³⁶, S. Dych¹⁰¹, B.S. Dziedzic⁸⁵, K.M. Ecker¹¹⁵, M.G. Eggleston⁴⁹, T. Eifert⁸, G. Eigen¹⁷, K. Einsweiler¹⁸, T. Ekelof¹⁷², H. El Jarrari^{35e}, R. El Kosseifi¹⁰², V. Ellajosyula¹⁷², M. Ellert¹⁷², F. Ellinghaus¹⁸², A.A. Elliot⁹³, N. Ellis³⁶, J. Elmsheuser²⁹, M. Elsing³⁶, D. Emelianov¹⁴⁴, A. Emerman³⁹, Y. Enari¹⁶³, M.B. Epland⁴⁹, J. Erdmann⁴⁷, A. Ereditato²⁰, P.A. Erland⁸⁵, M. Errenst³⁶, M. Escalier⁶⁵, C. Escobar¹⁷⁴, O. Estrada Pastor¹⁷⁴, E. Etzion¹⁶¹, H. Evans⁶⁶, A. Ezhilov¹³⁸, F. Fabbri⁵⁷, L. Fabbri^{23b,23a}, V. Fabiani¹¹⁹, G. Facini¹⁷⁸, R.M. Faisca Rodrigues Pereira^{140a}, R.M. Fakhрутdinov¹²³, S. Falciano^{73a}, P.J. Falke⁵, S. Falke⁵, J. Faltova¹⁴³, Y. Fang^{15a}, Y. Fang^{15a}, G. Fanourakis⁴⁴, M. Fanti^{69a,69b}, M. Faraj^{67a,67c,s}, A. Farbin⁸, A. Farilla^{75a}, E.M. Farina^{71a,71b}, T. Farooque¹⁰⁷, S.M. Farrington⁵⁰, P. Farthouat³⁶, F. Fassi^{35e}, P. Fassnacht³⁶, D. Fassouliotis⁹, M. Fauci Giannelli⁵⁰, W.J. Fawcett³², L. Fayard⁶⁵, O.L. Fedin^{138,o}, W. Fedorko¹⁷⁵, A. Fehr²⁰, M. Feickert¹⁷³, L. Felgioni¹⁰², A. Fell¹⁴⁹, C. Feng^{60b}, M. Feng⁴⁹, M.J. Fenton¹⁷¹, A.B. Fenyuk¹²³, S.W. Ferguson⁴³, J. Ferrando⁴⁶, A. Ferrante¹⁷³, A. Ferrari¹⁷², P. Ferrari¹²⁰, R. Ferrari^{71a}, D.E. Ferreira de Lima^{61b}, A. Ferrer¹⁷⁴, D. Ferrere⁵⁴, C. Ferretti¹⁰⁶, F. Fiedler¹⁰⁰, A. Filipčić⁹², F. Filthaut¹¹⁹, K.D. Finelli²⁵, M.C.N. Fiolhais^{140a,140c,a}, L. Fiorini¹⁷⁴, F. Fischer¹¹⁴, W.C. Fisher¹⁰⁷, I. Fleck¹⁵¹,

P. Fleischmann¹⁰⁶, T. Flick¹⁸², B.M. Flierl¹¹⁴, L. Flores¹³⁷, L.R. Flores Castillo^{63a},
 F.M. Follega^{76a,76b}, N. Fomin¹⁷, J.H. Foo¹⁶⁷, G.T. Forcolin^{76a,76b}, A. Formica¹⁴⁵, F.A. Förster¹⁴,
 A.C. Forti¹⁰¹, A.G. Foster²¹, M.G. Foti¹³⁵, D. Fournier⁶⁵, H. Fox⁹⁰, P. Francavilla^{72a,72b},
 S. Francescato^{73a,73b}, M. Franchini^{23b,23a}, S. Franchino^{61a}, D. Francis³⁶, L. Franconi²⁰,
 M. Franklin⁵⁹, A.N. Fray⁹³, P.M. Freeman²¹, B. Freund¹¹⁰, W.S. Freund^{81b}, E.M. Freundlich⁴⁷,
 D.C. Frizzell¹²⁹, D. Froidevaux³⁶, J.A. Frost¹³⁵, C. Fukunaga¹⁶⁴, E. Fullana Torregrosa¹⁷⁴,
 T. Fusayasu¹¹⁶, J. Fuster¹⁷⁴, A. Gabrielli^{23b,23a}, A. Gabrielli¹⁸, S. Gadatsch⁵⁴, P. Gadow¹¹⁵,
 G. Gagliardi^{55b,55a}, L.G. Gagnon¹¹⁰, B. Galhardo^{140a}, G.E. Gallardo¹³⁵, E.J. Gallas¹³⁵,
 B.J. Gallop¹⁴⁴, G. Galster⁴⁰, R. Gamboa Goni⁹³, K.K. Gan¹²⁷, S. Ganguly¹⁸⁰, J. Gao^{60a},
 Y. Gao⁵⁰, Y.S. Gao^{31,l}, C. García¹⁷⁴, J.E. García Navarro¹⁷⁴, J.A. García Pascual^{15a},
 C. Garcia-Argos⁵², M. Garcia-Sciveres¹⁸, R.W. Gardner³⁷, N. Garelli¹⁵³, S. Gargiulo⁵²,
 C.A. Garner¹⁶⁷, V. Garonne¹³⁴, S.J. Gasiorowski¹⁴⁸, P. Gaspar^{81b}, A. Gaudiello^{55b,55a},
 G. Gaudio^{71a}, I.L. Gavrilenko¹¹¹, A. Gavrilyuk¹²⁴, C. Gay¹⁷⁵, G. Gaycken⁴⁶, E.N. Gazis¹⁰,
 A.A. Geanta^{27b}, C.M. Gee¹⁴⁶, C.N.P. Gee¹⁴⁴, J. Geisen⁹⁷, M. Geisen¹⁰⁰, C. Gemme^{55b},
 M.H. Genest⁵⁸, C. Geng¹⁰⁶, S. Gentile^{73a,73b}, S. George⁹⁴, T. Gerialis⁴⁴, L.O. Gerlach⁵³,
 P. Gessinger-Befurt¹⁰⁰, G. Gessner⁴⁷, S. Ghasemi¹⁵¹, M. Ghasemi Bostanabad¹⁷⁶,
 M. Ghneimat¹⁵¹, A. Ghosh⁶⁵, A. Ghosh⁷⁸, B. Giacobbe^{23b}, S. Giagu^{73a,73b},
 N. Giangiacomi^{23b,23a}, P. Giannetti^{72a}, A. Giannini^{70a,70b}, G. Giannini¹⁴, S.M. Gibson⁹⁴,
 M. Gignac¹⁴⁶, D. Gillberg³⁴, G. Gilles¹⁸², D.M. Gingrich^{3,ao}, M.P. Giordani^{67a,67c},
 P.F. Giraud¹⁴⁵, G. Giugliarelli^{67a,67c}, D. Giugni^{69a}, F. Giuli^{74a,74b}, S. Gkaitatzis¹⁶², I. Gkialas^{9,g},
 E.L. Gkoukousis¹⁴, P. Gkoutoumis¹⁰, L.K. Gladilin¹¹³, C. Glasman⁹⁹, J. Glatzer¹⁴,
 P.C.F. Glaysher⁴⁶, A. Glazov⁴⁶, G.R. Gledhill¹³², M. Goblirsch-Kolb²⁶, D. Godin¹¹⁰,
 S. Goldfarb¹⁰⁵, T. Golling⁵⁴, D. Golubkov¹²³, A. Gomes^{140a,140b}, R. Goncalves Gama⁵³,
 R. Gonçalo^{140a}, G. Gonella¹³², L. Gonella²¹, A. Gongadze⁸⁰, F. Gonnella²¹, J.L. Gonski³⁹,
 S. González de la Hoz¹⁷⁴, S. Gonzalez Fernandez¹⁴, S. Gonzalez-Sevilla⁵⁴,
 G.R. Gonzalvo Rodriguez¹⁷⁴, L. Goossens³⁶, N.A. Gorasia²¹, P.A. Gorbounov¹²⁴, H.A. Gordon²⁹,
 B. Gorini³⁶, E. Gorini^{68a,68b}, A. Gorišek⁹², A.T. Goshaw⁴⁹, M.I. Gostkin⁸⁰, C.A. Gottardo¹¹⁹,
 M. Gouighri^{35b}, A.G. Goussiou¹⁴⁸, N. Govender^{33c}, C. Goy⁵, E. Gozani¹⁶⁰,
 I. Grabowska-Bold^{84a}, E.C. Graham⁹¹, J. Gramling¹⁷¹, E. Gramstad¹³⁴, S. Grancagnolo¹⁹,
 M. Grandi¹⁵⁶, V. Gratchev¹³⁸, P.M. Gravila^{27f}, F.G. Gravili^{68a,68b}, C. Gray⁵⁷, H.M. Gray¹⁸,
 C. Greife²⁴, K. Gregersen⁹⁷, I.M. Gregor⁴⁶, P. Grenier¹⁵³, K. Grevtsov⁴⁶, C. Grieco¹⁴,
 N.A. Grieser¹²⁹, A.A. Grillo¹⁴⁶, K. Grimm^{31,k}, S. Grinstein^{14,y}, J.-F. Grivaz⁶⁵, S. Groh¹⁰⁰,
 E. Gross¹⁸⁰, J. Grosse-Knetter⁵³, Z.J. Grout⁹⁵, C. Grud¹⁰⁶, A. Grummer¹¹⁸, L. Guan¹⁰⁶,
 W. Guan¹⁸¹, C. Gubbels¹⁷⁵, J. Guenther³⁶, A. Guerguichon⁶⁵, J.G.R. Guerrero Rojas¹⁷⁴,
 F. Guescini¹¹⁵, D. Guest¹⁷¹, R. Gugel⁵², T. Guillemain⁵, S. Guindon³⁶, U. Gul⁵⁷, J. Guo^{60c},
 W. Guo¹⁰⁶, Y. Guo^{60a}, Z. Guo¹⁰², R. Gupta⁴⁶, S. Gurbuz^{12c}, G. Gustavino¹²⁹, M. Guth⁵²,
 P. Gutierrez¹²⁹, C. Gutsche⁹⁵, C. Guyot¹⁴⁵, C. Gwenlan¹³⁵, C.B. Gwilliam⁹¹, A. Haas¹²⁵,
 C. Haber¹⁸, H.K. Hadavand⁸, A. Hadeef^{60a}, M. Haleem¹⁷⁷, J. Haley¹³⁰, G. Halladjian¹⁰⁷,
 G.D. Hallewell¹⁰², K. Hamacher¹⁸², P. Hamal¹³¹, K. Hamano¹⁷⁶, H. Hamdaoui^{35e}, M. Hamer²⁴,
 G.N. Hamity⁵⁰, K. Han^{60a,x}, L. Han^{60a}, S. Han^{15a}, Y.F. Han¹⁶⁷, K. Hanagaki^{82,v}, M. Hance¹⁴⁶,
 D.M. Handl¹¹⁴, B. Haney¹³⁷, R. Hankache¹³⁶, E. Hansen⁹⁷, J.B. Hansen⁴⁰, J.D. Hansen⁴⁰,
 M.C. Hansen²⁴, P.H. Hansen⁴⁰, E.C. Hanson¹⁰¹, K. Hara¹⁶⁹, T. Harenberg¹⁸², S. Harkusha¹⁰⁸,
 P.F. Harrison¹⁷⁸, N.M. Hartmann¹¹⁴, Y. Hasegawa¹⁵⁰, A. Hasib⁵⁰, S. Hassani¹⁴⁵, S. Haug²⁰,
 R. Hauser¹⁰⁷, L.B. Havener³⁹, M. Havranek¹⁴², C.M. Hawkes²¹, R.J. Hawkins³⁶, D. Hayden¹⁰⁷,
 C. Hayes¹⁰⁶, R.L. Hayes¹⁷⁵, C.P. Hays¹³⁵, J.M. Hays⁹³, H.S. Hayward⁹¹, S.J. Haywood¹⁴⁴,
 F. He^{60a}, M.P. Heath⁵⁰, V. Hedberg⁹⁷, S. Heer²⁴, K.K. Heidegger⁵², W.D. Heidorn⁷⁹,
 J. Heilman³⁴, S. Heim⁴⁶, T. Heim¹⁸, B. Heinemann^{46,am}, J.J. Heinrich¹³², L. Heinrich³⁶,
 J. Hejbal¹⁴¹, L. Helary^{61b}, A. Held¹²⁵, S. Hellesund¹³⁴, C.M. Helling¹⁴⁶, S. Hellman^{45a,45b},

C. Helsens³⁶, R.C.W. Henderson⁹⁰, Y. Heng¹⁸¹, L. Henkelmann^{61a}, S. Henkelmann¹⁷⁵,
A.M. Henriques Correia³⁶, H. Herde²⁶, V. Herget¹⁷⁷, Y. Hernández Jiménez^{33e}, H. Herr¹⁰⁰,
M.G. Herrmann¹¹⁴, T. Herrmann⁴⁸, G. Herten⁵², R. Hertenberger¹¹⁴, L. Hervás³⁶,
T.C. Herwig¹³⁷, G.G. Hesketh⁹⁵, N.P. Hessey^{168a}, A. Higashida¹⁶³, S. Higashino⁸²,
E. Higón-Rodríguez¹⁷⁴, K. Hildebrand³⁷, J.C. Hill³², K.K. Hill²⁹, K.H. Hiller⁴⁶, S.J. Hillier²¹,
M. Hils⁴⁸, I. Hinchliffe¹⁸, F. Hinterkeuser²⁴, M. Hirose¹³³, S. Hirose⁵², D. Hirschbuehl¹⁸²,
B. Hiti⁹², O. Hladik¹⁴¹, D.R. Hlaluku^{33e}, J. Hobbs¹⁵⁵, N. Hod¹⁸⁰, M.C. Hodgkinson¹⁴⁹,
A. Hoecker³⁶, D. Hohn⁵², D. Hohov⁶⁵, T. Holm²⁴, T.R. Holmes³⁷, M. Holzbock¹¹⁴,
L.B.A.H. Hommels³², S. Honda¹⁶⁹, T.M. Hong¹³⁹, J.C. Honig⁵², A. Hönle¹¹⁵,
B.H. Hooberman¹⁷³, W.H. Hopkins⁶, Y. Horii¹¹⁷, P. Horn⁴⁸, L.A. Horyn³⁷, S. Hou¹⁵⁸,
A. Hoummada^{35a}, J. Howarth¹⁰¹, J. Hoya⁸⁹, M. Hrabovsky¹³¹, J. Hrdinka⁷⁷, I. Hristova¹⁹,
J. Hrivnac⁶⁵, A. Hrynevich¹⁰⁹, T. Hryn'ova⁵, P.J. Hsu⁶⁴, S.-C. Hsu¹⁴⁸, Q. Hu²⁹, S. Hu^{60c},
Y.F. Hu^{15a,15d}, D.P. Huang⁹⁵, Y. Huang^{60a}, Y. Huang^{15a}, Z. Hubacek¹⁴², F. Hubaut¹⁰²,
M. Huebner²⁴, F. Huegging²⁴, T.B. Huffman¹³⁵, M. Huhtinen³⁶, R.F.H. Hunter³⁴, P. Huo¹⁵⁵,
N. Huseynov^{80,ae}, J. Huston¹⁰⁷, J. Huth⁵⁹, R. Hyneman¹⁰⁶, S. Hyrych^{28a}, G. Iacobucci⁵⁴,
G. Iakovidis²⁹, I. Ibragimov¹⁵¹, L. Iconomidou-Fayard⁶⁵, P. Iengo³⁶, R. Ignazzi⁴⁰,
O. Igonkina^{120,aa,*}, R. Iguchi¹⁶³, T. Iizawa⁵⁴, Y. Ikegami⁸², M. Ikeno⁸², D. Iliadis¹⁶²,
N. Ilic^{119,167,ad}, F. Iltzsche⁴⁸, G. Introzzi^{71a,71b}, M. Iodice^{75a}, K. Iordanidou^{168a},
V. Ippolito^{73a,73b}, M.F. Isacson¹⁷², M. Ishino¹⁶³, W. Islam¹³⁰, C. Issever^{19,46}, S. Istin¹⁶⁰,
F. Ito¹⁶⁹, J.M. Iturbe Ponce^{63a}, R. Iuppa^{76a,76b}, A. Ivina¹⁸⁰, H. Iwasaki⁸², J.M. Izen⁴³,
V. Izzo^{70a}, P. Jacka¹⁴¹, P. Jackson¹, R.M. Jacobs²⁴, B.P. Jaeger¹⁵², V. Jain², G. Jäkel¹⁸²,
K.B. Jakobi¹⁰⁰, K. Jakobs⁵², T. Jakoubek¹⁴¹, J. Jamieson⁵⁷, K.W. Janas^{84a}, R. Jansky⁵⁴,
M. Janus⁵³, P.A. Janus^{84a}, G. Jarlskog⁹⁷, N. Javadov^{80,ae}, T. Javůrek³⁶, M. Javurkova¹⁰³,
F. Jeanneau¹⁴⁵, L. Jeanty¹³², J. Jejelava^{159a}, A. Jelinskas¹⁷⁸, P. Jenni^{52,b}, N. Jeong⁴⁶,
S. Jézéquel⁵, H. Ji¹⁸¹, J. Jia¹⁵⁵, H. Jiang⁷⁹, Y. Jiang^{60a}, Z. Jiang^{153,p}, S. Jiggins⁵²,
F.A. Jimenez Morales³⁸, J. Jimenez Pena¹¹⁵, S. Jin^{15c}, A. Jinaru^{27b}, O. Jinnouchi¹⁶⁵,
H. Jivan^{33e}, P. Johansson¹⁴⁹, K.A. Johns⁷, C.A. Johnson⁶⁶, R.W.L. Jones⁹⁰, S.D. Jones¹⁵⁶,
S. Jones⁷, T.J. Jones⁹¹, J. Jongmanns^{61a}, P.M. Jorge^{140a}, J. Jovicevic³⁶, X. Ju¹⁸,
J.J. Junggeburth¹¹⁵, A. Juste Rozas^{14,y}, A. Kaczmarek⁸⁵, M. Kado^{73a,73b}, H. Kagan¹²⁷,
M. Kagan¹⁵³, A. Kahn³⁹, C. Kahra¹⁰⁰, T. Kaji¹⁷⁹, E. Kajomovitz¹⁶⁰, C.W. Kalderon²⁹,
A. Kaluza¹⁰⁰, A. Kamenshchikov¹²³, M. Kaneda¹⁶³, N.J. Kang¹⁴⁶, S. Kang⁷⁹, L. Kanjir⁹²,
Y. Kano¹¹⁷, J. Kanzaki⁸², L.S. Kaplan¹⁸¹, D. Kar^{33e}, K. Karava¹³⁵, M.J. Kareem^{168b},
S.N. Karpov⁸⁰, Z.M. Karpova⁸⁰, V. Kartvelishvili⁹⁰, A.N. Karyukhin¹²³, A. Kastanas^{45a,45b},
C. Kato^{60d,60c}, J. Katzy⁴⁶, K. Kawade¹⁵⁰, K. Kawagoe⁸⁸, T. Kawaguchi¹¹⁷, T. Kawamoto¹⁴⁵,
G. Kawamura⁵³, E.F. Kay¹⁷⁶, V.F. Kazanin^{122b,122a}, R. Keeler¹⁷⁶, R. Kehoe⁴², J.S. Keller³⁴,
E. Kellermann⁹⁷, D. Kelsey¹⁵⁶, J.J. Kempster²¹, J. Kendrick²¹, K.E. Kennedy³⁹, O. Kepka¹⁴¹,
S. Kersten¹⁸², B.P. Kerševan⁹², S. Ketabchi Haghighat¹⁶⁷, M. Khader¹⁷³, F. Khalil-Zada¹³,
M. Khandoga¹⁴⁵, A. Khanov¹³⁰, A.G. Kharlamov^{122b,122a}, T. Kharlamova^{122b,122a},
E.E. Khoda¹⁷⁵, A. Khodinov¹⁶⁶, T.J. Khoo⁵⁴, E. Khramov⁸⁰, J. Khubua^{159b}, S. Kido⁸³,
M. Kiehn⁵⁴, C.R. Kilby⁹⁴, E. Kim¹⁶⁵, Y.K. Kim³⁷, N. Kimura⁹⁵, O.M. Kind¹⁹, B.T. King^{91,*},
D. Kirchmeier⁴⁸, J. Kirk¹⁴⁴, A.E. Kiryunin¹¹⁵, T. Kishimoto¹⁶³, D.P. Kisluk¹⁶⁷, V. Kitali⁴⁶,
O. Kivernyk⁵, T. Klapdor-Kleingrothaus⁵², M. Klassen^{61a}, C. Klein³², M.H. Klein¹⁰⁶, M. Klein⁹¹,
U. Klein⁹¹, K. Kleinknecht¹⁰⁰, P. Klimek¹²¹, A. Klimentov²⁹, T. Klingl²⁴, T. Klioutchnikova³⁶,
F.F. Klitzner¹¹⁴, P. Kluit¹²⁰, S. Kluth¹¹⁵, E. Kneringer⁷⁷, E.B.F.G. Knoops¹⁰², A. Knue⁵²,
D. Kobayashi⁸⁸, T. Kobayashi¹⁶³, M. Kobel⁴⁸, M. Kocian¹⁵³, T. Kodama¹⁶³, P. Kodys¹⁴³,
P.T. Koenig²⁴, T. Koffas³⁴, N.M. Köhler³⁶, M. Kolb¹⁴⁵, I. Koletsou⁵, T. Komarek¹³¹,
T. Kondo⁸², K. Köneke⁵², A.X.Y. Kong¹, A.C. König¹¹⁹, T. Kono¹²⁶, V. Konstantinides⁹⁵,
N. Konstantinidis⁹⁵, B. Konya⁹⁷, R. Kopeliansky⁶⁶, S. Koperny^{84a}, K. Korcyl⁸⁵, K. Kordas¹⁶²,

G. Koren¹⁶¹, A. Korn⁹⁵, I. Korolkov¹⁴, E.V. Korolkova¹⁴⁹, N. Korotkova¹¹³, O. Kortner¹¹⁵, S. Kortner¹¹⁵, T. Kosek¹⁴³, V.V. Kostyukhin^{149,166}, A. Kotskechagia⁶⁵, A. Kotwal⁴⁹, A. Koulouris¹⁰, A. Kourkoumeli-Charalampidi^{71a,71b}, C. Kourkoumelis⁹, E. Kourlitis¹⁴⁹, V. Kouskoura²⁹, A.B. Kowalewska⁸⁵, R. Kowalewski¹⁷⁶, W. Kozanecki¹⁰¹, A.S. Kozhin¹²³, V.A. Kramarenko¹¹³, G. Kramberger⁹², D. Krasnopevtsev^{60a}, M.W. Krasny¹³⁶, A. Krasznahorkay³⁶, D. Krauss¹¹⁵, J.A. Kremer^{84a}, J. Kretzschmar⁹¹, P. Krieger¹⁶⁷, F. Krieter¹¹⁴, A. Krishnan^{61b}, K. Krizka¹⁸, K. Kroeninger⁴⁷, H. Kroha¹¹⁵, J. Kroll¹⁴¹, J. Kroll¹³⁷, K.S. Krowpman¹⁰⁷, U. Kruchonak⁸⁰, H. Krüger²⁴, N. Krumnack⁷⁹, M.C. Kruse⁴⁹, J.A. Krzysiak⁸⁵, T. Kubota¹⁰⁵, O. Kuchinskaia¹⁶⁶, S. Kunday^{4b}, J.T. Kuechler⁴⁶, S. Kuehn³⁶, A. Kugel^{61a}, T. Kuhl⁴⁶, V. Kukhtin⁸⁰, R. Kukla¹⁰², Y. Kulchitsky^{108,ag}, S. Kuleshov^{147d}, Y.P. Kulinich¹⁷³, M. Kuna⁵⁸, T. Kunigo⁸⁶, A. Kupco¹⁴¹, T. Kupfer⁴⁷, O. Kuprash⁵², H. Kurashige⁸³, L.L. Kurchaninov^{168a}, Y.A. Kurochkin¹⁰⁸, A. Kurova¹¹², M.G. Kurth^{15a,15d}, E.S. Kuwertz³⁶, M. Kuze¹⁶⁵, A.K. Kvam¹⁴⁸, J. Kvita¹³¹, T. Kwan¹⁰⁴, L. La Rotonda^{41b,41a}, F. La Ruffa^{41b,41a}, C. Lacasta¹⁷⁴, F. Lacava^{73a,73b}, D.P.J. Lack¹⁰¹, H. Lacker¹⁹, D. Lacour¹³⁶, E. Ladygin⁸⁰, R. Lafaye⁵, B. Laforge¹³⁶, T. Lagouri^{147b}, S. Lai⁵³, I.K. Lakomic^{84a}, S. Lammers⁶⁶, W. Lampl⁷, C. Lampoudis¹⁶², E. Lançon²⁹, U. Landgraf⁵², M.P.J. Landon⁹³, M.C. Lanfermann⁵⁴, V.S. Lang⁴⁶, J.C. Lange⁵³, R.J. Langenberg¹⁰³, A.J. Lankford¹⁷¹, F. Lanni²⁹, K. Lantzsck²⁴, A. Lanza^{71a}, A. Lapertosa^{55b,55a}, S. Laplace¹³⁶, J.F. Laporte¹⁴⁵, T. Lari^{69a}, F. Lasagni Manghi^{23b,23a}, M. Lassnig³⁶, T.S. Lau^{63a}, A. Laudrain⁶⁵, A. Laurier³⁴, M. Lavorgna^{70a,70b}, S.D. Lawlor⁹⁴, M. Lazzaroni^{69a,69b}, B. Le¹⁰⁵, E. Le Guirriec¹⁰², A. Lebedev⁷⁹, M. LeBlanc⁷, T. LeCompte⁶, F. Ledroit-Guillon⁵⁸, A.C.A. Lee⁹⁵, C.A. Lee²⁹, G.R. Lee¹⁷, L. Lee⁵⁹, S.C. Lee¹⁵⁸, S. Lee⁷⁹, B. Lefebvre^{168a}, H.P. Lefebvre⁹⁴, M. Lefebvre¹⁷⁶, C. Leggett¹⁸, K. Lehmann¹⁵², N. Lehmann¹⁸², G. Lehmann Miotto³⁶, W.A. Leight⁴⁶, A. Leisos^{162,w}, M.A.L. Leite^{81d}, C.E. Leitgeb¹¹⁴, R. Leitner¹⁴³, D. Lellouch^{180,*}, K.J.C. Leney⁴², T. Lenz²⁴, R. Leone⁷, S. Leone^{72a}, C. Leonidopoulos⁵⁰, A. Leopold¹³⁶, C. Leroy¹¹⁰, R. Les¹⁶⁷, C.G. Lester³², M. Levchenko¹³⁸, J. Levêque⁵, D. Levin¹⁰⁶, L.J. Levinson¹⁸⁰, D.J. Lewis²¹, B. Li^{15b}, B. Li¹⁰⁶, C-Q. Li^{60a}, F. Li^{60c}, H. Li^{60a}, H. Li^{60b}, J. Li^{60c}, K. Li¹⁴⁸, L. Li^{60c}, M. Li^{15a,15d}, Q. Li^{15a,15d}, Q.Y. Li^{60a}, S. Li^{60d,60c}, X. Li⁴⁶, Y. Li⁴⁶, Z. Li^{60b}, Z. Li¹⁰⁴, Z. Liang^{15a}, B. Liberti^{74a}, A. Liblong¹⁶⁷, K. Lie^{63c}, S. Lim²⁹, C.Y. Lin³², K. Lin¹⁰⁷, T.H. Lin¹⁰⁰, R.A. Linck⁶⁶, J.H. Lindon²¹, A.L. Lioni⁵⁴, E. Lipeles¹³⁷, A. Lipniacka¹⁷, T.M. Liss^{173,an}, A. Lister¹⁷⁵, J.D. Little⁸, B. Liu⁷⁹, B.L. Liu⁶, H.B. Liu²⁹, H. Liu¹⁰⁶, J.B. Liu^{60a}, J.K.K. Liu³⁷, K. Liu^{60d}, M. Liu^{60a}, P. Liu^{15a}, Y. Liu⁴⁶, Y. Liu^{15a,15d}, Y.L. Liu¹⁰⁶, Y.W. Liu^{60a}, M. Livan^{71a,71b}, A. Lleres⁵⁸, J. Llorente Merino¹⁵², S.L. Lloyd⁹³, C.Y. Lo^{63b}, E.M. Lobodzinska⁴⁶, P. Loch⁷, S. Loffredo^{74a,74b}, T. Lohse¹⁹, K. Lohwasser¹⁴⁹, M. Lokajicek¹⁴¹, J.D. Long¹⁷³, R.E. Long⁹⁰, L. Longo³⁶, K.A. Looper¹²⁷, J.A. Lopez^{147d}, I. Lopez Paz¹⁰¹, A. Lopez Solis¹⁴⁹, J. Lorenz¹¹⁴, N. Lorenzo Martinez⁵, A.M. Lory¹¹⁴, M. Losada^{22a}, P.J. Lösel¹¹⁴, A. Lösle⁵², X. Lou⁴⁶, X. Lou^{15a}, A. Lounis⁶⁵, J. Love⁶, P.A. Love⁹⁰, J.J. Lozano Bahilo¹⁷⁴, M. Lu^{60a}, Y.J. Lu⁶⁴, H.J. Lubatti¹⁴⁸, C. Luci^{73a,73b}, A. Lucotte⁵⁸, C. Luedtke⁵², F. Luehring⁶⁶, I. Luise¹³⁶, L. Luminari^{73a}, B. Lund-Jensen¹⁵⁴, M.S. Lutz¹⁰³, D. Lynn²⁹, H. Lyons⁹¹, R. Lysak¹⁴¹, E. Lytken⁹⁷, F. Lyu^{15a}, V. Lyubushkin⁸⁰, T. Lyubushkina⁸⁰, H. Ma²⁹, L.L. Ma^{60b}, Y. Ma⁹⁵, G. Maccarrone⁵¹, A. Macchiolo¹¹⁵, C.M. Macdonald¹⁴⁹, J. Machado Miguens¹³⁷, D. Madaffari¹⁷⁴, R. Madar³⁸, W.F. Mader⁴⁸, M. Madugoda Ralalage Don¹³⁰, N. Madysa⁴⁸, J. Maeda⁸³, T. Maeno²⁹, M. Maerker⁴⁸, V. Magerl⁵², N. Magini⁷⁹, J. Magro^{67a,67c,s}, D.J. Mahon³⁹, C. Maidantchik^{81b}, T. Maier¹¹⁴, A. Maio^{140a,140b,140d}, K. Maj^{84a}, O. Majersky^{28a}, S. Majewski¹³², Y. Makida⁸², N. Makovec⁶⁵, B. Malaescu¹³⁶, Pa. Malecki⁸⁵, V.P. Maleev¹³⁸, F. Malek⁵⁸, U. Mallik⁷⁸, D. Malon⁶, C. Malone³², S. Maltezos¹⁰, S. Malyukov⁸⁰, J. Mamuzic¹⁷⁴, G. Mancini⁵¹, I. Mandić⁹², L. Manhaes de Andrade Filho^{81a}, I.M. Maniatis¹⁶², J. Manjarres Ramos⁴⁸, K.H. Mankinen⁹⁷, A. Mann¹¹⁴, A. Manousos⁷⁷, B. Mansoulie¹⁴⁵,

I. Manthos¹⁶², S. Manzoni¹²⁰, A. Marantis¹⁶², G. Marceca³⁰, L. Marchese¹³⁵, G. Marchiori¹³⁶,
 M. Marcisovsky¹⁴¹, L. Marcoccia^{74a,74b}, C. Marcon⁹⁷, C.A. Marin Tobon³⁶, M. Marjanovic¹²⁹,
 Z. Marshall¹⁸, M.U.F. Martensson¹⁷², S. Marti-Garcia¹⁷⁴, C.B. Martin¹²⁷, T.A. Martin¹⁷⁸,
 V.J. Martin⁵⁰, B. Martin dit Latour¹⁷, L. Martinelli^{75a,75b}, M. Martinez^{14,y},
 V.I. Martinez Outschoorn¹⁰³, S. Martin-Haugh¹⁴⁴, V.S. Martoiu^{27b}, A.C. Martyniuk⁹⁵,
 A. Marzin³⁶, S.R. Maschek¹¹⁵, L. Masetti¹⁰⁰, T. Mashimo¹⁶³, R. Mashinistov¹¹¹, J. Masik¹⁰¹,
 A.L. Maslennikov^{122b,122a}, L. Massa^{23b,23a}, P. Massarotti^{70a,70b}, P. Mastrandrea^{72a,72b},
 A. Mastroberardino^{41b,41a}, T. Masubuchi¹⁶³, D. Matakias²⁹, A. Matic¹¹⁴, N. Matsuzawa¹⁶³,
 P. Mättig²⁴, J. Maurer^{27b}, B. Maček⁹², D.A. Maximov^{122b,122a}, R. Mazini¹⁵⁸, I. Maznas¹⁶²,
 S.M. Mazza¹⁴⁶, S.P. Mc Kee¹⁰⁶, T.G. McCarthy¹¹⁵, W.P. McCormack¹⁸, E.F. McDonald¹⁰⁵,
 J.A. Mcfayden³⁶, G. Mchedlidze^{159b}, M.A. McKay⁴², K.D. McLean¹⁷⁶, S.J. McMahon¹⁴⁴,
 P.C. McNamara¹⁰⁵, C.J. McNicol¹⁷⁸, R.A. McPherson^{176,ad}, J.E. Mdhluli^{33e}, Z.A. Meadows¹⁰³,
 S. Meehan³⁶, T. Megy⁵², S. Mehlhase¹¹⁴, A. Mehta⁹¹, T. Meideck⁵⁸, B. Meirose⁴³, D. Melini¹⁶⁰,
 B.R. Mellado Garcia^{33e}, J.D. Mellenthin⁵³, M. Melo^{28a}, F. Meloni⁴⁶, A. Melzer²⁴,
 S.B. Menary¹⁰¹, E.D. Mendes Gouveia^{140a,140e}, L. Meng³⁶, X.T. Meng¹⁰⁶, S. Menke¹¹⁵,
 E. Meoni^{41b,41a}, S. Mergelmeyer¹⁹, S.A.M. Merkt¹³⁹, C. Merlassino¹³⁵, P. Mermod⁵⁴,
 L. Merola^{70a,70b}, C. Meroni^{69a}, G. Merz¹⁰⁶, O. Meshkov^{113,111}, J.K.R. Meshreki¹⁵¹,
 A. Messina^{73a,73b}, J. Metcalfe⁶, A.S. Mete⁶, C. Meyer⁶⁶, J.P. Meyer¹⁴⁵,
 H. Meyer Zu Theenhausen^{61a}, F. Miano¹⁵⁶, M. Michetti¹⁹, R.P. Middleton¹⁴⁴, L. Mijović⁵⁰,
 G. Mikenberg¹⁸⁰, M. Mikesikova¹⁴¹, M. Mikuz⁹², H. Mildner¹⁴⁹, M. Milesi¹⁰⁵, A. Milic¹⁶⁷,
 C.D. Milke⁴², D.A. Millar⁹³, D.W. Miller³⁷, A. Milov¹⁸⁰, D.A. Milstead^{45a,45b}, R.A. Mina¹⁵³,
 A.A. Minaenko¹²³, M. Miñano Moya¹⁷⁴, I.A. Minashvili^{159b}, A.I. Mincer¹²⁵, B. Mindur^{84a},
 M. Mineev⁸⁰, Y. Minegishi¹⁶³, L.M. Mir¹⁴, A. Mirto^{68a,68b}, K.P. Mistry¹³⁷, T. Mitani¹⁷⁹,
 J. Mitrevski¹¹⁴, V.A. Mitsou¹⁷⁴, M. Mittal^{60c}, O. Miu¹⁶⁷, A. Miucci²⁰, P.S. Miyagawa¹⁴⁹,
 A. Mizukami⁸², J.U. Mjörnmark⁹⁷, T. Mkrtchyan^{61a}, M. Mlynarikova¹⁴³, T. Moa^{45a,45b},
 K. Mochizuki¹¹⁰, P. Mogg⁵², S. Mohapatra³⁹, R. Moles-Valls²⁴, M.C. Mondragon¹⁰⁷, K. Mönig⁴⁶,
 J. Monk⁴⁰, E. Monnier¹⁰², A. Montalbano¹⁵², J. Montejo Berlingen³⁶, M. Montella⁹⁵,
 F. Monticelli⁸⁹, S. Monzani^{69a}, N. Morange⁶⁵, D. Moreno^{22a}, M. Moreno Llacer¹⁷⁴,
 C. Moreno Martinez¹⁴, P. Morettini^{55b}, M. Morgenstern¹⁶⁰, S. Morgenstern⁴⁸, D. Mori¹⁵²,
 M. Morii⁵⁹, M. Morinaga¹⁷⁹, V. Morisbak¹³⁴, A.K. Morley³⁶, G. Mornacchi³⁶, A.P. Morris⁹⁵,
 L. Morvaj¹⁵⁵, P. Moschovakos³⁶, B. Moser¹²⁰, M. Mosidze^{159b}, T. Moskalets¹⁴⁵, H.J. Moss¹⁴⁹,
 J. Moss^{31,m}, E.J.W. Moyse¹⁰³, S. Muanza¹⁰², J. Mueller¹³⁹, R.S.P. Mueller¹¹⁴,
 D. Muenstermann⁹⁰, G.A. Mullier⁹⁷, D.P. Mungo^{69a,69b}, J.L. Munoz Martinez¹⁴,
 F.J. Munoz Sanchez¹⁰¹, P. Murin^{28b}, W.J. Murray^{178,144}, A. Murrone^{69a,69b}, M. Muškinja¹⁸,
 C. Mwewa^{33a}, A.G. Myagkov^{123,ai}, A.A. Myers¹³⁹, J. Myers¹³², M. Myska¹⁴², B.P. Nachman¹⁸,
 O. Nackenhorst⁴⁷, A.Nag Nag⁴⁸, K. Nagai¹³⁵, K. Nagano⁸², Y. Nagasaka⁶², J.L. Nagle²⁹,
 E. Nagy¹⁰², A.M. Nairz³⁶, Y. Nakahama¹¹⁷, K. Nakamura⁸², T. Nakamura¹⁶³, I. Nakano¹²⁸,
 H. Nanjo¹³³, F. Napolitano^{61a}, R.F. Naranjo Garcia⁴⁶, R. Narayan⁴², I. Naryshkin¹³⁸,
 T. Naumann⁴⁶, G. Navarro^{22a}, P.Y. Nechaeva¹¹¹, F. Nechansky⁴⁶, T.J. Neep²¹, A. Negri^{71a,71b},
 M. Negrini^{23b}, C. Nellist¹¹⁹, M.E. Nelson^{45a,45b}, S. Nemecek¹⁴¹, M. Nessi^{36,d}, M.S. Neubauer¹⁷³,
 F. Neuhaus¹⁰⁰, M. Neumann¹⁸², R. Newhouse¹⁷⁵, P.R. Newman²¹, C.W. Ng¹³⁹, Y.S. Ng¹⁹,
 Y.W.Y. Ng¹⁷¹, B. Ngair^{35e}, H.D.N. Nguyen¹⁰², T. Nguyen Manh¹¹⁰, E. Nibigira³⁸,
 R.B. Nickerson¹³⁵, R. Nicolaidou¹⁴⁵, D.S. Nielsen⁴⁰, J. Nielsen¹⁴⁶, N. Nikiforou¹¹,
 V. Nikolaenko^{123,ai}, I. Nikolic-Audit¹³⁶, K. Nikolopoulos²¹, P. Nilsson²⁹, H.R. Nindhito⁵⁴,
 Y. Ninomiya⁸², A. Nisati^{73a}, N. Nishu^{60c}, R. Nisius¹¹⁵, I. Nitsche⁴⁷, T. Nitta¹⁷⁹, T. Nobe¹⁶³,
 Y. Noguchi⁸⁶, I. Nomidis¹³⁶, M.A. Nomura²⁹, M. Nordberg³⁶, T. Novak⁹², O. Novgorodova⁴⁸,
 R. Novotny¹⁴², L. Nozka¹³¹, K. Ntekas¹⁷¹, E. Nurse⁹⁵, F.G. Oakham^{34,ao}, H. Oberlack¹¹⁵,
 J. Ocariz¹³⁶, A. Ochi⁸³, I. Ochoa³⁹, J.P. Ochoa-Ricoux^{147a}, K. O'Connor²⁶, S. Oda⁸⁸,

S. Odaka⁸², S. Oerdek⁵³, A. Ogrodnik^{84a}, A. Oh¹⁰¹, S.H. Oh⁴⁹, C.C. Ohm¹⁵⁴, H. Oide¹⁶⁵, M.L. Ojeda¹⁶⁷, H. Okawa¹⁶⁹, Y. Okazaki⁸⁶, M.W. O’Keefe⁹¹, Y. Okumura¹⁶³, T. Okuyama⁸², A. Olariu^{27b}, L.F. Oleiro Seabra^{140a}, S.A. Olivares Pino^{147a}, D. Oliveira Damazio²⁹, J.L. Oliver¹, M.J.R. Olsson¹⁷¹, A. Olszewski⁸⁵, J. Olszowska⁸⁵, D.C. O’Neil¹⁵², A.P. O’neill¹³⁵, A. Onofre^{140a,140e}, P.U.E. Onyisi¹¹, H. Oppen¹³⁴, M.J. Oreglia³⁷, G.E. Orellana⁸⁹, D. Orestano^{75a,75b}, N. Orlando¹⁴, R.S. Orr¹⁶⁷, V. O’Shea⁵⁷, R. Ospanov^{60a}, G. Otero y Garzon³⁰, H. Otono⁸⁸, P.S. Ott^{61a}, M. Ouchrif^{35d}, J. Ouellette²⁹, F. Ould-Saada¹³⁴, A. Ouraou¹⁴⁵, Q. Ouyang^{15a}, M. Owen⁵⁷, R.E. Owen²¹, V.E. Ozcan^{12c}, N. Ozturk⁸, J. Pacalt¹³¹, H.A. Pacey³², K. Pachal⁴⁹, A. Pacheco Pages¹⁴, C. Padilla Aranda¹⁴, S. Pagan Griso¹⁸, M. Paganini¹⁸³, G. Palacino⁶⁶, S. Palazzo⁵⁰, S. Palestini³⁶, M. Palka^{84b}, D. Pallin³⁸, P. Palni^{84a}, I. Panagoulas¹⁰, C.E. Pandini³⁶, J.G. Panduro Vazquez⁹⁴, P. Pani⁴⁶, G. Panizzo^{67a,67c}, L. Paolozzi⁵⁴, C. Papadatos¹¹⁰, K. Papageorgiou^{9,g}, S. Parajuli⁴², A. Paramonov⁶, D. Paredes Hernandez^{63b}, S.R. Paredes Saenz¹³⁵, B. Parida¹⁶⁶, T.H. Park¹⁶⁷, A.J. Parker³¹, M.A. Parker³², F. Parodi^{55b,55a}, E.W. Parrish¹²¹, J.A. Parsons³⁹, U. Parzefall⁵², L. Pascual Dominguez¹³⁶, V.R. Pascuzzi¹⁶⁷, J.M.P. Pasner¹⁴⁶, F. Pasquali¹²⁰, E. Pasqualucci^{73a}, S. Passaggio^{55b}, F. Pastore⁹⁴, P. Pasuwan^{45a,45b}, S. Patarraia¹⁰⁰, J.R. Pater¹⁰¹, A. Pathak^{181,i}, J. Patton⁹¹, T. Pauly³⁶, J. Parkes¹⁵³, B. Pearson¹¹⁵, M. Pedersen¹³⁴, L. Pedraza Diaz¹¹⁹, R. Pedro^{140a}, T. Peiffer⁵³, S.V. Peleganchuk^{122b,122a}, O. Penc¹⁴¹, H. Peng^{60a}, B.S. Peralva^{81a}, M.M. Perego⁶⁵, A.P. Pereira Peixoto^{140a}, L. Pereira Sanchez^{45a,45b}, D.V. Perepelitsa²⁹, F. Peri¹⁹, L. Perini^{69a,69b}, H. Pernegger³⁶, S. Perrella^{140a}, A. Perrevoort¹²⁰, K. Peters⁴⁶, R.F.Y. Peters¹⁰¹, B.A. Petersen³⁶, T.C. Petersen⁴⁰, E. Petit¹⁰², A. Petridis¹, C. Petridou¹⁶², P. Petroff⁶⁵, M. Petrov¹³⁵, F. Petrucci^{75a,75b}, M. Pettee¹⁸³, N.E. Pettersson¹⁰³, K. Petukhova¹⁴³, A. Peyaud¹⁴⁵, R. Pezoa^{147d}, L. Pezzotti^{71a,71b}, T. Pham¹⁰⁵, F.H. Phillips¹⁰⁷, P.W. Phillips¹⁴⁴, M.W. Phipps¹⁷³, G. Piacquadio¹⁵⁵, E. Pianori¹⁸, A. Picazio¹⁰³, R.H. Pickles¹⁰¹, R. Piegai³⁰, D. Pietreanu^{27b}, J.E. Pilcher³⁷, A.D. Pilkington¹⁰¹, M. Pinamonti^{67a,67c}, J.L. Pinfold³, M. Pitt¹⁶¹, L. Pizzimento^{74a,74b}, M.-A. Pleier²⁹, V. Pleskot¹⁴³, E. Plotnikova⁸⁰, P. Podberezko^{122b,122a}, R. Poettgen⁹⁷, R. Poggi⁵⁴, L. Poggioli¹³⁶, I. Pogrebnyak¹⁰⁷, D. Pohl²⁴, I. Pokharel⁵³, G. Polesello^{71a}, A. Poley¹⁸, A. Policicchio^{73a,73b}, R. Polifka¹⁴³, A. Polini^{23b}, C.S. Pollard⁴⁶, V. Polychronakos²⁹, D. Ponomarenko¹¹², L. Pontecorvo³⁶, S. Popa^{27a}, G.A. Popeneciu^{27d}, L. Portales⁵, D.M. Portillo Quintero⁵⁸, S. Pospisil¹⁴², K. Potamianos⁴⁶, I.N. Potrap⁸⁰, C.J. Potter³², H. Potti¹¹, T. Poulsen⁹⁷, J. Poveda³⁶, T.D. Powell¹⁴⁹, G. Pownall⁴⁶, M.E. Pozo Astigarraga³⁶, P. Pralavorio¹⁰², S. Prell⁷⁹, D. Price¹⁰¹, M. Primavera^{68a}, S. Prince¹⁰⁴, M.L. Proffitt¹⁴⁸, N. Proklova¹¹², K. Prokofiev^{63c}, F. Prokoshin⁸⁰, S. Protopopescu²⁹, J. Proudfoot⁶, M. Przybycien^{84a}, D. Pudzha¹³⁸, A. Puri¹⁷³, P. Puzo⁶⁵, J. Qian¹⁰⁶, Y. Qin¹⁰¹, A. Quadt⁵³, M. Queitsch-Maitland³⁶, A. Qureshi¹, M. Racko^{28a}, F. Ragusa^{69a,69b}, G. Rahal⁹⁸, J.A. Raine⁵⁴, S. Rajagopalan²⁹, A. Ramirez Morales⁹³, K. Ran^{15a,15d}, T. Rashid⁶⁵, S. Raspopov⁵, D.M. Rauch⁴⁶, F. Rauscher¹¹⁴, S. Rave¹⁰⁰, B. Ravina¹⁴⁹, I. Ravinovich¹⁸⁰, J.H. Rawling¹⁰¹, M. Raymond³⁶, A.L. Read¹³⁴, N.P. Readioff⁵⁸, M. Reale^{68a,68b}, D.M. Rebuffi^{71a,71b}, A. Redelbach¹⁷⁷, G. Redlinger²⁹, K. Reeves⁴³, L. Rehnisch¹⁹, J. Reichert¹³⁷, D. Reikher¹⁶¹, A. Reiss¹⁰⁰, A. Rej¹⁵¹, C. Rembser³⁶, A. Renardi⁴⁶, M. Renda^{27b}, M. Rescigno^{73a}, S. Resconi^{69a}, E.D. Resseguie¹⁸, S. Rettie⁹⁵, B. Reynolds¹²⁷, E. Reynolds²¹, O.L. Rezanova^{122b,122a}, P. Reznicek¹⁴³, E. Ricci^{76a,76b}, R. Richter¹¹⁵, S. Richter⁴⁶, E. Richter-Was^{84b}, O. Ricken²⁴, M. Ridel¹³⁶, P. Rieck¹¹⁵, O. Rifki⁴⁶, M. Rijssenbeek¹⁵⁵, A. Rimoldi^{71a,71b}, M. Rimoldi⁴⁶, L. Rinaldi^{23b}, G. Ripellino¹⁵⁴, I. Riu¹⁴, J.C. Rivera Vergara¹⁷⁶, F. Rizatdinova¹³⁰, E. Rizvi⁹³, C. Rizzi³⁶, R.T. Roberts¹⁰¹, S.H. Robertson^{104,ad}, M. Robin⁴⁶, D. Robinson³², C.M. Robles Gajardo^{147d}, M. Robles Manzano¹⁰⁰, A. Robson⁵⁷, A. Rocchi^{74a,74b}, E. Rocco¹⁰⁰, C. Roda^{72a,72b}, S. Rodriguez Bosca¹⁷⁴, A. Rodriguez Perez¹⁴, D. Rodriguez Rodriguez¹⁷⁴, A.M. Rodríguez Vera^{168b}, S. Roe³⁶, O. Røhne¹³⁴, R. Röhrig¹¹⁵, R.A. Rojas^{147d}, B. Roland⁵²,

C.P.A. Roland¹⁶⁶, J. Roloff²⁹, A. Romaniouk¹¹², M. Romano^{23b,23a}, N. Rompotis⁹¹, M. Ronzani¹²⁵, L. Roos¹³⁶, S. Rosati^{73a}, G. Rosin¹⁰³, B.J. Rosser¹³⁷, E. Rossi⁴⁶, E. Rossi^{75a,75b}, E. Rossi^{70a,70b}, L.P. Rossi^{55b}, L. Rossini^{69a,69b}, R. Rosten¹⁴, M. Rotaru^{27b}, J. Rothberg¹⁴⁸, B. Rottler⁵², D. Rousseau⁶⁵, G. Rovelli^{71a,71b}, A. Roy¹¹, D. Roy^{33e}, A. Rozanov¹⁰², Y. Rozen¹⁶⁰, X. Ruan^{33e}, F. Rühr⁵², A. Ruiz-Martinez¹⁷⁴, A. Rummeler³⁶, Z. Rurikova⁵², N.A. Rusakovich⁸⁰, H.L. Russell¹⁰⁴, L. Rustige^{38,47}, J.P. Rutherford⁷, E.M. Rüttinger¹⁴⁹, M. Rybar³⁹, G. Rybkin⁶⁵, E.B. Rye¹³⁴, A. Ryzhov¹²³, J.A. Sabater Iglesias⁴⁶, P. Sabatini⁵³, G. Sabato¹²⁰, S. Sacerdoti⁶⁵, H.F-W. Sadrozinski¹⁴⁶, R. Sadykov⁸⁰, F. Safai Tehrani^{73a}, B. Safarzadeh Samani¹⁵⁶, M. Safdari¹⁵³, P. Saha¹²¹, S. Saha¹⁰⁴, M. Sahinsoy^{61a}, A. Sahu¹⁸², M. Saimpert⁴⁶, M. Saito¹⁶³, T. Saito¹⁶³, H. Sakamoto¹⁶³, D. Salamani⁵⁴, G. Salamanna^{75a,75b}, J.E. Salazar Loyola^{147d}, A. Salnikov¹⁵³, J. Salt¹⁷⁴, D. Salvatore^{41b,41a}, F. Salvatore¹⁵⁶, A. Salvucci^{63a,63b,63c}, A. Salzburger³⁶, J. Samarati³⁶, D. Sammel⁵², D. Sampsonidis¹⁶², D. Sampsonidou¹⁶², J. Sánchez¹⁷⁴, A. Sanchez Pineda^{67a,36,67c}, H. Sandaker¹³⁴, C.O. Sander⁴⁶, I.G. Sanderswood⁹⁰, M. Sandhoff¹⁸², C. Sandoval^{22a}, D.P.C. Sankey¹⁴⁴, M. Sannino^{55b,55a}, Y. Sano¹¹⁷, A. Sansoni⁵¹, C. Santoni³⁸, H. Santos^{140a,140b}, S.N. Santpur¹⁸, A. Santra¹⁷⁴, A. Saponov⁸⁰, J.G. Saraiva^{140a,140d}, O. Sasaki⁸², K. Sato¹⁶⁹, F. Sauerburger⁵², E. Sauvan⁵, P. Savard^{167,ao}, R. Sawada¹⁶³, C. Sawyer¹⁴⁴, L. Sawyer^{96,ah}, C. Sbarra^{23b}, A. Sbrizzi^{23a}, T. Scanlon⁹⁵, J. Schaarschmidt¹⁴⁸, P. Schacht¹¹⁵, B.M. Schachtner¹¹⁴, D. Schaefer³⁷, L. Schaefer¹³⁷, J. Schaeffer¹⁰⁰, S. Schaepe³⁶, U. Schäfer¹⁰⁰, A.C. Schaffer⁶⁵, D. Schaile¹¹⁴, R.D. Schamberger¹⁵⁵, N. Scharmberg¹⁰¹, V.A. Schegelsky¹³⁸, D. Scheirich¹⁴³, F. Schenck¹⁹, M. Schernau¹⁷¹, C. Schiavi^{55b,55a}, L.K. Schildgen²⁴, Z.M. Schillaci²⁶, E.J. Schioppa³⁶, M. Schioppa^{41b,41a}, K.E. Schleicher⁵², S. Schlenker³⁶, K.R. Schmidt-Sommerfeld¹¹⁵, K. Schmieden³⁶, C. Schmitt¹⁰⁰, S. Schmitt⁴⁶, S. Schmitz¹⁰⁰, J.C. Schmoeckel⁴⁶, L. Schoeffel¹⁴⁵, A. Schoening^{61b}, P.G. Scholer⁵², E. Schopf¹³⁵, M. Schott¹⁰⁰, J.F.P. Schouwenberg¹¹⁹, J. Schovancova³⁶, S. Schramm⁵⁴, F. Schroeder¹⁸², A. Schulte¹⁰⁰, H-C. Schultz-Coulon^{61a}, M. Schumacher⁵², B.A. Schumm¹⁴⁶, Ph. Schune¹⁴⁵, A. Schwartzman¹⁵³, T.A. Schwarz¹⁰⁶, Ph. Schwemling¹⁴⁵, R. Schwienhorst¹⁰⁷, A. Sciandra¹⁴⁶, G. Sciolla²⁶, M. Scodreggio⁴⁶, M. Scornajenghi^{41b,41a}, F. Scuri^{72a}, F. Scutti¹⁰⁵, L.M. Scyboz¹¹⁵, C.D. Sebastiani^{73a,73b}, P. Seema¹⁹, S.C. Seidel¹¹⁸, A. Seiden¹⁴⁶, B.D. Seidlitz²⁹, T. Seiss³⁷, J.M. Seixas^{81b}, G. Sekhniaidze^{70a}, S.J. Sekula⁴², N. Semprini-Cesari^{23b,23a}, S. Sen⁴⁹, C. Serfon⁷⁷, L. Serin⁶⁵, L. Serkin^{67a,67b}, M. Sessa^{60a}, H. Severini¹²⁹, S. Sevova¹⁵³, T. Šfiligoj⁹², F. Sforza^{55b,55a}, A. Sfyrta⁵⁴, E. Shabalina⁵³, J.D. Shahinian¹⁴⁶, N.W. Shaikh^{45a,45b}, D. Shaked Renous¹⁸⁰, L.Y. Shan^{15a}, M. Shapiro¹⁸, A. Sharma¹³⁵, A.S. Sharma¹, P.B. Shatalov¹²⁴, K. Shaw¹⁵⁶, S.M. Shaw¹⁰¹, M. Shehade¹⁸⁰, Y. Shen¹²⁹, A.D. Sherman²⁵, P. Sherwood⁹⁵, L. Shi¹⁵⁸, S. Shimizu⁸², C.O. Shimmin¹⁸³, Y. Shimogama¹⁷⁹, M. Shimojima¹¹⁶, I.P.J. Shipsey¹³⁵, S. Shirabe¹⁶⁵, M. Shiyakova^{80,ab}, J. Shlomi¹⁸⁰, A. Shmeleva¹¹¹, M.J. Shochet³⁷, J. Shojaii¹⁰⁵, D.R. Shope¹²⁹, S. Shrestha¹²⁷, E.M. Shrif^{33e}, E. Shulga¹⁸⁰, P. Sicho¹⁴¹, A.M. Sickles¹⁷³, P.E. Sidebo¹⁵⁴, E. Sideras Haddad^{33e}, O. Sidiropoulou³⁶, A. Sidoti^{23b,23a}, F. Siegert⁴⁸, Dj. Sijacki¹⁶, M.Jr. Silva¹⁸¹, M.V. Silva Oliveira^{81a}, S.B. Silverstein^{45a}, S. Simion⁶⁵, R. Simoniello¹⁰⁰, C.J. Simpson-allso²¹, S. Simsek^{12b}, P. Sinervo¹⁶⁷, V. Sinetckii¹¹³, S. Singh¹⁵², M. Sioli^{23b,23a}, I. Siral¹³², S.Yu. Sivoklov¹¹³, J. Sjölin^{45a,45b}, E. Skorda⁹⁷, P. Skubic¹²⁹, M. Slawinska⁸⁵, K. Sliwa¹⁷⁰, R. Slovak¹⁴³, V. Smakhtin¹⁸⁰, B.H. Smart¹⁴⁴, J. Smiesko^{28b}, N. Smirnov¹¹², S.Yu. Smirnov¹¹², Y. Smirnov¹¹², L.N. Smirnova^{113,t}, O. Smirnova⁹⁷, J.W. Smith⁵³, M. Smizanska⁹⁰, K. Smolek¹⁴², A. Smykiewicz⁸⁵, A.A. Snesarev¹¹¹, H.L. Snoek¹²⁰, I.M. Snyder¹³², S. Snyder²⁹, R. Sobie^{176,ad}, A. Soffer¹⁶¹, A. Sogaard⁵⁰, F. Sohns⁵³, C.A. Solans Sanchez³⁶, E.Yu. Soldatov¹¹², U. Soldevila¹⁷⁴, A.A. Solodkov¹²³, A. Soloshenko⁸⁰, O.V. Solovyanov¹²³, V. Solovyev¹³⁸, P. Sommer¹⁴⁹, H. Son¹⁷⁰, W. Song¹⁴⁴, W.Y. Song^{168b}, A. Sopczak¹⁴², A.L. Sopio⁹⁵, F. Sopkova^{28b}, C.L. Sotiropoulou^{72a,72b}, S. Sottocornola^{71a,71b}, R. Soualah^{67a,67c,f}, A.M. Soukharev^{122b,122a}, D. South⁴⁶, S. Spagnolo^{68a,68b}, M. Spalla¹¹⁵,

M. Spangenberg¹⁷⁸, F. Spanò⁹⁴, D. Sperlich⁵², T.M. Spieker^{61a}, G. Spigo³⁶, M. Spina¹⁵⁶,
 D.P. Spiteri⁵⁷, M. Spousta¹⁴³, A. Stabile^{69a,69b}, B.L. Stamas¹²¹, R. Stamen^{61a},
 M. Stamenkovic¹²⁰, E. Stanecka⁸⁵, B. Stanislaus¹³⁵, M.M. Stanitzki⁴⁶, M. Stankaityte¹³⁵,
 B. Stapf¹²⁰, E.A. Starchenko¹²³, G.H. Stark¹⁴⁶, J. Stark⁵⁸, P. Staroba¹⁴¹, P. Starovoitov^{61a},
 S. Stärz¹⁰⁴, R. Staszewski⁸⁵, G. Stavropoulos⁴⁴, M. Stegler⁴⁶, P. Steinberg²⁹, A.L. Steinhebel¹³²,
 B. Stelzer¹⁵², H.J. Stelzer¹³⁹, O. Stelzer-Chilton^{168a}, H. Stenzel⁵⁶, T.J. Stevenson¹⁵⁶,
 G.A. Stewart³⁶, M.C. Stockton³⁶, G. Stoicea^{27b}, M. Stolarski^{140a}, S. Stonjek¹¹⁵, A. Straessner⁴⁸,
 J. Strandberg¹⁵⁴, S. Strandberg^{45a,45b}, M. Strauss¹²⁹, P. Strizenec^{28b}, R. Ströhmer¹⁷⁷,
 D.M. Strom¹³², R. Stroynowski⁴², A. Strubig⁵⁰, S.A. Stucci²⁹, B. Stugu¹⁷, J. Stupak¹²⁹,
 N.A. Styles⁴⁶, D. Su¹⁵³, W. Su^{60c}, S. Suchek^{61a}, V.V. Sulin¹¹¹, M.J. Sullivan⁹¹, D.M.S. Sultan⁵⁴,
 S. Sultansoy^{4c}, T. Sumida⁸⁶, S. Sun¹⁰⁶, X. Sun¹⁰¹, K. Suruliz¹⁵⁶, C.J.E. Suster¹⁵⁷,
 M.R. Sutton¹⁵⁶, S. Suzuki⁸², M. Svatos¹⁴¹, M. Swiatlowski³⁷, S.P. Swift², T. Swirski¹⁷⁷,
 A. Sydorenko¹⁰⁰, I. Sykora^{28a}, M. Sykora¹⁴³, T. Sykora¹⁴³, D. Ta¹⁰⁰, K. Tackmann^{46,z},
 J. Taenzer¹⁶¹, A. Taffard¹⁷¹, R. Tafirout^{168a}, R. Takashima⁸⁷, K. Takeda⁸³, T. Takeshita¹⁵⁰,
 E.P. Takeva⁵⁰, Y. Takubo⁸², M. Talby¹⁰², A.A. Talyshv^{122b,122a}, N.M. Tamir¹⁶¹, J. Tanaka¹⁶³,
 M. Tanaka¹⁶⁵, R. Tanaka⁶⁵, S. Tapia Araya¹⁷³, S. Tapprogge¹⁰⁰,
 A. Tarek Abouelfadl Mohamed¹³⁶, S. Tarem¹⁶⁰, K. Tariq^{60b}, G. Tarna^{27b,c}, G.F. Tartarelli^{69a},
 P. Tas¹⁴³, M. Tasevsky¹⁴¹, T. Tashiro⁸⁶, E. Tassi^{41b,41a}, A. Tavares Delgado^{140a}, Y. Tayalati^{35e},
 A.J. Taylor⁵⁰, G.N. Taylor¹⁰⁵, W. Taylor^{168b}, A.S. Tee⁹⁰, R. Teixeira De Lima¹⁵³,
 P. Teixeira-Dias⁹⁴, H. Ten Kate³⁶, J.J. Teoh¹²⁰, S. Terada⁸², K. Terashi¹⁶³, J. Terron⁹⁹,
 S. Terzo¹⁴, M. Testa⁵¹, R.J. Teuscher^{167,ad}, S.J. Thais¹⁸³, T. Theveneaux-Pelzer⁴⁶, F. Thiele⁴⁰,
 D.W. Thomas⁹⁴, J.O. Thomas⁴², J.P. Thomas²¹, P.D. Thompson²¹, L.A. Thomsen¹⁸³,
 E. Thomson¹³⁷, E.J. Thorpe⁹³, R.E. Ticse Torres⁵³, V.O. Tikhomirov^{111,aj},
 Yu.A. Tikhonov^{122b,122a}, S. Timoshenko¹¹², P. Tipton¹⁸³, S. Tisserant¹⁰², K. Todome^{23b,23a},
 S. Todorova-Nova¹⁴³, S. Todt⁴⁸, J. Tojo⁸⁸, S. Tokár^{28a}, K. Tokushuku⁸², E. Tolley¹²⁷,
 K.G. Tomiwa^{33e}, M. Tomoto¹¹⁷, L. Tompkins^{153,p}, B. Tong⁵⁹, P. Tornambe¹⁰³, E. Torrence¹³²,
 H. Torres⁴⁸, E. Torró Pastor¹⁴⁸, C. Tosciri¹³⁵, J. Toth^{102,ac}, D.R. Tovey¹⁴⁹, A. Traeet¹⁷,
 C.J. Treado¹²⁵, T. Trefzger¹⁷⁷, F. Tresoldi¹⁵⁶, A. Tricoli²⁹, I.M. Trigger^{168a},
 S. Trincaz-Duvoid¹³⁶, D.A. Trischuk¹⁷⁵, W. Trischuk¹⁶⁷, B. Trocme⁵⁸, A. Trofymov¹⁴⁵,
 C. Troncon^{69a}, F. Trovato¹⁵⁶, L. Truong^{33c}, M. Trzebinski⁸⁵, A. Trzupek⁸⁵, F. Tsai⁴⁶,
 J.C-L. Tseng¹³⁵, P.V. Tsiarshka^{108,ag}, A. Tsirigotis^{162,w}, V. Tsiskaridze¹⁵⁵,
 E.G. Tskhadadze^{159a}, M. Tsopoulou¹⁶², I.I. Tsukerman¹²⁴, V. Tsulaia¹⁸, S. Tsuno⁸²,
 D. Tsybychev¹⁵⁵, Y. Tu^{63b}, A. Tudorache^{27b}, V. Tudorache^{27b}, T.T. Tulbure^{27a}, A.N. Tuna⁵⁹,
 S. Turchikhin⁸⁰, D. Turgeman¹⁸⁰, I. Turk Cakir^{4b,u}, R.J. Turner²¹, R.T. Turra^{69a}, P.M. Tuts³⁹,
 S. Tzamarias¹⁶², E. Tzovara¹⁰⁰, G. Ucchielli⁴⁷, K. Uchida¹⁶³, F. Ukegawa¹⁶⁹, G. Unal³⁶,
 A. Undrus²⁹, G. Unel¹⁷¹, F.C. Ungaro¹⁰⁵, Y. Unno⁸², K. Uno¹⁶³, J. Urban^{28b}, P. Urquijo¹⁰⁵,
 G. Usai⁸, Z. Uysal^{12d}, V. Vacek¹⁴², B. Vachon¹⁰⁴, K.O.H. Vadla¹³⁴, A. Vaidya⁹⁵,
 C. Valderanis¹¹⁴, E. Valdes Santurio^{45a,45b}, M. Valente⁵⁴, S. Valentinetti^{23b,23a}, A. Valero¹⁷⁴,
 L. Valéry⁴⁶, R.A. Vallance²¹, A. Vallier³⁶, J.A. Valls Ferrer¹⁷⁴, T.R. Van Daalen¹⁴,
 P. Van Gemmeren⁶, I. Van Vulpen¹²⁰, M. Vanadia^{74a,74b}, W. Vandelli³⁶, M. Vandenbroucke¹⁴⁵,
 E.R. Vandewall¹³⁰, A. Vaniachine¹⁶⁶, D. Vannicola^{73a,73b}, R. Vari^{73a}, E.W. Varnes⁷,
 C. Varni^{55b,55a}, T. Varol¹⁵⁸, D. Varouchas⁶⁵, K.E. Varvell¹⁵⁷, M.E. Vasile^{27b}, G.A. Vasquez¹⁷⁶,
 F. Vazeille³⁸, D. Vazquez Furelos¹⁴, T. Vazquez Schroeder³⁶, J. Veatch⁵³, V. Vecchio^{75a,75b},
 M.J. Veen¹²⁰, L.M. Veloce¹⁶⁷, F. Veloso^{140a,140c}, S. Veneziano^{73a}, A. Ventura^{68a,68b},
 N. Venturi³⁶, A. Verbytskyi¹¹⁵, V. Vercesi^{71a}, M. Verducci^{72a,72b}, C.M. Vergel Infante⁷⁹,
 C. Vergis²⁴, W. Verkerke¹²⁰, A.T. Vermeulen¹²⁰, J.C. Vermeulen¹²⁰, M.C. Vetterli^{152,ao},
 N. Viaux Maira^{147d}, M. Vicente Barreto Pinto⁵⁴, T. Vickey¹⁴⁹, O.E. Vickey Boeriu¹⁴⁹,
 G.H.A. Viehhauser¹³⁵, L. Vignani^{61b}, M. Villa^{23b,23a}, M. Villaplana Perez³, E. Vilucchi⁵¹,

M.G. Vincter³⁴, G.S. Virdee²¹, A. Vishwakarma⁴⁶, C. Vittori^{23b,23a}, I. Vivarelli¹⁵⁶, M. Vogel¹⁸², P. Vokac¹⁴², S.E. von Buddenbrock^{33e}, E. Von Toerne²⁴, V. Vorobel¹⁴³, K. Vorobev¹¹², M. Vos¹⁷⁴, J.H. Vosseveld⁹¹, M. Vozak¹⁰¹, N. Vranjes¹⁶, M. Vranjes Milosavljevic¹⁶, V. Vrba¹⁴², M. Vreeswijk¹²⁰, R. Vuillermet³⁶, I. Vukotic³⁷, P. Wagner²⁴, W. Wagner¹⁸², J. Wagner-Kuhr¹¹⁴, S. Wahdan¹⁸², H. Wahlberg⁸⁹, V.M. Walbrecht¹¹⁵, J. Walder⁹⁰, R. Walker¹¹⁴, S.D. Walker⁹⁴, W. Walkowiak¹⁵¹, V. Wallangen^{45a,45b}, A.M. Wang⁵⁹, A.Z. Wang¹⁸¹, C. Wang^{60c}, F. Wang¹⁸¹, H. Wang¹⁸, H. Wang³, J. Wang^{63a}, J. Wang^{61b}, P. Wang⁴², Q. Wang¹²⁹, R.-J. Wang¹⁰⁰, R. Wang^{60a}, R. Wang⁶, S.M. Wang¹⁵⁸, W.T. Wang^{60a}, W. Wang^{15c}, W.X. Wang^{60a}, Y. Wang^{60a}, Z. Wang^{60c}, C. Wanotayaroj⁴⁶, A. Warburton¹⁰⁴, C.P. Ward³², D.R. Wardrope⁹⁵, N. Warrack⁵⁷, A. Washbrook⁵⁰, A.T. Watson²¹, M.F. Watson²¹, G. Watts¹⁴⁸, B.M. Waugh⁹⁵, A.F. Webb¹¹, S. Webb¹⁰⁰, C. Weber¹⁸³, M.S. Weber²⁰, S.A. Weber³⁴, S.M. Weber^{61a}, A.R. Weidberg¹³⁵, J. Weingarten⁴⁷, M. Weirich¹⁰⁰, C. Weiser⁵², P.S. Wells³⁶, T. Wenaus²⁹, T. Wengler³⁶, S. Wenig³⁶, N. Wermes²⁴, M.D. Werner⁷⁹, M. Wessels^{61a}, T.D. Weston²⁰, K. Whalen¹³², N.L. Whallon¹⁴⁸, A.M. Wharton⁹⁰, A.S. White¹⁰⁶, A. White⁸, M.J. White¹, D. Whiteson¹⁷¹, B.W. Whitmore⁹⁰, W. Wiedenmann¹⁸¹, C. Wiel⁴⁸, M. Wielers¹⁴⁴, N. Wieseotte¹⁰⁰, C. Wiglesworth⁴⁰, L.A.M. Wiik-Fuchs⁵², H.G. Wilkens³⁶, L.J. Wilkins⁹⁴, H.H. Williams¹³⁷, S. Williams³², C. Willis¹⁰⁷, S. Willocq¹⁰³, I. Wingerter-Seez⁵, E. Winkels¹⁵⁶, F. Winklmeier¹³², O.J. Winston¹⁵⁶, B.T. Winter⁵², M. Wittgen¹⁵³, M. Wobisch⁹⁶, A. Wolf¹⁰⁰, T.M.H. Wolf¹²⁰, R. Wolff¹⁰², R. Wölker¹³⁵, J. Wollrath⁵², M.W. Wolter⁸⁵, H. Wolters^{140a,140c}, V.W.S. Wong¹⁷⁵, N.L. Woods¹⁴⁶, S.D. Worm⁴⁶, B.K. Wosiek⁸⁵, K.W. Woźniak⁸⁵, K. Wraight⁵⁷, S.L. Wu¹⁸¹, X. Wu⁵⁴, Y. Wu^{60a}, T.R. Wyatt¹⁰¹, B.M. Wynne⁵⁰, S. Xella⁴⁰, Z. Xi¹⁰⁶, L. Xia¹⁷⁸, X. Xiao¹⁰⁶, I. Xiotidis¹⁵⁶, D. Xu^{15a}, H. Xu^{60a}, H. Xu^{60a}, L. Xu²⁹, T. Xu¹⁴⁵, W. Xu¹⁰⁶, Z. Xu^{60b}, Z. Xu¹⁵³, B. Yabsley¹⁵⁷, S. Yacoob^{33a}, K. Yajima¹³³, D.P. Yallup⁹⁵, N. Yamaguchi⁸⁸, Y. Yamaguchi¹⁶⁵, A. Yamamoto⁸², M. Yamatani¹⁶³, T. Yamazaki¹⁶³, Y. Yamazaki⁸³, J. Yan^{60c}, Z. Yan²⁵, H.J. Yang^{60c,60d}, H.T. Yang¹⁸, S. Yang^{60a}, T. Yang^{63c}, X. Yang^{60b,58}, Y. Yang¹⁶³, W-M. Yao¹⁸, Y.C. Yap⁴⁶, Y. Yasu⁸², E. Yatsenko^{60c,60d}, H. Ye^{15c}, J. Ye⁴², S. Ye²⁹, I. Yeletsikh⁸⁰, M.R. Yexley⁹⁰, E. Yigitbasi²⁵, K. Yorita¹⁷⁹, K. Yoshihara¹³⁷, C.J.S. Young³⁶, C. Young¹⁵³, J. Yu⁷⁹, R. Yuan^{60b,h}, X. Yue^{61a}, M. Zaazoua^{35e}, B. Zabinski⁸⁵, G. Zacharis¹⁰, E. Zaffaroni⁵⁴, J. Zahreddine¹³⁶, A.M. Zaitsev^{123,ai}, T. Zakareishvili^{159b}, N. Zakharchuk³⁴, S. Zambito⁵⁹, D. Zanzi³⁶, D.R. Zaripovas⁵⁷, S.V. Zeiβner⁴⁷, C. Zeitnitz¹⁸², G. Zemaityte¹³⁵, J.C. Zeng¹⁷³, O. Zenin¹²³, T. Ženiš^{28a}, D. Zerwas⁶⁵, M. Zgubić¹³⁵, B. Zhang^{15c}, D.F. Zhang^{15b}, G. Zhang^{15b}, H. Zhang^{15c}, J. Zhang⁶, L. Zhang^{15c}, L. Zhang^{60a}, M. Zhang¹⁷³, R. Zhang¹⁸¹, S. Zhang¹⁰⁶, X. Zhang^{60c}, X. Zhang^{60b}, Y. Zhang^{15a,15d}, Z. Zhang^{63a}, Z. Zhang⁶⁵, P. Zhao⁴⁹, Z. Zhao^{60a}, A. Zhemchugov⁸⁰, Z. Zheng¹⁰⁶, D. Zhong¹⁷³, B. Zhou¹⁰⁶, C. Zhou¹⁸¹, M.S. Zhou^{15a,15d}, M. Zhou¹⁵⁵, N. Zhou^{60c}, Y. Zhou⁷, C.G. Zhu^{60b}, C. Zhu^{15a,15d}, H.L. Zhu^{60a}, H. Zhu^{15a}, J. Zhu¹⁰⁶, Y. Zhu^{60a}, X. Zhuang^{15a}, K. Zhukov¹¹¹, V. Zhulanov^{122b,122a}, D. Zieminska⁶⁶, N.I. Zimine⁸⁰, S. Zimmermann⁵², Z. Zinonos¹¹⁵, M. Ziolkowski¹⁵¹, L. Živković¹⁶, G. Zobernig¹⁸¹, A. Zoccoli^{23b,23a}, K. Zoch⁵³, T.G. Zorbas¹⁴⁹, R. Zou³⁷, L. Zwalinski³⁶.

¹ Department of Physics, University of Adelaide, Adelaide; Australia

² Physics Department, SUNY Albany, Albany NY; U.S.A.

³ Department of Physics, University of Alberta, Edmonton AB; Canada

⁴ (a) Department of Physics, Ankara University, Ankara; (b) Istanbul Aydin University, Istanbul;

(c) Division of Physics, TOBB University of Economics and Technology, Ankara; Turkey

⁵ LAPP, Université Grenoble Alpes, Université Savoie Mont Blanc, CNRS/IN2P3, Annecy; France

⁶ High Energy Physics Division, Argonne National Laboratory, Argonne IL; U.S.A.

⁷ Department of Physics, University of Arizona, Tucson AZ; U.S.A.

⁸ Department of Physics, University of Texas at Arlington, Arlington TX; U.S.A.

⁹ Physics Department, National and Kapodistrian University of Athens, Athens; Greece

- ¹⁰ *Physics Department, National Technical University of Athens, Zografou; Greece*
- ¹¹ *Department of Physics, University of Texas at Austin, Austin TX; U.S.A.*
- ¹² ^(a) *Bahcesehir University, Faculty of Engineering and Natural Sciences, Istanbul;* ^(b) *Istanbul Bilgi University, Faculty of Engineering and Natural Sciences, Istanbul;* ^(c) *Department of Physics, Bogazici University, Istanbul;* ^(d) *Department of Physics Engineering, Gaziantep University, Gaziantep; Turkey*
- ¹³ *Institute of Physics, Azerbaijan Academy of Sciences, Baku; Azerbaijan*
- ¹⁴ *Institut de Física d'Altes Energies (IFAE), Barcelona Institute of Science and Technology, Barcelona; Spain*
- ¹⁵ ^(a) *Institute of High Energy Physics, Chinese Academy of Sciences, Beijing;* ^(b) *Physics Department, Tsinghua University, Beijing;* ^(c) *Department of Physics, Nanjing University, Nanjing;* ^(d) *University of Chinese Academy of Science (UCAS), Beijing; China*
- ¹⁶ *Institute of Physics, University of Belgrade, Belgrade; Serbia*
- ¹⁷ *Department for Physics and Technology, University of Bergen, Bergen; Norway*
- ¹⁸ *Physics Division, Lawrence Berkeley National Laboratory and University of California, Berkeley CA; U.S.A.*
- ¹⁹ *Institut für Physik, Humboldt Universität zu Berlin, Berlin; Germany*
- ²⁰ *Albert Einstein Center for Fundamental Physics and Laboratory for High Energy Physics, University of Bern, Bern; Switzerland*
- ²¹ *School of Physics and Astronomy, University of Birmingham, Birmingham; U.K.*
- ²² ^(a) *Facultad de Ciencias y Centro de Investigaciones, Universidad Antonio Nariño, Bogotá;* ^(b) *Departamento de Física, Universidad Nacional de Colombia, Bogotá, Colombia; Colombia*
- ²³ ^(a) *INFN Bologna and Università di Bologna, Dipartimento di Fisica;* ^(b) *INFN Sezione di Bologna; Italy*
- ²⁴ *Physikalisches Institut, Universität Bonn, Bonn; Germany*
- ²⁵ *Department of Physics, Boston University, Boston MA; U.S.A.*
- ²⁶ *Department of Physics, Brandeis University, Waltham MA; U.S.A.*
- ²⁷ ^(a) *Transilvania University of Brasov, Brasov;* ^(b) *Horia Hulubei National Institute of Physics and Nuclear Engineering, Bucharest;* ^(c) *Department of Physics, Alexandru Ioan Cuza University of Iasi, Iasi;* ^(d) *National Institute for Research and Development of Isotopic and Molecular Technologies, Physics Department, Cluj-Napoca;* ^(e) *University Politehnica Bucharest, Bucharest;* ^(f) *West University in Timisoara, Timisoara; Romania*
- ²⁸ ^(a) *Faculty of Mathematics, Physics and Informatics, Comenius University, Bratislava;* ^(b) *Department of Subnuclear Physics, Institute of Experimental Physics of the Slovak Academy of Sciences, Kosice; Slovak Republic*
- ²⁹ *Physics Department, Brookhaven National Laboratory, Upton NY; U.S.A.*
- ³⁰ *Departamento de Física, Universidad de Buenos Aires, Buenos Aires; Argentina*
- ³¹ *California State University, CA; U.S.A.*
- ³² *Cavendish Laboratory, University of Cambridge, Cambridge; U.K.*
- ³³ ^(a) *Department of Physics, University of Cape Town, Cape Town;* ^(b) *iThemba Labs, Western Cape;* ^(c) *Department of Mechanical Engineering Science, University of Johannesburg, Johannesburg;* ^(d) *University of South Africa, Department of Physics, Pretoria;* ^(e) *School of Physics, University of the Witwatersrand, Johannesburg; South Africa*
- ³⁴ *Department of Physics, Carleton University, Ottawa ON; Canada*
- ³⁵ ^(a) *Faculté des Sciences Ain Chock, Réseau Universitaire de Physique des Hautes Energies - Université Hassan II, Casablanca;* ^(b) *Faculté des Sciences, Université Ibn-Tofail, Kénitra;* ^(c) *Faculté des Sciences Semlalia, Université Cadi Ayyad, LPHEA-Marrakech;* ^(d) *Faculté des Sciences, Université Mohamed Premier and LPTPM, Oujda;* ^(e) *Faculté des sciences, Université Mohammed V, Rabat; Morocco*
- ³⁶ *CERN, Geneva; Switzerland*
- ³⁷ *Enrico Fermi Institute, University of Chicago, Chicago IL; U.S.A.*
- ³⁸ *LPC, Université Clermont Auvergne, CNRS/IN2P3, Clermont-Ferrand; France*

- 39 *Nevis Laboratory, Columbia University, Irvington NY; U.S.A.*
- 40 *Niels Bohr Institute, University of Copenhagen, Copenhagen; Denmark*
- 41 ^(a) *Dipartimento di Fisica, Università della Calabria, Rende;* ^(b) *INFN Gruppo Collegato di Cosenza, Laboratori Nazionali di Frascati; Italy*
- 42 *Physics Department, Southern Methodist University, Dallas TX; U.S.A.*
- 43 *Physics Department, University of Texas at Dallas, Richardson TX; U.S.A.*
- 44 *National Centre for Scientific Research “Demokritos”, Agia Paraskevi; Greece*
- 45 ^(a) *Department of Physics, Stockholm University;* ^(b) *Oskar Klein Centre, Stockholm; Sweden*
- 46 *Deutsches Elektronen-Synchrotron DESY, Hamburg and Zeuthen; Germany*
- 47 *Lehrstuhl für Experimentelle Physik IV, Technische Universität Dortmund, Dortmund; Germany*
- 48 *Institut für Kern- und Teilchenphysik, Technische Universität Dresden, Dresden; Germany*
- 49 *Department of Physics, Duke University, Durham NC; U.S.A.*
- 50 *SUPA - School of Physics and Astronomy, University of Edinburgh, Edinburgh; U.K.*
- 51 *INFN e Laboratori Nazionali di Frascati, Frascati; Italy*
- 52 *Physikalisches Institut, Albert-Ludwigs-Universität Freiburg, Freiburg; Germany*
- 53 *II. Physikalisches Institut, Georg-August-Universität Göttingen, Göttingen; Germany*
- 54 *Département de Physique Nucléaire et Corpusculaire, Université de Genève, Genève; Switzerland*
- 55 ^(a) *Dipartimento di Fisica, Università di Genova, Genova;* ^(b) *INFN Sezione di Genova; Italy*
- 56 *II. Physikalisches Institut, Justus-Liebig-Universität Giessen, Giessen; Germany*
- 57 *SUPA - School of Physics and Astronomy, University of Glasgow, Glasgow; U.K.*
- 58 *LPSC, Université Grenoble Alpes, CNRS/IN2P3, Grenoble INP, Grenoble; France*
- 59 *Laboratory for Particle Physics and Cosmology, Harvard University, Cambridge MA; U.S.A.*
- 60 ^(a) *Department of Modern Physics and State Key Laboratory of Particle Detection and Electronics, University of Science and Technology of China, Hefei;* ^(b) *Institute of Frontier and Interdisciplinary Science and Key Laboratory of Particle Physics and Particle Irradiation (MOE), Shandong University, Qingdao;* ^(c) *School of Physics and Astronomy, Shanghai Jiao Tong University, KLPPAC-MoE, SKLPPC, Shanghai;* ^(d) *Tsung-Dao Lee Institute, Shanghai; China*
- 61 ^(a) *Kirchhoff-Institut für Physik, Ruprecht-Karls-Universität Heidelberg, Heidelberg;*
- ^(b) *Physikalisches Institut, Ruprecht-Karls-Universität Heidelberg, Heidelberg; Germany*
- 62 *Faculty of Applied Information Science, Hiroshima Institute of Technology, Hiroshima; Japan*
- 63 ^(a) *Department of Physics, Chinese University of Hong Kong, Shatin, N.T., Hong Kong;*
- ^(b) *Department of Physics, University of Hong Kong, Hong Kong;* ^(c) *Department of Physics and Institute for Advanced Study, Hong Kong University of Science and Technology, Clear Water Bay, Kowloon, Hong Kong; China*
- 64 *Department of Physics, National Tsing Hua University, Hsinchu; Taiwan*
- 65 *IJCLab, Université Paris-Saclay, CNRS/IN2P3, 91195, Orsay; France*
- 66 *Department of Physics, Indiana University, Bloomington IN; U.S.A.*
- 67 ^(a) *INFN Gruppo Collegato di Udine, Sezione di Trieste, Udine;* ^(b) *ICTP, Trieste;* ^(c) *Dipartimento Politecnico di Ingegneria e Architettura, Università di Udine, Udine; Italy*
- 68 ^(a) *INFN Sezione di Lecce;* ^(b) *Dipartimento di Matematica e Fisica, Università del Salento, Lecce; Italy*
- 69 ^(a) *INFN Sezione di Milano;* ^(b) *Dipartimento di Fisica, Università di Milano, Milano; Italy*
- 70 ^(a) *INFN Sezione di Napoli;* ^(b) *Dipartimento di Fisica, Università di Napoli, Napoli; Italy*
- 71 ^(a) *INFN Sezione di Pavia;* ^(b) *Dipartimento di Fisica, Università di Pavia, Pavia; Italy*
- 72 ^(a) *INFN Sezione di Pisa;* ^(b) *Dipartimento di Fisica E. Fermi, Università di Pisa, Pisa; Italy*
- 73 ^(a) *INFN Sezione di Roma;* ^(b) *Dipartimento di Fisica, Sapienza Università di Roma, Roma; Italy*
- 74 ^(a) *INFN Sezione di Roma Tor Vergata;* ^(b) *Dipartimento di Fisica, Università di Roma Tor Vergata, Roma; Italy*
- 75 ^(a) *INFN Sezione di Roma Tre;* ^(b) *Dipartimento di Matematica e Fisica, Università Roma Tre, Roma; Italy*
- 76 ^(a) *INFN-TIFPA;* ^(b) *Università degli Studi di Trento, Trento; Italy*
- 77 *Institut für Astro- und Teilchenphysik, Leopold-Franzens-Universität, Innsbruck; Austria*

- 78 *University of Iowa, Iowa City IA; U.S.A.*
- 79 *Department of Physics and Astronomy, Iowa State University, Ames IA; U.S.A.*
- 80 *Joint Institute for Nuclear Research, Dubna; Russia*
- 81 ^(a) *Departamento de Engenharia Elétrica, Universidade Federal de Juiz de Fora (UFJF), Juiz de Fora;* ^(b) *Universidade Federal do Rio De Janeiro COPPE/EE/IF, Rio de Janeiro;* ^(c) *Universidade Federal de São João del Rei (UFSJ), São João del Rei;* ^(d) *Instituto de Física, Universidade de São Paulo, São Paulo; Brazil*
- 82 *KEK, High Energy Accelerator Research Organization, Tsukuba; Japan*
- 83 *Graduate School of Science, Kobe University, Kobe; Japan*
- 84 ^(a) *AGH University of Science and Technology, Faculty of Physics and Applied Computer Science, Krakow;* ^(b) *Marian Smoluchowski Institute of Physics, Jagiellonian University, Krakow; Poland*
- 85 *Institute of Nuclear Physics Polish Academy of Sciences, Krakow; Poland*
- 86 *Faculty of Science, Kyoto University, Kyoto; Japan*
- 87 *Kyoto University of Education, Kyoto; Japan*
- 88 *Research Center for Advanced Particle Physics and Department of Physics, Kyushu University, Fukuoka; Japan*
- 89 *Instituto de Física La Plata, Universidad Nacional de La Plata and CONICET, La Plata; Argentina*
- 90 *Physics Department, Lancaster University, Lancaster; U.K.*
- 91 *Oliver Lodge Laboratory, University of Liverpool, Liverpool; U.K.*
- 92 *Department of Experimental Particle Physics, Jožef Stefan Institute and Department of Physics, University of Ljubljana, Ljubljana; Slovenia*
- 93 *School of Physics and Astronomy, Queen Mary University of London, London; U.K.*
- 94 *Department of Physics, Royal Holloway University of London, Egham; U.K.*
- 95 *Department of Physics and Astronomy, University College London, London; U.K.*
- 96 *Louisiana Tech University, Ruston LA; U.S.A.*
- 97 *Fysiska institutionen, Lunds universitet, Lund; Sweden*
- 98 *Centre de Calcul de l'Institut National de Physique Nucléaire et de Physique des Particules (IN2P3), Villeurbanne; France*
- 99 *Departamento de Física Teórica C-15 and CIAFF, Universidad Autónoma de Madrid, Madrid; Spain*
- 100 *Institut für Physik, Universität Mainz, Mainz; Germany*
- 101 *School of Physics and Astronomy, University of Manchester, Manchester; U.K.*
- 102 *CPPM, Aix-Marseille Université, CNRS/IN2P3, Marseille; France*
- 103 *Department of Physics, University of Massachusetts, Amherst MA; U.S.A.*
- 104 *Department of Physics, McGill University, Montreal QC; Canada*
- 105 *School of Physics, University of Melbourne, Victoria; Australia*
- 106 *Department of Physics, University of Michigan, Ann Arbor MI; U.S.A.*
- 107 *Department of Physics and Astronomy, Michigan State University, East Lansing MI; U.S.A.*
- 108 *B.I. Stepanov Institute of Physics, National Academy of Sciences of Belarus, Minsk; Belarus*
- 109 *Research Institute for Nuclear Problems of Byelorussian State University, Minsk; Belarus*
- 110 *Group of Particle Physics, University of Montreal, Montreal QC; Canada*
- 111 *P.N. Lebedev Physical Institute of the Russian Academy of Sciences, Moscow; Russia*
- 112 *National Research Nuclear University MEPhI, Moscow; Russia*
- 113 *D.V. Skobeltsyn Institute of Nuclear Physics, M.V. Lomonosov Moscow State University, Moscow; Russia*
- 114 *Fakultät für Physik, Ludwig-Maximilians-Universität München, München; Germany*
- 115 *Max-Planck-Institut für Physik (Werner-Heisenberg-Institut), München; Germany*
- 116 *Nagasaki Institute of Applied Science, Nagasaki; Japan*
- 117 *Graduate School of Science and Kobayashi-Maskawa Institute, Nagoya University, Nagoya; Japan*
- 118 *Department of Physics and Astronomy, University of New Mexico, Albuquerque NM; U.S.A.*
- 119 *Institute for Mathematics, Astrophysics and Particle Physics, Radboud University Nijmegen/Nikhef, Nijmegen; Netherlands*

- 120 *Nikhef National Institute for Subatomic Physics and University of Amsterdam, Amsterdam; Netherlands*
- 121 *Department of Physics, Northern Illinois University, DeKalb IL; U.S.A.*
- 122 ^(a) *Budker Institute of Nuclear Physics and NSU, SB RAS, Novosibirsk;* ^(b) *Novosibirsk State University Novosibirsk; Russia*
- 123 *Institute for High Energy Physics of the National Research Centre Kurchatov Institute, Protvino; Russia*
- 124 *Institute for Theoretical and Experimental Physics named by A.I. Alikhanov of National Research Centre “Kurchatov Institute”, Moscow; Russia*
- 125 *Department of Physics, New York University, New York NY; U.S.A.*
- 126 *Ochanomizu University, Otsuka, Bunkyo-ku, Tokyo; Japan*
- 127 *Ohio State University, Columbus OH; U.S.A.*
- 128 *Faculty of Science, Okayama University, Okayama; Japan*
- 129 *Homer L. Dodge Department of Physics and Astronomy, University of Oklahoma, Norman OK; U.S.A.*
- 130 *Department of Physics, Oklahoma State University, Stillwater OK; U.S.A.*
- 131 *Palacký University, RCPTM, Joint Laboratory of Optics, Olomouc; Czech Republic*
- 132 *Institute for Fundamental Science, University of Oregon, Eugene, OR; U.S.A.*
- 133 *Graduate School of Science, Osaka University, Osaka; Japan*
- 134 *Department of Physics, University of Oslo, Oslo; Norway*
- 135 *Department of Physics, Oxford University, Oxford; U.K.*
- 136 *LPNHE, Sorbonne Université, Université de Paris, CNRS/IN2P3, Paris; France*
- 137 *Department of Physics, University of Pennsylvania, Philadelphia PA; U.S.A.*
- 138 *Konstantinov Nuclear Physics Institute of National Research Centre “Kurchatov Institute”, PNPI, St. Petersburg; Russia*
- 139 *Department of Physics and Astronomy, University of Pittsburgh, Pittsburgh PA; U.S.A.*
- 140 ^(a) *Laboratório de Instrumentação e Física Experimental de Partículas - LIP, Lisboa;*
^(b) *Departamento de Física, Faculdade de Ciências, Universidade de Lisboa, Lisboa;*
^(c) *Departamento de Física, Universidade de Coimbra, Coimbra;* ^(d) *Centro de Física Nuclear da Universidade de Lisboa, Lisboa;* ^(e) *Departamento de Física, Universidade do Minho, Braga;*
^(f) *Departamento de Física Teórica y del Cosmos, Universidad de Granada, Granada (Spain);*
^(g) *Dep Física and CEFITEC of Faculdade de Ciências e Tecnologia, Universidade Nova de Lisboa, Caparica;* ^(h) *Instituto Superior Técnico, Universidade de Lisboa, Lisboa; Portugal*
- 141 *Institute of Physics of the Czech Academy of Sciences, Prague; Czech Republic*
- 142 *Czech Technical University in Prague, Prague; Czech Republic*
- 143 *Charles University, Faculty of Mathematics and Physics, Prague; Czech Republic*
- 144 *Particle Physics Department, Rutherford Appleton Laboratory, Didcot; U.K.*
- 145 *IRFU, CEA, Université Paris-Saclay, Gif-sur-Yvette; France*
- 146 *Santa Cruz Institute for Particle Physics, University of California Santa Cruz, Santa Cruz CA; U.S.A.*
- 147 ^(a) *Departamento de Física, Pontificia Universidad Católica de Chile, Santiago;* ^(b) *Universidad Andres Bello, Department of Physics, Santiago;* ^(c) *Instituto de Alta Investigación, Universidad de Tarapacá;* ^(d) *Departamento de Física, Universidad Técnica Federico Santa María, Valparaíso; Chile*
- 148 *Department of Physics, University of Washington, Seattle WA; U.S.A.*
- 149 *Department of Physics and Astronomy, University of Sheffield, Sheffield; U.K.*
- 150 *Department of Physics, Shinshu University, Nagano; Japan*
- 151 *Department Physik, Universität Siegen, Siegen; Germany*
- 152 *Department of Physics, Simon Fraser University, Burnaby BC; Canada*
- 153 *SLAC National Accelerator Laboratory, Stanford CA; U.S.A.*
- 154 *Physics Department, Royal Institute of Technology, Stockholm; Sweden*
- 155 *Departments of Physics and Astronomy, Stony Brook University, Stony Brook NY; U.S.A.*
- 156 *Department of Physics and Astronomy, University of Sussex, Brighton; U.K.*

- 157 *School of Physics, University of Sydney, Sydney; Australia*
- 158 *Institute of Physics, Academia Sinica, Taipei; Taiwan*
- 159 ^(a) *E. Andronikashvili Institute of Physics, Iv. Javakhishvili Tbilisi State University, Tbilisi; ^(b) High Energy Physics Institute, Tbilisi State University, Tbilisi; Georgia*
- 160 *Department of Physics, Technion, Israel Institute of Technology, Haifa; Israel*
- 161 *Raymond and Beverly Sackler School of Physics and Astronomy, Tel Aviv University, Tel Aviv; Israel*
- 162 *Department of Physics, Aristotle University of Thessaloniki, Thessaloniki; Greece*
- 163 *International Center for Elementary Particle Physics and Department of Physics, University of Tokyo, Tokyo; Japan*
- 164 *Graduate School of Science and Technology, Tokyo Metropolitan University, Tokyo; Japan*
- 165 *Department of Physics, Tokyo Institute of Technology, Tokyo; Japan*
- 166 *Tomsk State University, Tomsk; Russia*
- 167 *Department of Physics, University of Toronto, Toronto ON; Canada*
- 168 ^(a) *TRIUMF, Vancouver BC; ^(b) Department of Physics and Astronomy, York University, Toronto ON; Canada*
- 169 *Division of Physics and Tomonaga Center for the History of the Universe, Faculty of Pure and Applied Sciences, University of Tsukuba, Tsukuba; Japan*
- 170 *Department of Physics and Astronomy, Tufts University, Medford MA; U.S.A.*
- 171 *Department of Physics and Astronomy, University of California Irvine, Irvine CA; U.S.A.*
- 172 *Department of Physics and Astronomy, University of Uppsala, Uppsala; Sweden*
- 173 *Department of Physics, University of Illinois, Urbana IL; U.S.A.*
- 174 *Instituto de Física Corpuscular (IFIC), Centro Mixto Universidad de Valencia - CSIC, Valencia; Spain*
- 175 *Department of Physics, University of British Columbia, Vancouver BC; Canada*
- 176 *Department of Physics and Astronomy, University of Victoria, Victoria BC; Canada*
- 177 *Fakultät für Physik und Astronomie, Julius-Maximilians-Universität Würzburg, Würzburg; Germany*
- 178 *Department of Physics, University of Warwick, Coventry; U.K.*
- 179 *Waseda University, Tokyo; Japan*
- 180 *Department of Particle Physics, Weizmann Institute of Science, Rehovot; Israel*
- 181 *Department of Physics, University of Wisconsin, Madison WI; U.S.A.*
- 182 *Fakultät für Mathematik und Naturwissenschaften, Fachgruppe Physik, Bergische Universität Wuppertal, Wuppertal; Germany*
- 183 *Department of Physics, Yale University, New Haven CT; U.S.A.*
- ^a *Also at Borough of Manhattan Community College, City University of New York, New York NY; U.S.A.*
- ^b *Also at CERN, Geneva; Switzerland*
- ^c *Also at CPPM, Aix-Marseille Université, CNRS/IN2P3, Marseille; France*
- ^d *Also at Département de Physique Nucléaire et Corpusculaire, Université de Genève, Genève; Switzerland*
- ^e *Also at Departament de Física de la Universitat Autònoma de Barcelona, Barcelona; Spain*
- ^f *Also at Department of Applied Physics and Astronomy, University of Sharjah, Sharjah; United Arab Emirates*
- ^g *Also at Department of Financial and Management Engineering, University of the Aegean, Chios; Greece*
- ^h *Also at Department of Physics and Astronomy, Michigan State University, East Lansing MI; U.S.A.*
- ⁱ *Also at Department of Physics and Astronomy, University of Louisville, Louisville, KY; U.S.A.*
- ^j *Also at Department of Physics, Ben Gurion University of the Negev, Beer Sheva; Israel*
- ^k *Also at Department of Physics, California State University, East Bay; U.S.A.*

- ^l Also at Department of Physics, California State University, Fresno; U.S.A.
- ^m Also at Department of Physics, California State University, Sacramento; U.S.A.
- ⁿ Also at Department of Physics, King's College London, London; U.K.
- ^o Also at Department of Physics, St. Petersburg State Polytechnical University, St. Petersburg; Russia
- ^p Also at Department of Physics, Stanford University, Stanford CA; U.S.A.
- ^q Also at Department of Physics, University of Adelaide, Adelaide; Australia
- ^r Also at Department of Physics, University of Fribourg, Fribourg; Switzerland
- ^s Also at Dipartimento di Matematica, Informatica e Fisica, Università di Udine, Udine; Italy
- ^t Also at Faculty of Physics, M.V. Lomonosov Moscow State University, Moscow; Russia
- ^u Also at Giresun University, Faculty of Engineering, Giresun; Turkey
- ^v Also at Graduate School of Science, Osaka University, Osaka; Japan
- ^w Also at Hellenic Open University, Patras; Greece
- ^x Also at IJCLab, Université Paris-Saclay, CNRS/IN2P3, 91405, Orsay; France
- ^y Also at Institutio Catalana de Recerca i Estudis Avancats, ICREA, Barcelona; Spain
- ^z Also at Institut für Experimentalphysik, Universität Hamburg, Hamburg; Germany
- ^{aa} Also at Institute for Mathematics, Astrophysics and Particle Physics, Radboud University Nijmegen/Nikhef, Nijmegen; Netherlands
- ^{ab} Also at Institute for Nuclear Research and Nuclear Energy (INRNE) of the Bulgarian Academy of Sciences, Sofia; Bulgaria
- ^{ac} Also at Institute for Particle and Nuclear Physics, Wigner Research Centre for Physics, Budapest; Hungary
- ^{ad} Also at Institute of Particle Physics (IPP), Vancouver; Canada
- ^{ae} Also at Institute of Physics, Azerbaijan Academy of Sciences, Baku; Azerbaijan
- ^{af} Also at Instituto de Física Teórica, IFT-UAM/CSIC, Madrid; Spain
- ^{ag} Also at Joint Institute for Nuclear Research, Dubna; Russia
- ^{ah} Also at Louisiana Tech University, Ruston LA; U.S.A.
- ^{ai} Also at Moscow Institute of Physics and Technology State University, Dolgoprudny; Russia
- ^{aj} Also at National Research Nuclear University MEPhI, Moscow; Russia
- ^{ak} Also at Physics Department, An-Najah National University, Nablus; Palestine
- ^{al} Also at Physics Dept, University of South Africa, Pretoria; South Africa
- ^{am} Also at Physikalisches Institut, Albert-Ludwigs-Universität Freiburg, Freiburg; Germany
- ^{an} Also at The City College of New York, New York NY; U.S.A.
- ^{ao} Also at TRIUMF, Vancouver BC; Canada
- ^{ap} Also at Università di Napoli Parthenope, Napoli; Italy
- * Deceased